Electronic Supplementary Material (ESI) for ChemComm.

Supporting Information

Chemically and Electrochemically Induced Expansion and Contraction of a Ferrocene Rotor

*Synøve Ø. Scottwell,[a] Anastasia B. S. Elliott,[a,b] Karl J. Shaffer,[a] Ayman Nafady,[c] C. John McAdam,[a] Keith C. Gordon,[a,b] and James D. Crowley[a]**

[a] Department of Chemistry, University of Otago, PO Box 56, Dunedin, New Zealand; Fax: +64 3 479 7906; Tel: +64 3 479 7731.

[b] MacDiarmid Institute for Advanced Materials and Nanotechnology, New Zealand

[c] Department of Chemistry, College of Science, King Saud University, PO Box 2455, Riyadh 11451, Saudi Arabia

***jcrowley@chemistry.otago.ac.nz**

Contents

1 Experimental Procedures

1.1 General

Unless otherwise stated, all reagents were purchased from commercial sources and used without further purification. The solvents used were laboratory grade, with petrol referring to the fraction of petroleum ether boiling in the range 40-60 ˚C, and ether referring to diethyl ether. Dry tetrahydrofuran (THF), acetonitrile (CH_3CN), dichloromethane (CH_2Cl_2) and chloroform ($CHCl_3$) were obtained by passing them through an activated alumina column using a PureSolv TM solvent purification system (Innovative Technologies Inc., MA). Dry tetramethylethylenediamine (TMEDA) was obtained by distillation over CaH_2. 0.1 M Ammonium hydroxide/ethylenediaminetetraacetic acid (NH_4OH/EDTA) solution was made up by mixing 30 g EDTA with 900 mL water and 100 mL NH_4OH. Microwave-assisted reactions were performed in a CEM Focused Microwave Synthesis System, Discover S-Class (CEM Corporation, NC), at 300 W.

^1H and ^{13}C NMR spectra were recorded on either a 400 MHz Varian/Agilent 400-MR or Varian 500 MHz AR spectrometer at 298 K. Chemical shifts (δ) are reported in parts per million (ppm) and referenced to residual solvent peaks ($CDCl_3$: ^1H δ 7.26 ppm, ^{13}C δ 77.16 ppm; d_6-acetone: ^1H δ 2.05 ppm; ^{13}C δ 29.84 & 206.26 ppm; CD_3CN: ^1H δ 1.94 ppm, ^{13}C δ 1.32 & 118.26 ppm). Coupling constants (*J*) are reported in Hertz (Hz). Standard abbreviations indicating multiplicity were used as follows: m = multiplet, q = quartet, t = triplet, dt = double triplet, d = doublet, dd = double doublet, s = singlet. IR spectra were recorded on a Bruker ALPHA FT-IR spectrometer with an attached ALPHA-P measurement module. Microanalyses were conducted at the Campbell Microanalytical Laboratory at the University of Otago. Electrospray mass spectra (ESMS) were collected on a Bruker micrOTOF-Q spectrometer. Melting points were determined using a Leica VMHB melting bar. UV-visible absorption spectra were acquired with a Jasco V550 UV/VIS spectrophotometer.

1.2 Ligand Synthesis

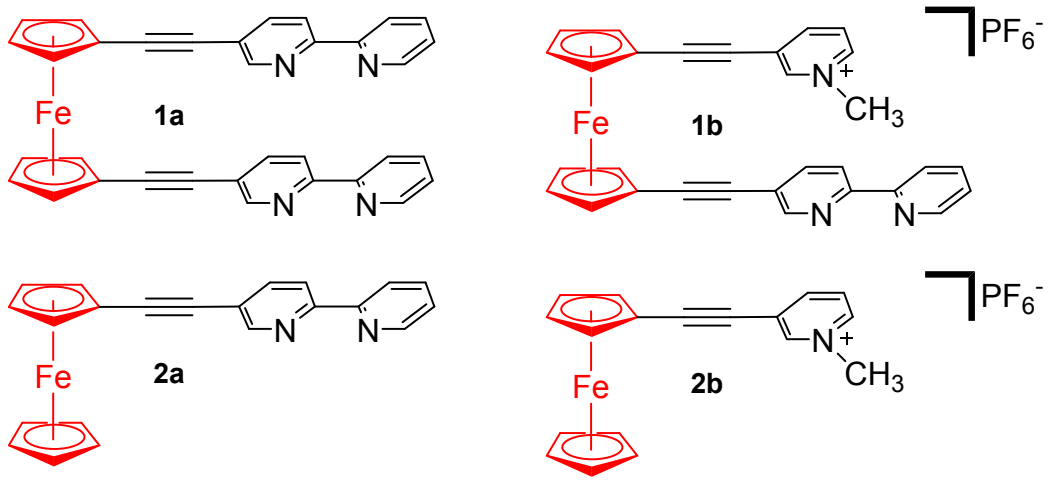

Figure S1 The ferrocene rotor molecules (**1a-b**) and the model systems (**2a-b**) studied.

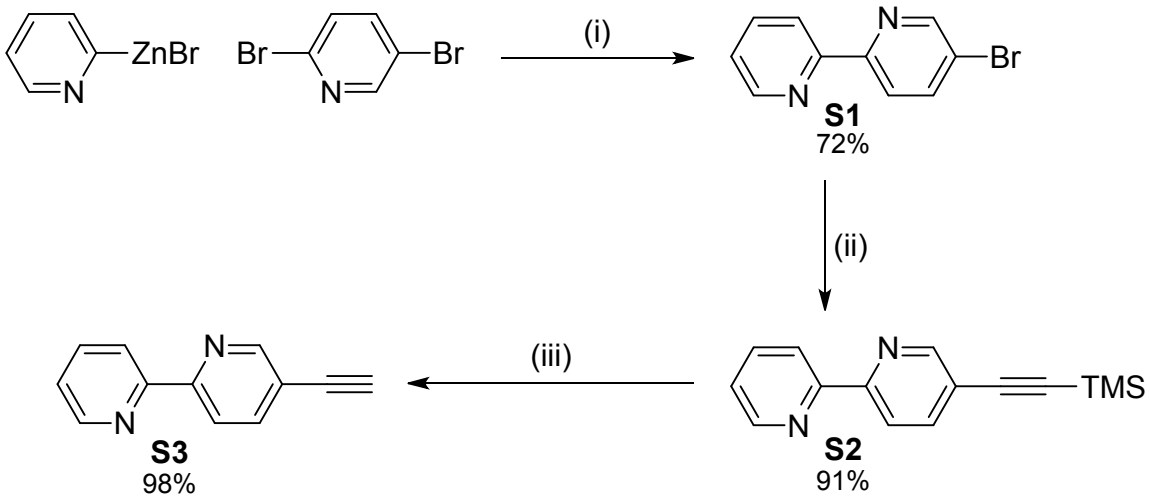

Scheme S2 Synthetic strategy for the formation of the functionalised bipyridine intermediates. (i) $[Pd(PPh_3)_4]$, THF, reflux (5 h), r.t. (16 h); (ii) Triethylamine, $[Pd(PPh_3)_2Cl_2]$, CuI, ethynyltrimethylsilane, THF, reflux (2.5 days); (iii) K_2CO_3, methanol, r.t. (1 h).

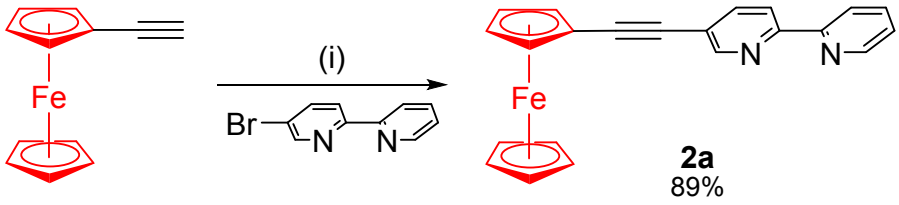

Scheme S3 Synthetic strategy for the formation of the model ligand **2a**. (i) Triethylamine, $[Pd(PPh_3)_2Cl_2]$, CuI, THF, reflux (16 h).

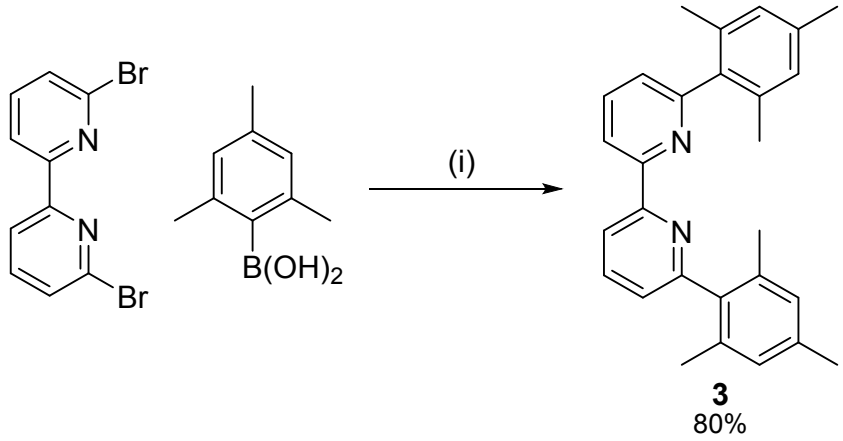

Scheme S4 Synthetic strategy for the formation of ligand **3**. (i) $[Pd(PPh_3)_4]$, $NaCO_3$ (2 M), toluene, methanol, reflux (3 days).

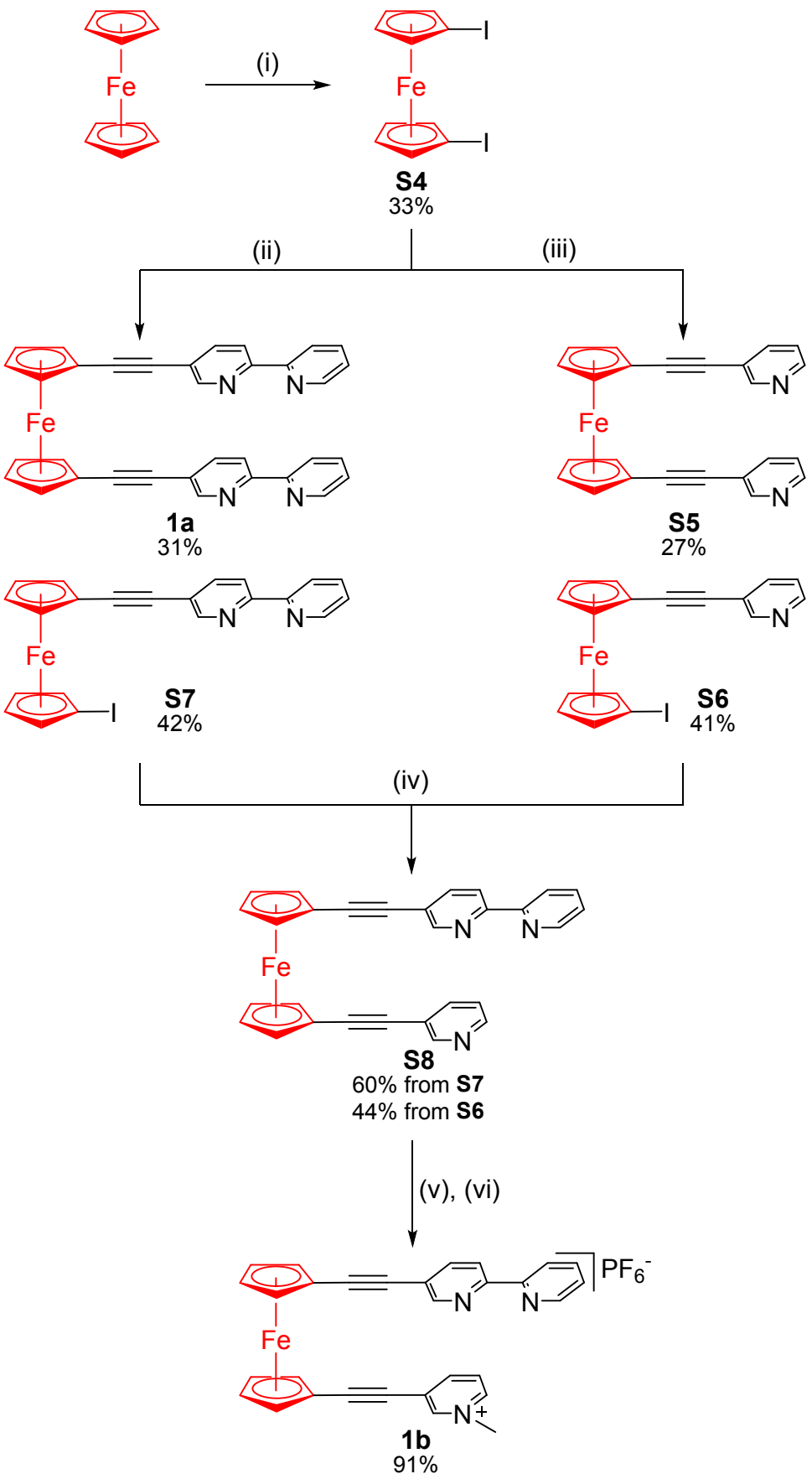

Scheme S5 Synthetic strategy for the formation of the two ferrocene-based switches **1a** and **1b**. (i) *n*-BuLi, TMEDA, I_2, ether, r.t. (16 h), -78 °C (30 min); (ii) **S3**, $[Pd(CH_3CN)_2Cl_2]$, $[PH(^tBu)_3]BF_4$, CuI, diisopropylamine, reflux (24 h); (iii) 3-ethynylpyridine, $[Pd(CH_3CN)_2Cl_2]$, $[PH(^tBu)_3]BF_4$, CuI, diisopropylamine, reflux (24 h); (iv) 3-ethynylpyridine OR **S3**,

[$Pd(CH_3CN)_2Cl_2$], [$PH(^tBu)_3]BF_4$, CuI, diisopropylamine, reflux (24 h); (v) CH_3I, CH_2Cl_2, r.t. (2 days); (vi) $AgPF_6$, acetone, r.t. (10 min).

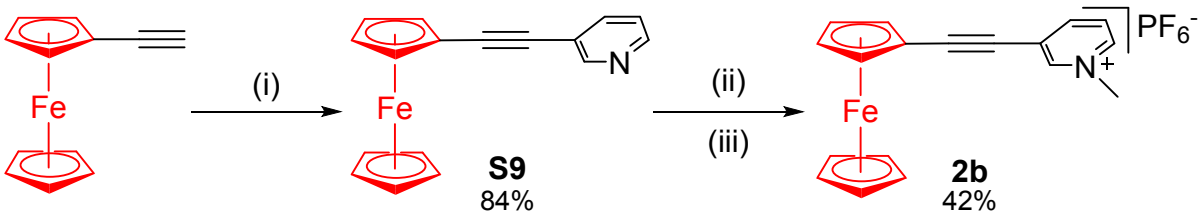

Scheme S6 Synthetic strategy for the formation of model **2b**. (i) 3-bromopyridine, [$Pd(CH_3CN)_2Cl_2$], [$PH(^tBu)_3]BF_4$, CuI, diisopropylamine, reflux (24 h); (ii) CH_3I, CH_2Cl_2, r.t. (2 days); (iii) $AgPF_6$, acetone, r.t. (10 min).

1.2.1 Synthesis of 5-bromo-2,2'-bipyridine (S1)

The synthesis of this compound has previously been reported by Rieke in 72% yield.[1]

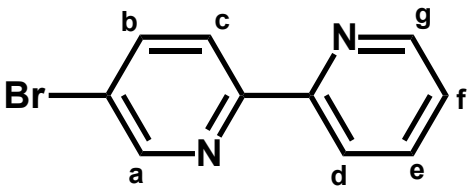

Under a nitrogen atmosphere, a solution of 2-pyridylzinc(II) bromide (THF, 0.5 M, 50 mL, 25.0 mmol, 1.10 eq.) was added to a solution of THF (20 mL) containing 2,5-dibromopyridine (5.38 g, 22.7 mmol, 1.00 eq.) and *tetrakis*(triphenylphosphine)palladium(0) (0.53 g, 0.46 mmol, 0.02 eq.). The resulting suspension was refluxed for five hours, before stirring at room temperature overnight (16 hours). NH_4OH/EDTA (200 mL) and CH_2Cl2 (150 mL) were added and the mixture allowed to stir for four hours. The organic phase was washed with water (2 × 50 mL) and saturated aqueous NaCl (2 × 50 mL), then dried over Na_2SO_4 and excess solvent removed *in vacuo*. Column chromatography (silica gel, gradient 100% petrol, then 1:1 petrol /CH_2Cl_2, then 95:5 CH_2Cl_2/acetone) was used to obtain a colourless solid. The solid residue was dissolved in CH_3CN and vapour diffused diethyl ether to provide colourless crystals. Yield: 3.84 g, 72%. Mp 82 ˚C; ^{1}H NMR (400 MHz, $CDCl_3$) δ 8.72 (dd, *J* = 2.4, 0.7 Hz, 1H, H_a), 8.67 (ddd, *J* = 4.8, 1.8, 0.9 Hz, 1H, H_g), 8.37 (dt, *J* = 8.0, 1.1 Hz, 1H, H_d), 8.32 (dd, *J* = 8.5, 0.7 Hz, 1H, H_c), 7.93 (dd, *J* = 8.5, 2.4 Hz, 1H, H_b), 7.81 (ddd, *J* = 8.1, 7.5, 1.8 Hz, 1H, H_e), 7.33 (ddd, *J* = 7.5, 4.8, 1.2 Hz, 1H, H_f); ^{13}C NMR (125 MHz, $CDCl_3$) δ 155.3, 154.8, 150.3, 149.4, 139.6, 137.2, 124.1, 122.5, 121.3, 121.1; IR (ATR): ν (cm^{-1}) 3089, 1549, 1431, 1363, 1001, 786, 733, 631; HRESI-MS (MeOH): *m/z* = 234.9870 [**S1**+H]$^+$ (calc. for $C_{10}H_7BrN_2H$ 234.9865), *m/z* = 256.9684 [**S1**+Na]$^+$ (calc. for $C_{10}H_7BrN_2Na$ 256.9685); Anal. Calc. for $C_{10}H_7BrN_2$: C, 51.09; H, 3.00; N, 11.92. Found: C, 51.09; H, 2.93; N, 11.65.

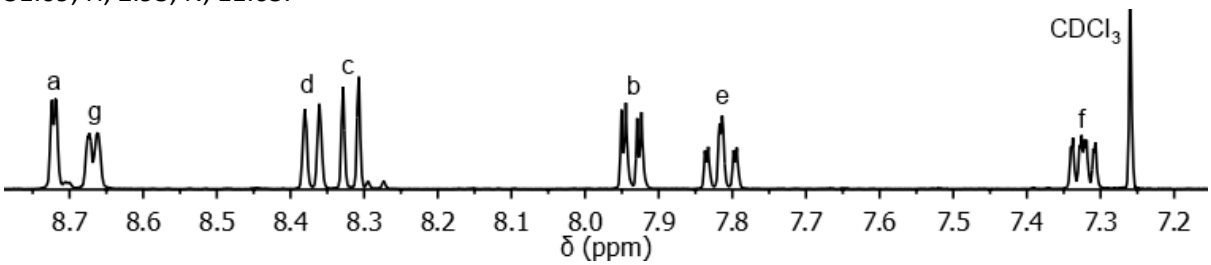

Figure S2 ^{1}H NMR spectrum (400 MHz, $CDCl_3$) of **S1**.

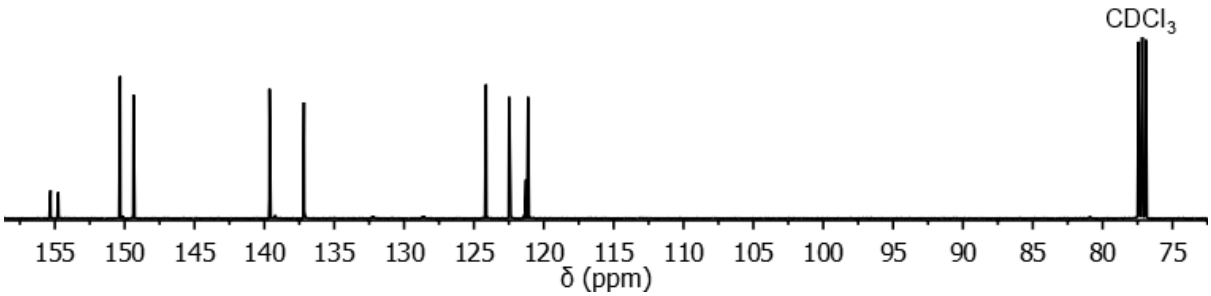

Figure S3 ^{13}C NMR spectrum (125 MHz, $CDCl_3$) of **S1**.

1.2.2 Synthesis of 5-(trimethylsilyl)ethynyl-2,2'-bipyridine (S2)

The synthesis of this compound has previously been reported by Ziessel in 77% yield.[2]

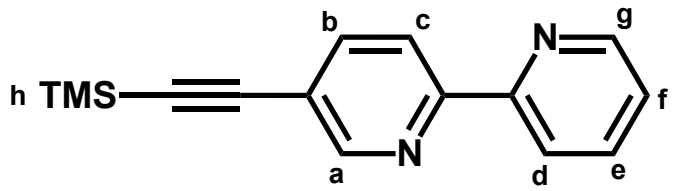

Triethylamine (3.56 mL, 25.5 mmol, 6.00 eq.) and dry THF (50 mL) were added to $[Pd(PPh_3)_2Cl_2]$ (0.090 g, 0.13 mmol, 0.03 eq.), CuI (0.081 g, 0.43 mmol, 0.10 eq.), and **S1** (1.00 g, 4.25 mmol, 1.00 eq.) under a nitrogen atmosphere. Ethynyltrimethylsilane (0.90 mL, 6.38 mmol, 1.50 eq.) was hence added and the resulting solution refluxed for 2.5 days. The reaction was quenched with NH_4OH/EDTA (200 mL), then extracted with CH_2Cl_2 (4 x 50 mL). The organic extracts were washed with NH_4OH/EDTA (2 x 50 mL), water (2 x 50 mL) and saturated aqueous NaCl (2 x 50 mL), then dried over Na_2SO_4 and the solvent removed *in vacuo*. Column chromatography (silica gel, gradient 100% petrol to 100% CH_2Cl_2) was used to obtain a colourless solid. Yield: 0.975 g, 91%. Mp 60 ˚C; ^{1}H NMR (400 MHz, $CDCl_3$) δ 8.74 (d, *J* = 1.3 Hz, 1H, H_a), 8.68 (dd, *J* = 4.8, 0.8 Hz, 1H, H_g), 8.41 (d, *J* = 8.0 Hz, 1H, H_d), 8.37 (d, *J* = 8.2 Hz, 1H, H_c) 7.87 (dd, *J* = 8.3, 2.1 Hz, 1H, H_b), 7.83 (dt, *J* = 7.7, 1.8 Hz, 1H, H_e), 7.32 (ddd, *J* = 7.5, 4.8, 1.1 Hz, 1H, H_f), 0.28 (s, 9H, H_h); ^{13}C NMR (125 MHz, $CDCl_3$) δ 155.5, 155.0, 152.1, 149.3, 139.8, 137.0, 124.0, 121.5, 120.2, 120.2, 101.9, 99.2, 0.1; IR (ATR): ν (cm^{-1}) 2959, 2158, 1455, 1248, 858, 835, 795, 740, 642; HRESI-MS (MeOH): *m/z* = 235.1142 [**S2**+H]$^+$ (calc. for $C_{15}H_{17}N_2Si$ 253.1156); Anal. Calc. for $C_{15}H_{16}N_2Si$: C, 71.38; H, 6.39; N, 11.10. Found: C, 71.39; H, 6.23; N, 11.18.

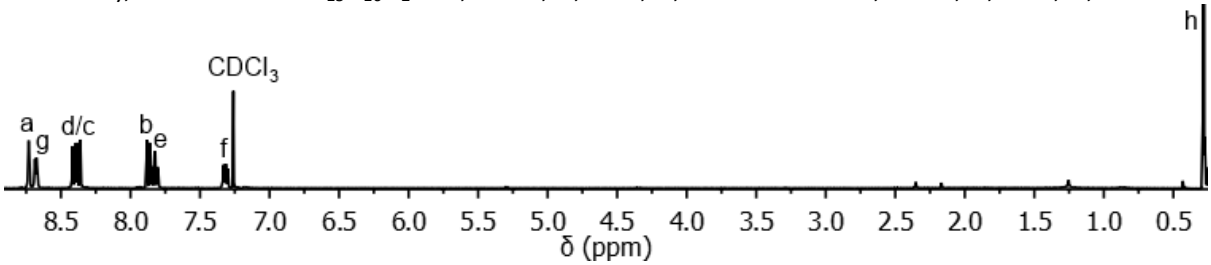

Figure S4 ^{1}H NMR spectrum (400 MHz, $CDCl_3$) of **S2**.

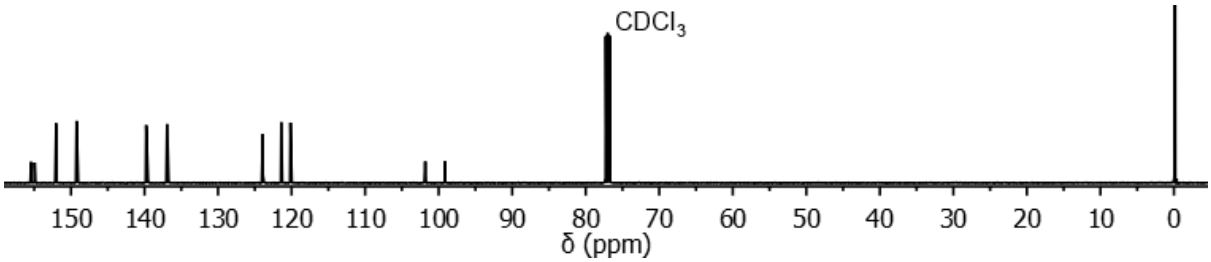

Figure S5 ^{13}C NMR spectrum (125 MHz, $CDCl_3$) of **S2**.

1.2.3 Synthesis of 5-ethynyl-2,2'-bipyridine (S3)

The synthesis of this compound has previously been reported by Ziessel in 83% yield.[2]

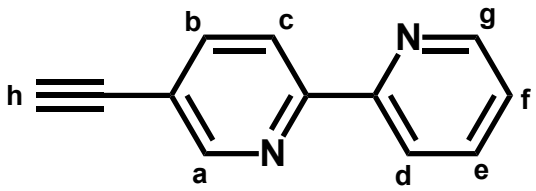

S2 (0.54 g, 2.1 mmol, 1.00 eq.) and K_2CO_3 (0.59 g, 4.2 mmol, 2.00 eq.) were combined in methanol (50 mL) and stirred for one hour at room temperature. The suspended K_2CO_3 was filtered out through Celite, before the solvent was removed *in vacuo*. The resulting colourless solid was purified by passing it through a short plug (silica gel, gradient 100% CH_2Cl_2 to 95:5 CH_2Cl_2/acetone). Yield: 0.376 g, 98%. Mp 96 ˚C; ^{1}H NMR (400 MHz, $CDCl_3$) δ 8.78 (dd, *J* = 2.0, 0.7 Hz, 1H, H_a), 8.69 (ddd, *J* = 4.8, 1.8, 0.9 Hz, 1H, H_g), 8.41 (dt, *J* = 8.0, 1.0 Hz, 1H, H_d), 8.40 (dd, *J* = 8.2, 0.8 Hz, 1H, H_c), 7.91 (dd, *J* = 8.2, 2.1 Hz, 1H, H_b), 7.83 (dt, *J* = 7.6, 1.8 Hz, 1H, H_e), 7.33 (ddd, *J* = 7.5, 4.8, 1.2 Hz 1H, H_f), 3.29 (s, 1H, H_h); ^{13}C NMR (125 MHz, $CDCl_3$) δ 155.6, 155.5, 152.4, 149.4, 140.2, 137.1, 124.2, 121.6, 120.4, 119.3, 81.5, 80.8; IR (ATR): ν (cm^{-1}) 2094, 1585, 1543, 1456, 1433, 1366, 857, 795, 744, 522; HRESI-MS (MeOH) *m/z* = 181.0769 [**S3**+H]$^+$ (calc. for $C_{12}H_9N_2$ 181.0760), *m/z* = 203.0592 [**S3**+Na]$^+$ (calc. for $C_{12}H_8N_2Na$ 203.0580); Anal. Calc. for $C_{12}H_8N_2 \bullet 0.5H_2O$: C, 79.58; H, 4.51; N, 15.47. Found: C, 79.43; H, 4.51; N, 15.42.

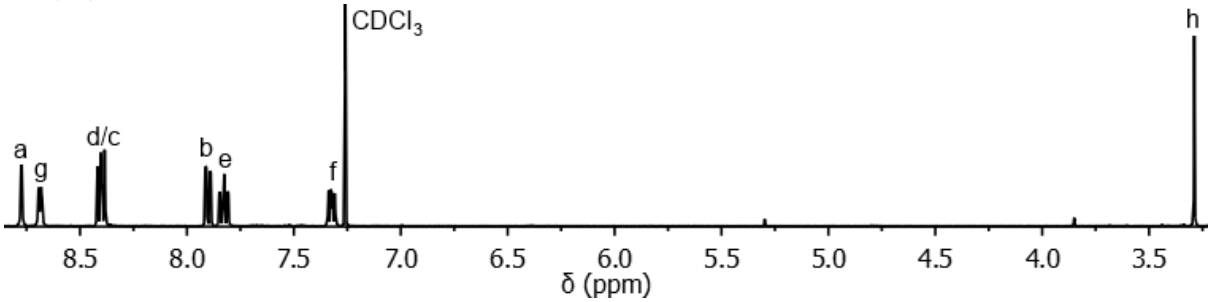

Figure S6 ^{1}H NMR spectrum (400 MHz, $CDCl_3$) of **S3**.

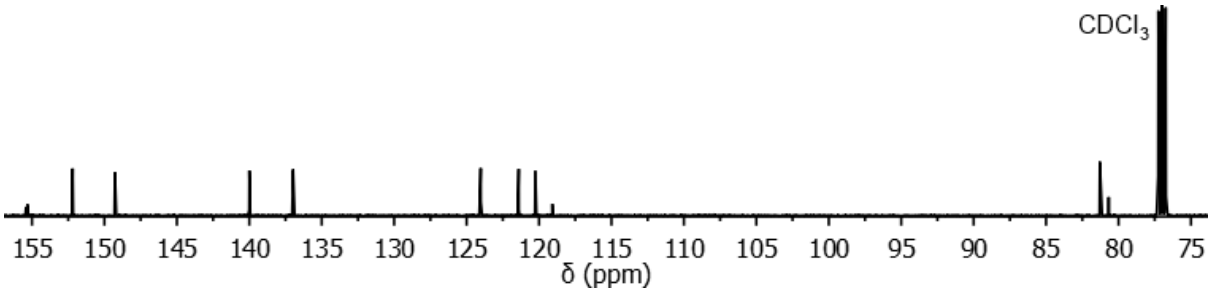

Figure S7 ^{13}C NMR spectrum (125 MHz, $CDCl_3$) of **S3**.

1.2.4 Synthesis of 1,1'-diiodoferrocene (S4)

The synthesis of this compound has previously been reported by Long in 19% yield.[3]

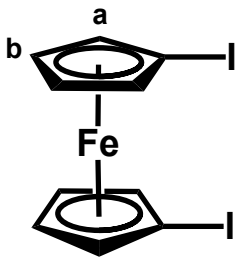

n-Butyllithium in hexanes (1.6 M, 100 mL, 160 mmol, 2.20 eq.) and TMEDA (24 mL, 160 mmol, 2.20 eq.) were added sequentially to dry ether (50 mL) under a nitrogen atmosphere, then stirred for 20 minutes. This was then added to a solution of ferrocene (13.5 g, 72.7 mmol, 1.00 eq.) in dry ether (100 mL) and stirred at room temperature overnight (16 hours). The resultant suspension of red di-lithiated ferrocene was cooled to -78 °C, and a solution of iodine (40.6 g, 160 mmol, 2.20 eq.) in dry ether (300 mL) was slowly added. The mixture was stirred at -78 °C for 30 minutes, then allowed to reach room temperature and stirred for a further 30 minutes. The reaction mixture was filtered through a Buchner funnel to remove any precipitates before the solvent was removed *in vacuo*. The crude product was extracted into *n*-hexane (200 mL) and washed with 0.5 M $FeCl_3$ solution (~15 x 200 mL) until the aqueous layer no longer turned green. The oxidative purification was monitored via ^{1}H NMR. The organic fraction was then passed through a silica plug, eluting with petrol, and the solvent removed *in vacuo* to give a deep red oil. Yield: 10.562 g, 33%. ^{1}H NMR (400 MHz, $CDCl_3$) δ 4.39 (s, 4H, H_a), 4.19 (s, 4H, H_b).

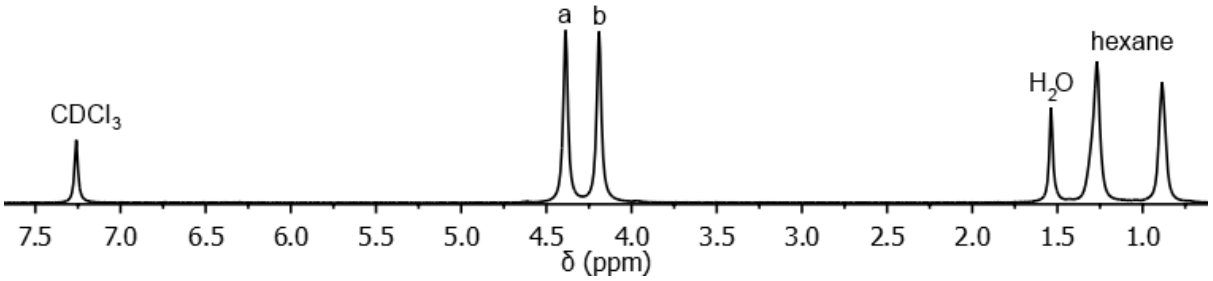

Figure S8 ^{1}H NMR spectrum (400 MHz, $CDCl_3$) of **S4**.

1.2.5 Synthesis of 1-(3-yl-ethynylpyridine)ferrocene (S9)

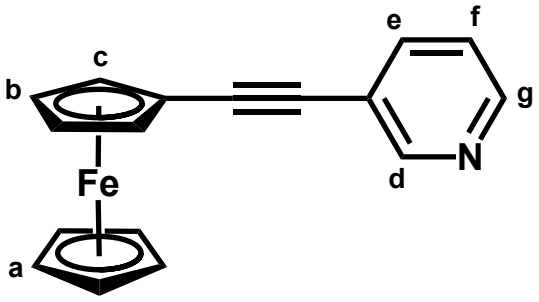

Ethynylferrocene (0.50 g, 2.38 mmol, 1.00 eq.), 3-bromopyridine (0.46 mL, 4.76 mmol, 2.00 eq.), CuI (0.091 g, 0.48 mmol, 0.20 eq.), $[Pd(CH_3CN)_2Cl_2]$ (0.037 g, 0.14 mmol, 0.06 eq.), and $[PH(^tBu)_3]BF_4$ (0.083 g, 0.29 mmol, 0.12 eq.) were combined under an argon atmosphere. Diisopropylamine (50 mL) was added, and the solution was refluxed for 24 hours. CH_2Cl_2 (50 mL) and NH_4OH/EDTA (50 mL) were added, and the aqueous layer extracted with CH_2Cl_2 (3 x 50 mL). The organic phase was washed with saturated aqueous NaCl (100 mL), dried over Na_2SO_4, and the solvent removed *in vacuo*. Column chromatography (silica gel, gradient 100% CH_2Cl_2, then 95:5 CH_2Cl_2/acetone, then 9:1 CH_2Cl_2/acetone) was used to obtain an orange solid. Yield: 0.571 g, 84%. Mp 98 ˚C; ^{1}H NMR (400 MHz, d_6-acetone) δ 8.67 (s, 1H, H_d), 8.53 (d, J = 3.8 Hz, 1H, H_g), 7.85(dt, J = 7.9, 1.8 Hz, 1H, H_e), 7.38 (dd, J = 7.8, 4.9 Hz, 1H, H_f), 4.55 (t, J = 1.8 Hz, 2H, H_c), 4.34 (t, J = 1.8 Hz, 2H, H_b), 4.27 (s, 5H, H_a); ^{13}C NMR (125 MHz, d_6-acetone) δ 152.6, 149.1, 138.7, 124.1, 121.8, 92.6, 83.0, 72.3, 70.8, 70.0, 65.2; IR: ν (cm^{-1}) 2205, 1405, 804, 702, 483; HRESI-MS (MeOH): m/z = 288.0464 [**S9**+H]$^+$ (calc. for $C_{17}H_{14}NFe$ 288.0470); UV-Vis (CH_2Cl_2) λ_{max} (ε/ L mol^{-1} cm^{-1}): 302 (12700), 354 (3100), 434 (800); Anal. Calc. for $C_{17}H_{13}NFe•0.25H_2O$: C, 70.01; H, 4.67; N, 4.80. Found: C, 69.98; H, 4.60; N, 4.85.

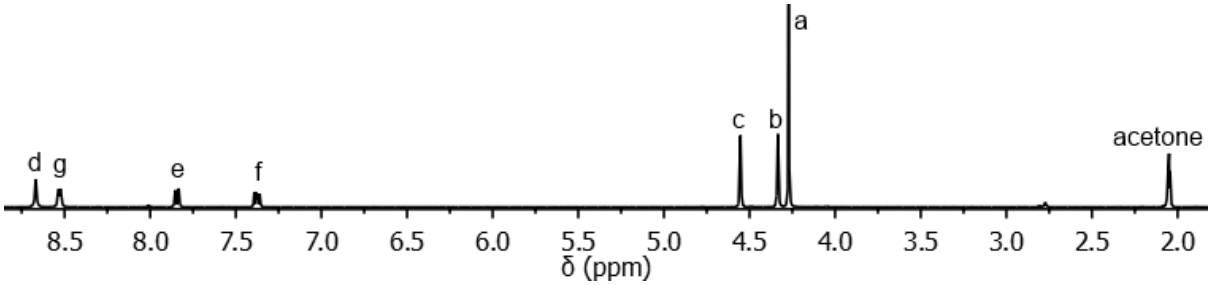

Figure S9 ^{1}H NMR spectrum (400 MHz, d_6-acetone) of **S9**.

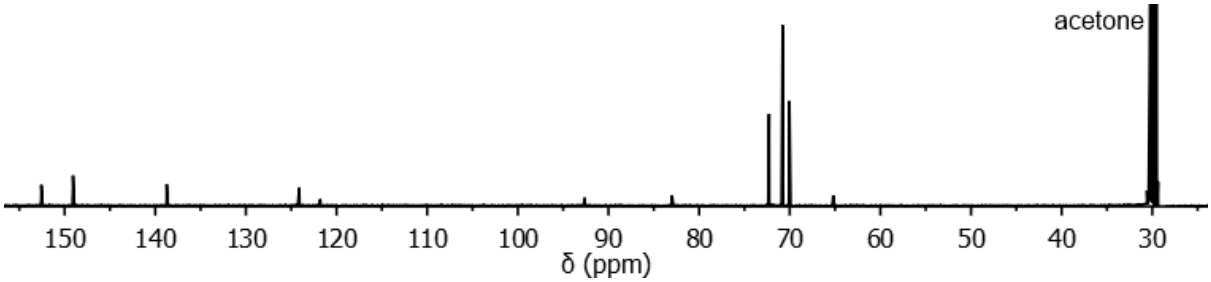

Figure S10 ^{13}C NMR spectrum (125 MHz, d_6-acetone) of **S9**.

1.2.6 Synthesis of 1-(3-yl-ethynylpyridine)-1'-iodo-ferrocene (S6)

The synthesis of this compound has previously been reported by Long in 72% yield.[4]

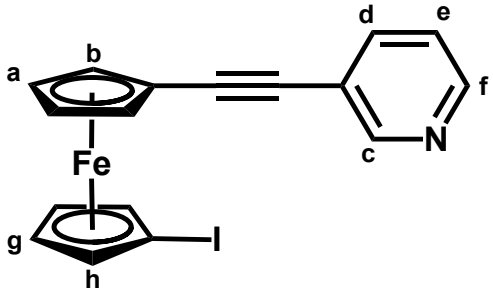

S4 (1.00 g, 2.28 mmol, 1.00 eq.), 3-ethynylpyridine (0.26 g, 2.51 mmol, 1.10 eq.), CuI (0.087 g, 0.46 mmol, 0.20 eq.), $[Pd(CH_3CN)_2Cl_2]$ (0.036 g, 0.14 mmol, 0.06 eq.), and $[PH(^tBu)_3]BF_4$ (0.080 g, 0.27 mmol, 0.12 eq.) were combined under an argon atmosphere. Diisopropylamine (20 mL) was added, and the solution was refluxed for 24 hours. CH_2Cl_2 (50 mL) and NH_4OH/EDTA (50 mL) were added, and the aqueous layer extracted with CH_2Cl_2 (3 x 50 mL). The organic phase was washed with saturated aqueous NaCl (100 mL), dried over Na_2SO_4, and the solvent removed *in vacuo*. Column chromatography (silica gel, gradient 100% CH_2Cl_2, then 9:1 CH_2Cl_2/acetone, then 4:1 CH_2Cl_2/acetone) was used to obtain the desired mono-substituted product as an orange solid (0.383 g, 41%), as well as the doubly-substituted byproduct (**S5**), also as an orange solid (0.240 g, 27%).Mp 102 ˚C; ^{1}H NMR (400 MHz, d_6-acetone) δ 8.71 (s, 1H, H_c), 8.55 (d, *J* = 4.4 Hz, 1H, H_f), 7.89 (dt, *J* = 7.7, 1.4 Hz, 1H, H_d), 7.39 (dd, *J* = 7.9, 4.9 Hz, 1H, H_e), 4.52 (t, *J* = 2.0 Hz, 2H, H_b or H_h), 4.51 (t, *J* = 1.7 Hz, 2H, H_b or H_h), 4.38 (t, *J* = 1.9 Hz, 2H, H_a or H_g), 4.34 (t, *J* = 1.9 Hz, 2H, H_a or H_g); ^{13}C NMR (125 MHz, d_6-acetone) δ 152.7, 149.3, 138.9, 124.1, 121.7, 91.3, 84.3, 77.4, 75.0, 72.9, 71.8, 67.7, 41.7; IR: ν (cm^{-1}) 2208, 1403, 1022, 800, 698, 482; HRESI-MS (MeOH) *m/z* = 413.9415 [**S6**+H]$^+$ (calc. for $C_{17}H_{13}FeIN$ 413.9437); Anal. Calc. for $C_{17}H_{12}FeIN•0.3(CH_3)_2CO$: C, 49.95; H, 3.23; N, 3.25. Found: C, 50.21; H, 3.07; N, 3.48.

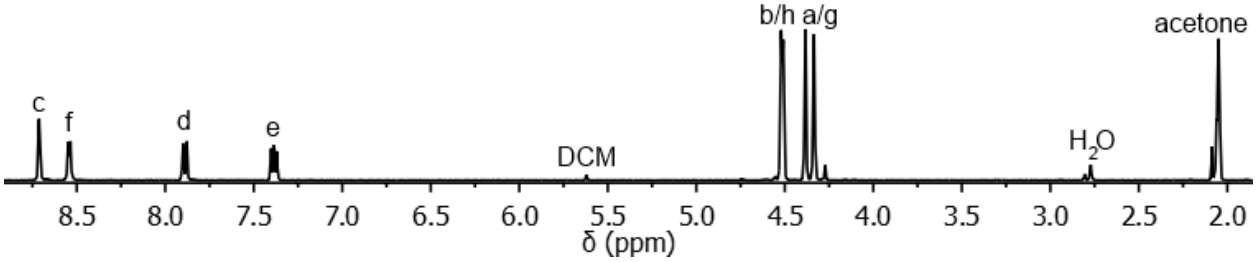

Figure S11 ^{1}H NMR spectrum (400 MHz, d_6-acetone) of **S6**.

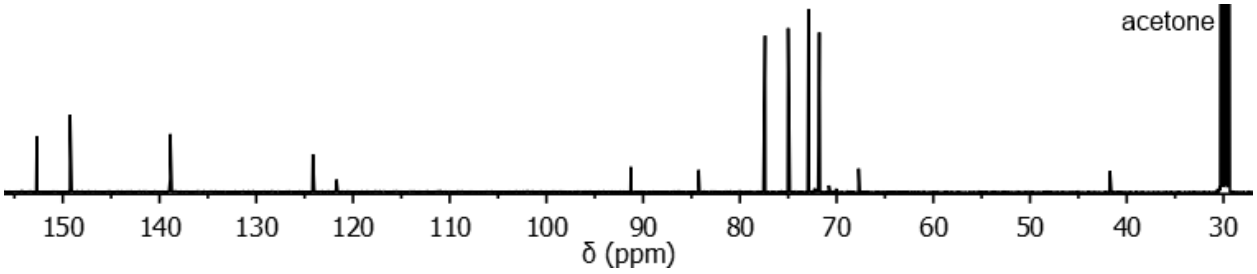

Figure S12 ^{13}C NMR spectrum (125 MHz, d_6-acetone) of **S6**.

1.2.7 Synthesis of 1,1'-di(3-yl-ethynylpyridine)ferrocene (S5)

The synthesis of this compound has previously been reported by Lindner in 30% yield,[5] and more recently by Long in 23% yield.[4]

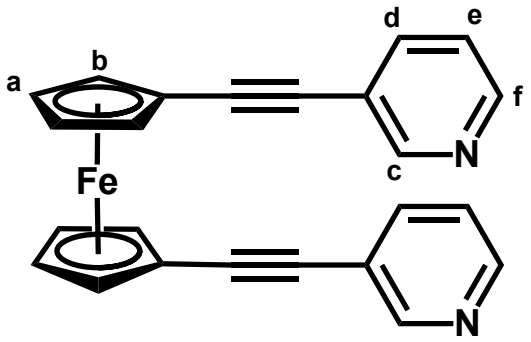

The synthesis of **S5** was inadvertent and it was isolated as a byproduct of the reaction to form **S6**. Mp 194 ˚C; ^{1}H NMR (400 MHz, d_6-acetone) δ 8.58 (s, 2H, H_c), 8.47 (d, J = 4.8 Hz, 2H, H_f), 7.71 (dt, J = 7.8, 1.7 Hz, 2H, H_d), 7.26 (dd, J = 7.9, 4.9 Hz, 2H, H_e), 4.63 (t, J = 1.7 Hz, 4H, H_b), 4.45 (t, J = 1.7 Hz, 4H, H_a); ^{13}C NMR (125 MHz, d_6-acetone) δ 152.5, 149.0, 138.6, 124.0, 121.6, 91.1, 84.2, 73.9, 72.0, 67.5; IR: ν (cm^{-1}) 2205, 1486, 1403, 1165, 1019, 799, 699, 497, 489, 433; HRESI-MS (MeOH) *m/z* = 389.0754 [**S5**+H]$^+$ (calc. for $C_{24}H_{17}FeN_2$ 389.0736), *m/z* = 411.0579 [**S5**+Na]$^+$ (calc. for $C_{24}H_{16}FeN_2Na$ 411.0555); UV-Vis (CH_2Cl_2) λ_{max} (ε/ L mol^{-1} cm^{-1}): 308 (21100), 456 (1500); Anal. Calc. for $C_{24}H_{16}FeN_2 \bullet 0.1H_2O$: C, 73.90; H, 4.19; N, 7.18. Found: C, 73.92; H, 4.13; N, 7.24.

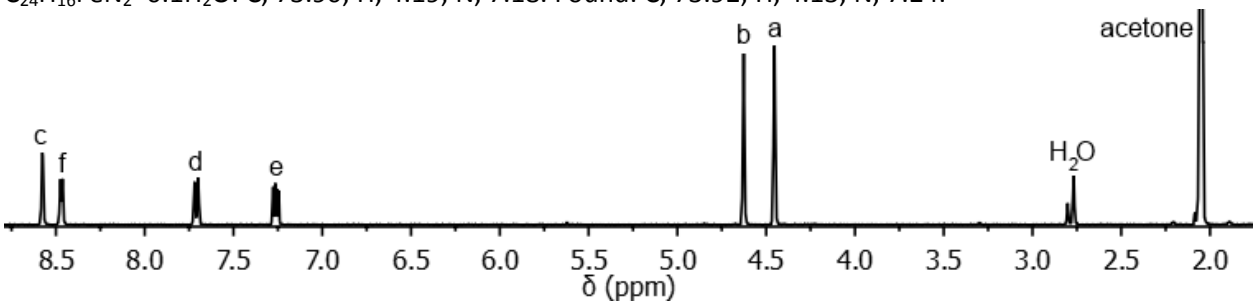

Figure S13 ^{1}H NMR spectrum (400 MHz, d_6-acetone) of **S5**.

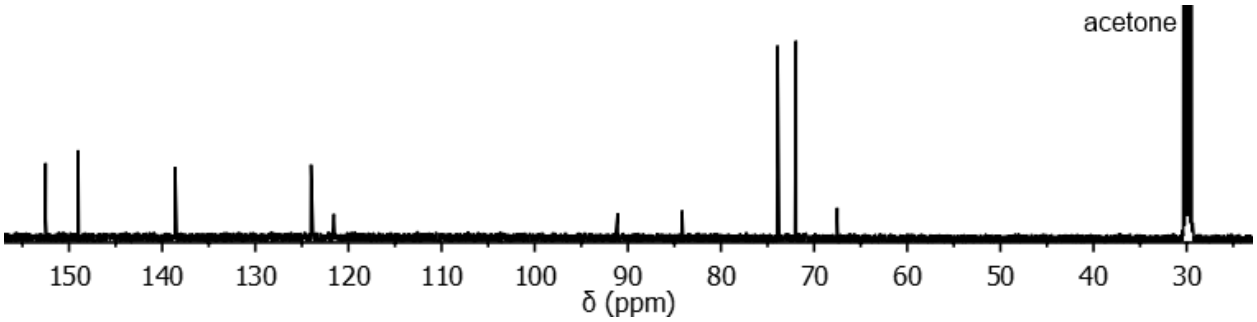

Figure S14 ^{13}C NMR spectrum (125 MHz, d_6-acetone) of **S5**.

1.2.8 Synthesis of 1-(5-yl-ethynyl-2,2'-bipyridine)ferrocene (2a)

The synthesis of this compound has previously been reported by Lang in 68% yield.[6]

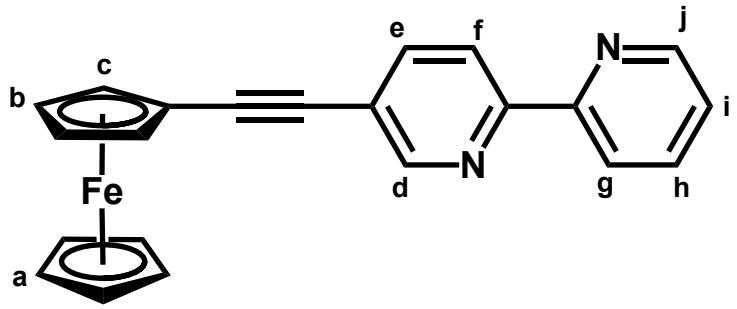

Ethynylferrocene (0.30 g, 1.428 mmol, 1.10 eq.), **S1** (0.305 g, 1.298 mmol, 1.00 eq.), CuI (0.025 g, 0.130 mmol, 0.10 eq.), and $[PdCl_2(PPh_3)_2]$ (0.027 g, 0.039 mmol, 0.03 eq.) were combined under a nitrogen atmosphere. Dry triethylamine (2.2 mL, 15.58 mmol, 12.00 eq.) and dry THF (50 mL) were added and the solution refluxed overnight (16 hours). CH_2Cl_2 (50 mL) and NH_4OH/EDTA (100 mL) were added, and the aqueous layer extracted with CH_2Cl_2 (2 x 50 mL). The organic phase was washed with saturated aqueous NaCl (2 x 50 mL), dried over Na_2SO_4, and the solvent removed *in vacuo*. Column chromatography (silica gel, gradient 100% CH_2Cl_2, then 99:1 CH_2Cl_2/acetone, then 98:2 CH_2Cl_2/acetone) was used to obtain the product as an orange solid (0.420 g, 89%). Mp 163 ˚C; ^{1}H NMR (400 MHz, $CDCl_3$) δ 8.76 (d, *J* = 1.3 Hz, 1H, H_d), 8.69 (d, *J* = 4.3 Hz, 1H, H_j), 8.41 (d, *J* = 8.0 Hz, 1H, H_g), 8.38 (d, *J* = 8.2 Hz, 1H, H_f), 7.89 (dd, *J* = 8.3, 2.1 Hz, 1H, H_e), 7.82 (dt, *J* = 7.9, 1.8 Hz, 1H, H_h), 7.31 (ddd, *J* = 7.4, 4.8, 1.0 Hz, 1H, H_i), 4.55 (t, *J* = 1.9 Hz, 2H, H_c), 4.29 (t, *J* = 1.9 Hz, 2H, H_b), 4.27 (s, 5H, H_a); ^{13}C NMR (125 MHz, $CDCl_3$) δ 155.8, 154.3, 151.6, 149.4, 139.2, 137.1, 123.9, 121.4, 121.2, 120.4, 93.3, 83.0, 71.7, 70.2, 69.3, 64.5; IR: ν (cm^{-1}) 1587, 1467, 1449, 821, 798, 755, 504, 486; HRESI-MS (MeOH) *m/z* = 365.0728 [**2a**+H]$^+$ (calc. for $C_{22}H_{17}FeN_2$ 365.0736), *m/z* = 387.0550 [**2a**+Na]$^+$ (calc. for $C_{22}H_{16}FeN_2Na$ 387.0555); UV-Vis ($CHCl_3$) λ_{max} (ε/ L mol^{-1} cm^{-1}): 317 (36500), 368 (6300), 447 (1900); Anal. Calc. for $C_{22}H_{16}FeN_2 \bullet 0.25H_2O$: C, 71.66; H, 4.51; N, 7.60. Found: C, 71.54; H, 4.41; N, 7.33.

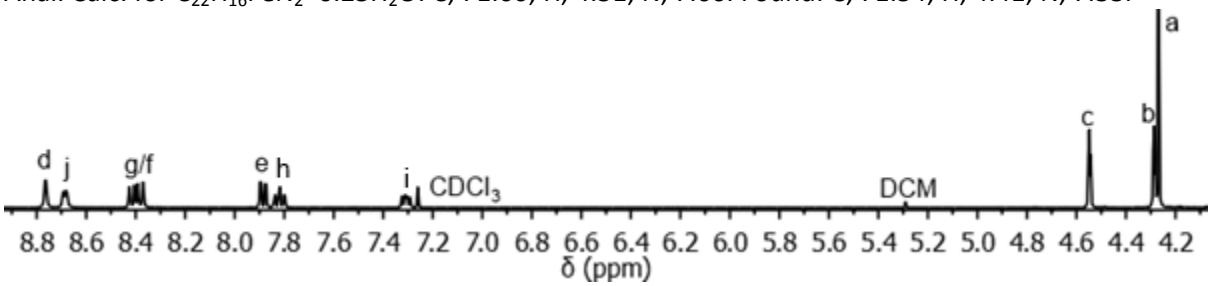

Figure S15 ^{1}H NMR spectrum (400 MHz, $CDCl_3$) of **2a**.

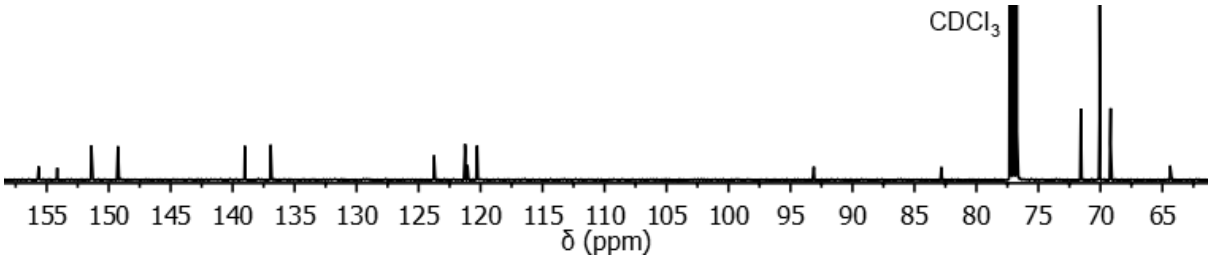

Figure S16 ^{13}C NMR spectrum (125 MHz, $CDCl_3$) of **2a**.

1.2.9 Synthesis of 1-(5-yl-ethynyl-2,2'-bipyridine)-1'-iodo-ferrocene (S7)

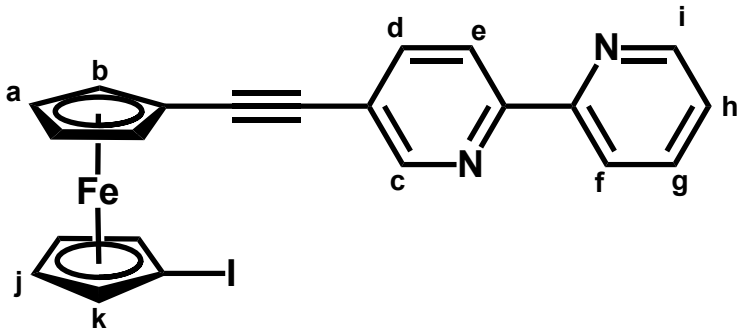

S4 (0.663 g, 1.513 mmol, 1.00 eq.), **S3** (0.300 g, 1.665 mmol, 1.10 eq.), CuI (0.058 g, 0.303 mmol, 0.20 eq.), $[Pd(CH_3CN)_2Cl_2]$ (0.024 g, 0.091 mmol, 0.06 eq.), and $[PH(^tBu)_3]BF_4$ (0.053 g, 0.182 mmol, 0.12 eq.) were combined under an argon atmosphere. Diisopropylamine (20 mL) was added, and the solution was refluxed for 24 hours. CH_2Cl_2 (50 mL) and NH_4OH/EDTA (50 mL) were added, and the aqueous layer extracted with CH_2Cl_2 (3 x 50 mL). The organic phase was washed with saturated aqueous NaCl (100 mL), dried over Na_2SO_4, and the solvent removed *in vacuo*. Column chromatography (silica gel, gradient 100% $CHCl_3$, then 95:5 $CHCl_3$/acetone, then 4:1 $CHCl_3$/acetone) was used to obtain the desired mono-substituted product as an orange solid (0.309 g, 42%). Mp 106 ˚C; ^{1}H NMR (400 MHz, $CDCl_3$) δ 8.80 (d, *J* = 2.0 Hz, 1H, H_c), 8.69 (d, *J* = 4.8 Hz, 1H, H_i), 8.41 (d, *J* = 8.0 Hz, 1H, H_f), 8.38 (d, *J* = 8.3 Hz, 1H, H_e), 7.91 (dd, *J* = 8.3, 2.1 Hz, 1H, H_d), 7.82 (dt, *J* = 8.0, 1.8 Hz, 1H, H_g), 7.31 (ddd, *J* = 7.4, 5.2, 1.0 Hz, 1H, H_h), 4.51 (t, *J* = 2.0 Hz, 2H, H_b or H_k), 4.47 (t, *J* = 1.9 Hz, 2H, H_b or H_k), 4.30 (t, *J* = 1.9 Hz, 2H, H_a or H_j), 4.25 (t, *J* = 1.9 Hz, 2H, H_a or H_j); ^{13}C NMR (125 MHz, $CDCl_3$) δ 155.7, 154.5, 151.6, 149.4, 139.2, 137.1, 123.9, 121.4, 121.0, 120.4, 91.9, 84.2, 76.6, 74.3, 72.4, 71.0, 70.2, 67.0; IR: ν (cm^{-1}) 2205, 1585, 1571, 1543, 1448, 1431, 1017, 846, 793, 742, 478; HRESI-MS (MeOH) *m/z* = 490.9730 [**S7**+H]$^+$ (calc. for $C_{22}H_{16}FeIN_2$ 490.9702), *m/z* = 512.9538 [**S7**+Na]$^+$ (calc. for $C_{22}H_{15}FeIN_2Na$ 512.9522); Anal. Calc. for $C_{22}H_{15}FeN_2I$: C, 53.91; H, 3.08; N, 5.72. Found: C, 53.83; H, 3.04; N, 5.64.

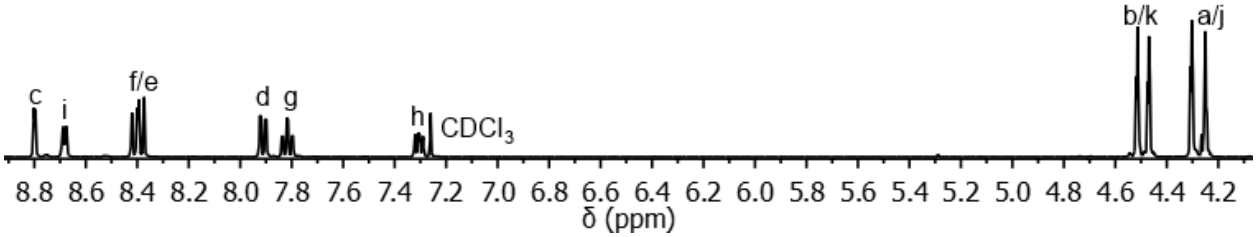

Figure S17 ^{1}H NMR spectrum (400 MHz, $CDCl_3$) of **S7**.

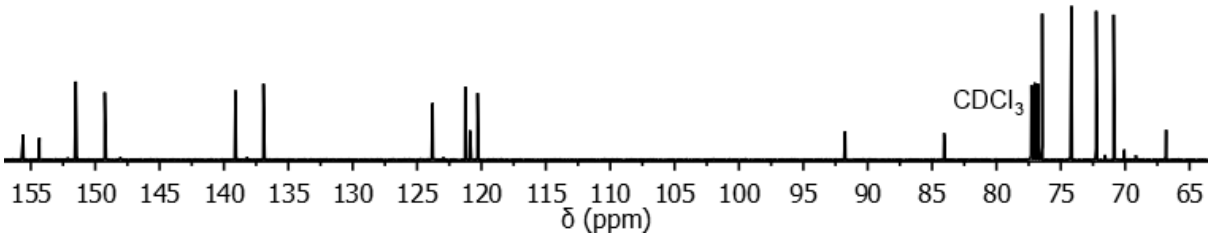

Figure S18 ^{13}C NMR spectrum (125 MHz, $CDCl_3$) of **S7**.

1.2.10 Synthesis of 1,1'-di(5-yl-ethynyl-2,2'-bipyridine)ferrocene (1a)

The synthesis of this compound has previously been reported by Lindner in 19% yield.[7]

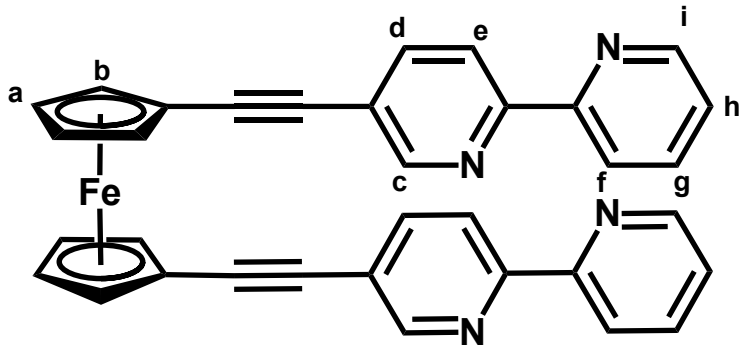

S4 (0.310 g, 0.708 mmol, 1.00 eq.), **S3** (0.281 g, 1.558 mmol, 2.20 eq.), CuI (0.027 g, 0.142 mmol, 0.20 eq.), $[Pd(CH_3CN)_2Cl_2]$ (0.011 g, 0.042 mmol, 0.06 eq.), and $[PH(^tBu)_3]BF_4$ (0.025 g, 0.084 mmol, 0.12 eq.) were combined under an argon atmosphere. Diisopropylamine (20 mL) was added, and the solution was refluxed for 24 hours. CH_2Cl_2 (50 mL) and NH_4OH/EDTA (50 mL) were added, and the aqueous layer extracted with CH_2Cl_2 (5 x 50 mL). The organic phase was washed with saturated aqueous NaCl (200 mL), dried over Na_2SO_4, and the solvent removed *in vacuo*. Column chromatography (silica gel, gradient 100% $CHCl_3$, then 95:5 $CHCl_3$/acetone, then 4:1 $CHCl_3$/acetone) was used to obtain the desired mono-substituted product as an orange solid (0.120 g, 31%). Mp >230 ˚C; ^{1}H NMR (400 MHz, $CDCl_3$) δ 8.61 (s, 2H, H_c), 8.57 (d, *J* = 4.3 Hz, 2H, H_i), 8.24 (d, *J* = 8.2 Hz, 2H, H_f), 8.20 (d, *J* = 8.3 Hz, 2H, H_e), 7.73 (dd, *J* = 8.3, 2.1 Hz, 2H, H_d), 7.69 (dt, *J* = 7.8, 1.6 Hz, 2H, H_g), 7.23 (dd, *J* = 6.9, 5.2 Hz, 1H, H_h), 4.62 (t, *J* = 1.8 Hz, 4H, H_b), 4.39 (t, *J* = 1.9 Hz, 4H, H_a); ^{13}C NMR (125 MHz, $CDCl_3$) δ 155.6, 154.1, 151.4, 149.2, 138.9, 136.9, 123.7, 121.3, 120.9, 120.3, 91.4, 84.5, 73.1, 71.1, 67.2; IR: ν (cm^{-1}) 2206, 1586, 1570, 1538, 1449, 1431, 1367, 1021, 793, 739, 510, 490; HRESI-MS (MeOH) *m/z* = 565.1116 [**1a**+Na]$^+$ (calc. for $C_{34}H_{22}FeN_4Na$ 565.1087); UV-Vis ($CHCl_3$) λ_{max} (ε/ L mol^{-1} cm^{-1}): 314 (74000), 337 (52700), 372 (15100), 432 (4000); Anal. Calc. for $C_{34}H_{22}FeN_4 \bullet 0.75H_2O$: C, 73.46; H, 4.26; N, 10.08. Found: C, 73.49; H, 3.98; N, 10.20.

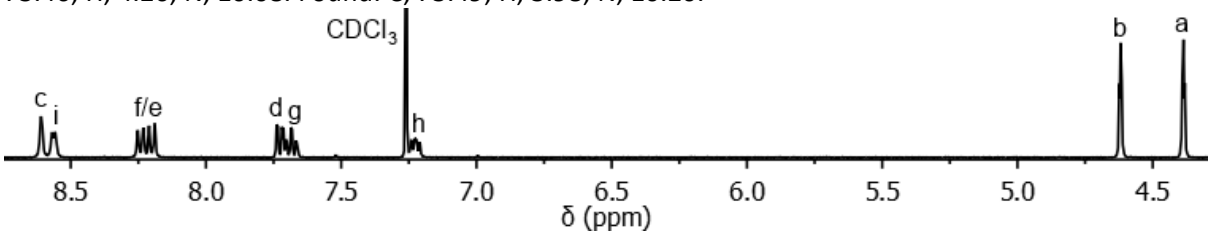

Figure S19 ^{1}H NMR spectrum (400 MHz, $CDCl_3$) of **1a**.

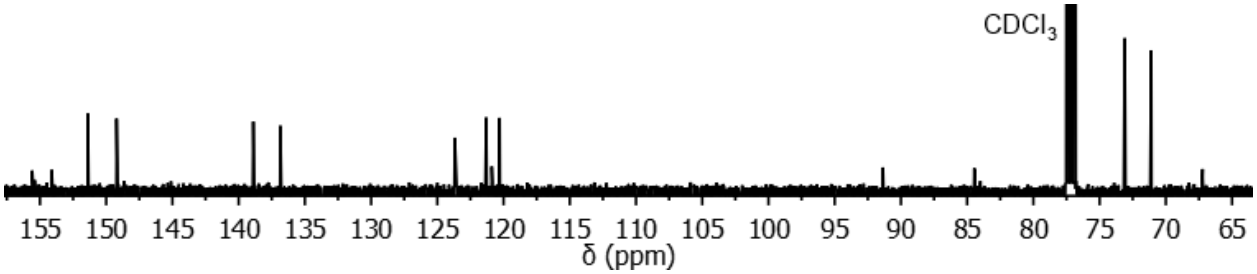

Figure S20 ^{13}C NMR spectrum (125 MHz, $CDCl_3$) of **1a**.

1.2.11 Synthesis of 1-(5-yl-ethynyl-2,2'-bipyridine)-1'-(3-yl-ethynylpyridine)ferrocene (S8)

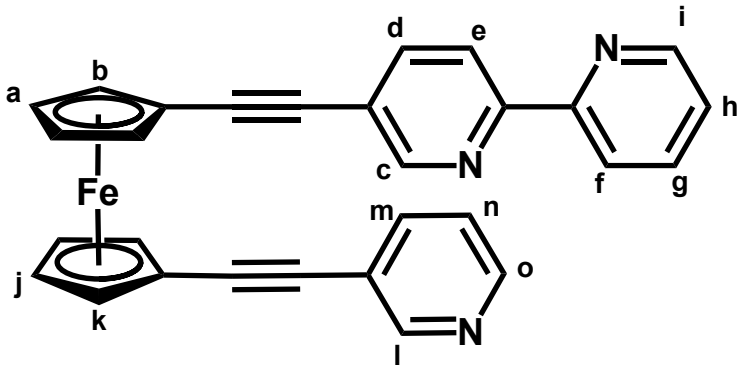

Method A: **S7** (0.200 g, 0.408 mmol, 1.00 eq.), 3-ethynylpyridine (0.046 g, 0.449 mmol, 1.10 eq.), CuI (0.016 g, 0.082 mmol, 0.20 eq.), $[Pd(CH_3CN)_2Cl_2]$ (0.00635 g, 0.024 mmol, 0.06 eq.), and $[PH(^tBu)_3]BF_4$ (0.014 g, 0.049 mmol, 0.12 eq.) were combined under an argon atmosphere. Diisopropylamine (20 mL) was added, and the solution was refluxed for 24 hours. CH_2Cl_2 (50 mL) and NH_4OH/EDTA (50 mL) were added, and the aqueous layer extracted with CH_2Cl_2 (3 x 50 mL). The organic phase was washed with saturated aqueous NaCl (100 mL), dried over Na_2SO_4, and the solvent removed *in vacuo*. Column chromatography (silica gel, gradient 100% CH_2Cl_2, then 95:5 CH_2Cl_2/acetone, then 4:1 CH_2Cl_2/acetone) was used to obtain the product as an orange solid (0.113 g, 60%).

Method B: **S6** (0.500 g, 1.211 mmol, 1.00 eq.), **S3** (0.262 g, 1.453 mmol, 1.20 eq.), CuI (0.046 g, 0.242 mmol, 0.20 eq.), $[Pd(CH_3CN)_2Cl_2]$ (0.019 g, 0.073 mmol, 0.06 eq.), and $[PH(^tBu)_3]BF_4$ (0.042 g, 0.145 mmol, 0.12 eq.) were combined under an argon atmosphere. Diisopropylamine (40 mL) was added, and the solution was refluxed for 24 hours. CH_2Cl_2 (50 mL) and NH_4OH/EDTA (50 mL) were added, and the aqueous layer extracted with CH_2Cl_2 (3 x 50 mL). The organic phase was washed with saturated aqueous NaCl (100 mL), dried over Na_2SO_4, and the solvent removed *in vacuo*. Column chromatography (silica gel, gradient 100% CH_2Cl_2, then 95:5 CH_2Cl_2/acetone, then 4:1 CH_2Cl_2/acetone) was used to obtain the product as an orange solid (0.248 g, 44%). Although the yield was slightly lower using method B, the product was easier to separate from the reaction mixture.

Mp 133 ˚C; ^{1}H NMR (400 MHz, d_6-acetone) δ 8.66 (ddd, *J* = 4.8, 1.7, 0.9 Hz, 1H, H_i), 8.59 (dd, *J* = 2.1, 0.8 Hz, 1H, H_c), 8.54 (d, *J* = 1.5 Hz, 1H, H_l), 8.41 (dt, *J* = 7.9, 0.9 Hz, 1H, H_f), 8.35 (dd, *J* = 4.8, 1.6 Hz, 1H, H_o), 8.32 (dd, *J* = 8.2, 0.8 Hz, 1H, H_e), 7.90 (dt, *J* = 7.6, 1.8 Hz, 1H, H_g), 7.80 (dd, *J* = 8.3, 2.2 Hz, 1H, H_d), 7.67 (dt, *J* = 7.9, 1.8 Hz, 1H, H_m), 7.39 (ddd, *J* = 7.5, 4.8, 1.2 Hz, 1H, H_h), 7.17 (ddd, *J* = 7.9, 4.8, 0.8 Hz, 1H, H_n), 4.62 (t, *J* = 1.9 Hz, 2H, H_b or H_k), 4.61 (t, *J* = 1.9 Hz, 2H, H_b or H_k), 4.44 (t, *J* = 1.8 Hz, 2H, H_a or H_j), 4.43 (t, *J* = 1.8 Hz, 2H, H_a or H_j); ^{13}C NMR (125 MHz, $CDCl_3$) δ 155.7, 154.3, 152.1, 151.4, 149.4, 148.0, 139.0, 138.1, 137.1, 123.9, 123.0, 121.4, 121.0, 120.9, 120.4, 91.7, 90.6, 84.1, 83.7, 73.2, 73.2, 71.3, 71.2, 66.8, 66.8; IR: ν (cm^{-1}) 2208, 1673, 1586, 1468, 794, 744, 702, 496, 439; HRESI-MS (MeOH) *m/z* = 466.0979 [**S8**+H]$^+$ (calc. for $C_{29}H_{20}FeN_3$ 466.1001), *m/z* = 488.0802 [**S8**+Na]$^+$ (calc. for $C_{29}H_{19}FeN_3Na$ 488.0821); UV-Vis (acetone) λ_{max} (ε/ L mol^{-1} cm^{-1}): 371 (8500), 451 (2300); Anal. Calc. for $C_{29}H_{19}FeN_3$•0.25CH_3CN: C, 74.50; H, 4.19; N, 9.57. Found: C, 74.66; H, 4.27; N, 9.73.

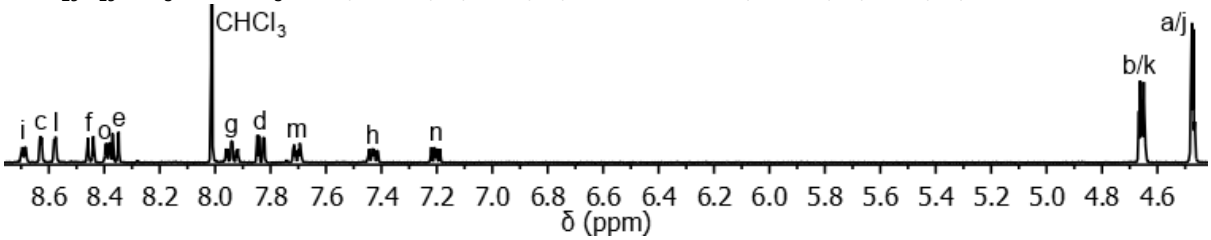

Figure S21 ^{1}H NMR spectrum (400 MHz, d_6-acetone) of **S8**.

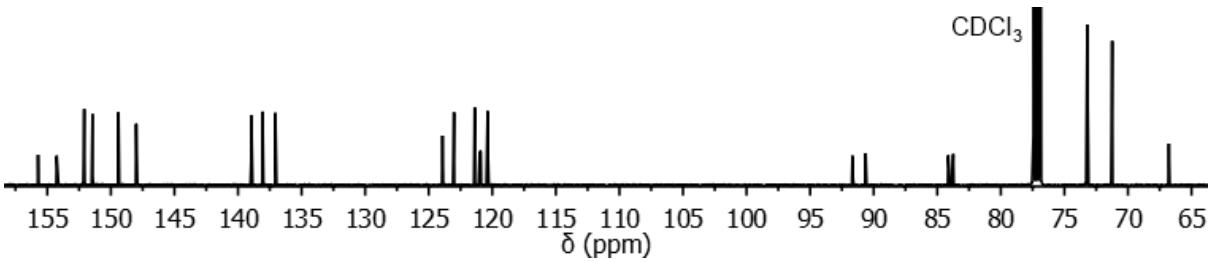

Figure S22 ^{13}C NMR spectrum (125 MHz, $CDCl_3$) of **S8**.

1.2.12 Synthesis of 6,6'-dimesityl-2,2'-bipyridine (3)

The synthesis of this compound has previously been reported by Schmittel in 72% yield.[8]

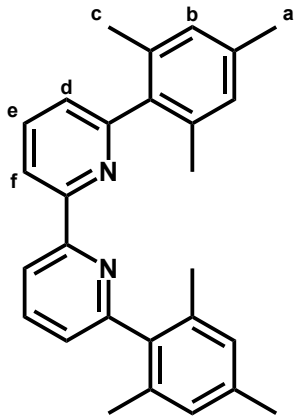

Under a nitrogen atmosphere, 6,6'-dibromo-2,2'-bipyridine (0.20 g, 0.64 mmol, 1.00 eq.) and *tetrakis*(triphenylphosphine)palladium(0) (0.006 g, 5.2 µmol, 0.008 eq.) were dissolved in degassed boiling toluene. A solution of mesitylboronic acid (0.25 g, 1.52 mmol, 2.40 eq.) in methanol (5 mL) and 2 M Na_2CO_3 (8 mL, 16.0 mmol, 25.1 eq.) were added, and the mixture refluxed for four hours. An additional 0.1 g of mesitylboronic acid was then added, and heating was continued for a further three days. After cooling, the solvent layers were separated, and the organic layer washed with a saturated aqueous solution of Na_2CO_3 containing a small amount of ammonia. The aqueous layer was extracted with CH_2Cl_2 (2 x 50 mL), which in turn was washed with the Na_2CO_3 solution. The organic layers were combined, dried over Na_2SO_4 and the solvent removed *in vacuo*. Column chromatography (silica, CH_2Cl_2) was used to isolate the white product (0.199 g, 80%). Mp 211 ˚C; ^{1}H NMR (400 MHz, $CDCl_3$) δ 8.38 (d, *J* = 7.9 Hz, 2H, H_f), 7.80 (t, *J* = 7.8 Hz, 2H, H_e), 7.21 (d, *J* = 7.6 Hz, 2H, H_d), 6.98 (s, 4H, H_b), 2.35 (s, 6H, H_a), 2.12 (s, 12H, H_c); ^{13}C NMR (125 MHz, $CDCl_3$) δ 159.2, 156.4, 138.2, 137.6, 137.0, 136.1, 128.6, 124.8, 119.3, 21.3, 20.6; IR: ν (cm^{-1}) 2915, 1561, 1438, 851, 815, 631; HRESI-MS (MeOH): *m/z* = 393.2329 [**3**+H]$^+$ (calc. for $C_{28}H_{28}N_2H$ 393.23), *m/z* = 415.2158 [**3**+Na]$^+$ (calc. for $C_{28}H_{28}N_2Na$ 415.53); Anal. Calc. for $C_{28}H_{28}N_2$: C, 85.67; H, 7.19; N, 7.14. Found: C, 85.43; H, 7.28; N, 7.28.

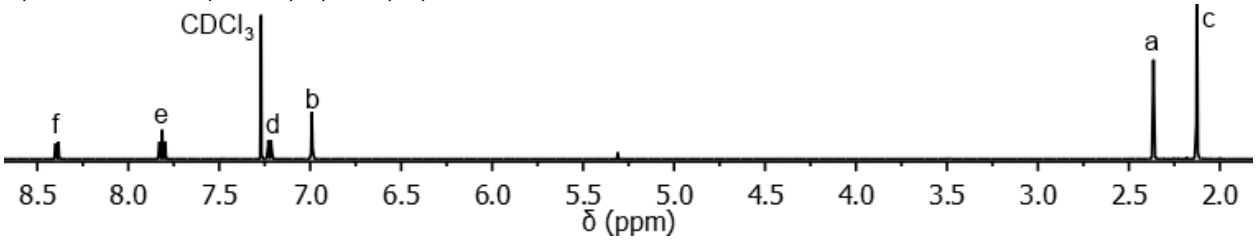

Figure S23 ^{1}H NMR spectrum (400 MHz, $CDCl_3$) of **3**.

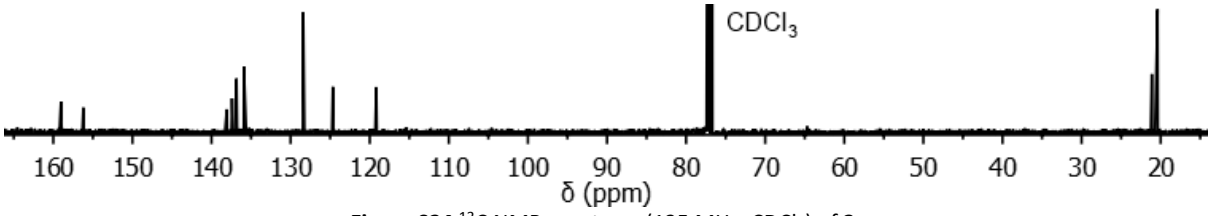

Figure S24 ^{13}C NMR spectrum (125 MHz, $CDCl_3$) of **3**.

1.3 Methylation

1.3.1 Synthesis of [1-(N-methyl-3-yl-ethynylpyridine)ferrocene]PF_6 (2b)

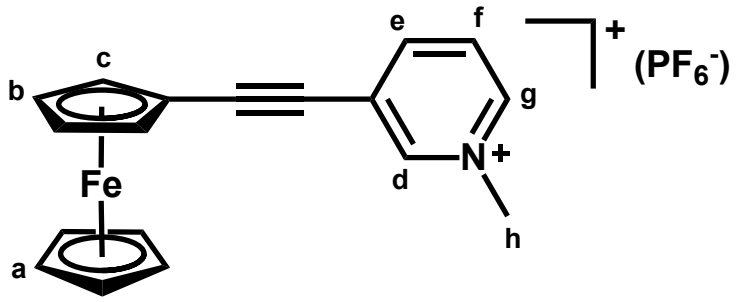

Methyl iodide (0.867 mL, 13.93 mmol, 20.00 eq.) was added to a solution of **S9** (0.2 g, 0.697 mmol, 1.00 eq.) in CH_2Cl_2 (2 mL) and the mixture stirred at room temperature for two days. The solvent and excess methyl iodide was removed *in vacuo*, then the residue taken up in acetone. $AgPF_6$ (0.176 g, 0.697 mmol, 1.00 eq.) was added, the resultant AgI precipitate filtered out through celite, and the solvent again removed *in vacuo*. The crude product was recrystallized from MeOH/H_2O to give deep red crystals. Yield: 0.130 g, 42% (quantitative by crude NMR). Mp 170 ˚C; ^{1}H NMR (400 MHz, d_6-acetone) δ 9.28 (s, 1H, H_d), 9.07 (d, *J* = 6.3 Hz, 1H, H_g), 8.71 (d, *J* = 8.7 Hz, 1H, H_e), 8.25 (t, *J* = 7.0 Hz, 1H, H_f), 4.67 (s, 3H, H_h), 4.64 (t, *J* = 1.9 Hz, 1H, H_c), 4.45 (t, *J* = 1.9 Hz, 1H, H_b), 1.30 (s, 5H, H_a); ^{13}C NMR (125 MHz, d_6-acetone) δ 148.2, 147.1, 144.7, 129.0, 126.2, 99.3, 79.4, 72.8, 71.1, 71.0, 62.7, 49.4; IR: ν (cm^{-1}) 3104, 2217, 1514, 1210, 816, 671, 555, 506, 487; HRESI-MS (MeOH) *m/z* = 302.0604 [**2b**-PF_6]$^+$ (calc. for $C_{18}H_{16}FeN$ 302.0627); UV-Vis (CH_2Cl_2) λ_{max} (ε/ L mol^{-1} cm^{-1}): 314 (3600), 508 (600); Anal. Calc. for $C_{18}H_{16}FeNPF_6$: C, 48.35; H, 3.61; N, 3.13. Found: C, 48.63; H, 3.39; N, 3.12.

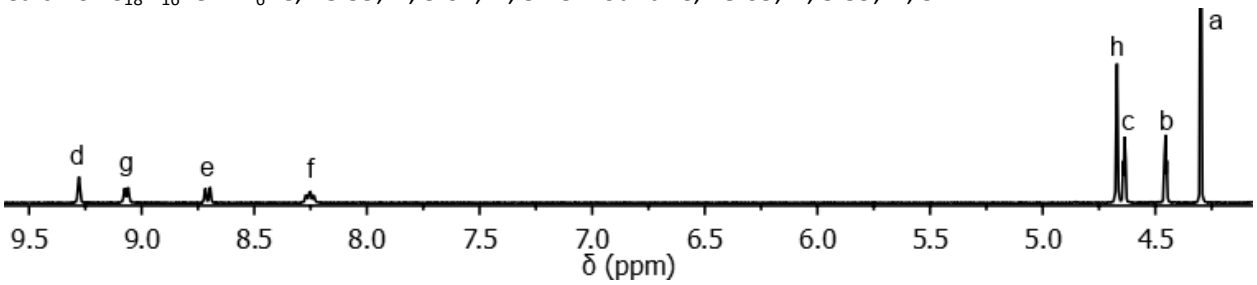

Figure S25 ^{1}H NMR spectrum (400 MHz, d_6-acetone) of **2b**.

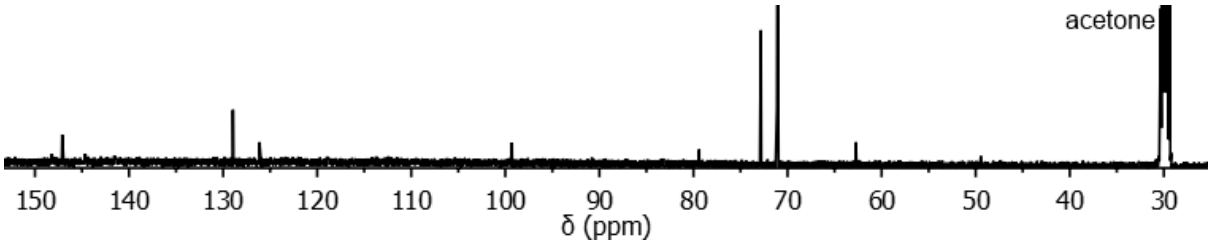

Figure S26 ^{13}C NMR spectrum (125 MHz, d_6-acetone) of **2b**.

1.3.2 Synthesis of [1-(5-yl-ethynyl-2,2'-bipyridine)-1'-(N-methyl-3-yl-ethynylpyridine)ferrocene]PF_6 (1b)

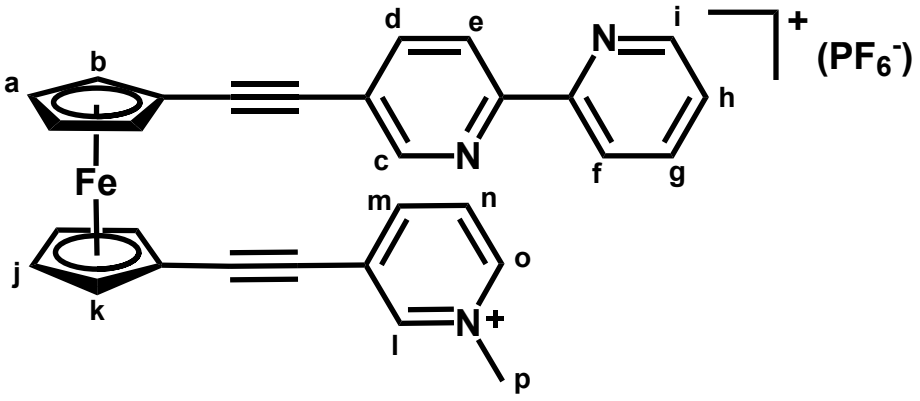

Under an argon atmosphere, methyl iodide (0.124 mL, 2.149 mmol, 20.00 eq.) was added to a solution of **S8** (0.05 g, 0.107 mmol, 1.00 eq.) in CH_2Cl_2 (2 mL) and the mixture stirred at room temperature for two days. The solvent and excess methyl iodide was removed *in vacuo*, then the residue taken up in acetone. $AgPF_6$ (0.027 g, 0.107 mmol, 1.00 eq.) was added, the resultant AgI precipitate filtered out through celite, and the solvent again removed *in vacuo*. The product was isolated as a deep red solid. Yield: 0.061 g, 91%. Mp >230 ˚C; ^{1}H NMR (400 MHz, d_6-acetone) δ 9.14 (s, 1H, H_l), 8.81 (d, *J* = 6.1 Hz, 1H, H_o), 8.73 (ddd, *J* = 4.7, 1.7, 0.9 Hz, 1H, H_i), 8.56 (dd, *J* = 2.2, 0.8 Hz, 1H, H_c), 8.49 (d, *J* = 8.0 Hz, 1H, H_m), 8.44 (dt, *J* = 8.0, 1.0 Hz, 1H, H_f), 8.33 (dd, *J* = 8.2, 0.8 Hz, 1H, H_e), 7.99-7.95 (m, 2H, $H_{i/n}$), 7.83 (dd, *J* = 8.2, 2.2 Hz, 1H, H_d), 7.47 (ddd, *J* = 7.5, 4.8, 1.2 Hz, 1H, H_h), 4.72 (t, *J* = 1.9 Hz, 2H, H_b or H_k), 4.69 (t, *J* = 1.9 Hz, 2H, H_b or H_k), 4.58 (t, *J* = 1.9 Hz, 2H, H_a or H_j), 4.51 (t, *J* = 1.9 Hz, 2H, H_a or H_j), 4.51 (s, 3H, H_p); ^{13}C NMR (125 MHz, d_6-acetone) δ 156.0, 155.1, 151.9, 150.4, 147.9, 146.7, 144.3, 139.7, 138.1, 128.9, 126.2, 125.2, 121.7, 120.8, 110.9, 97.5, 91.8, 84.9, 80.9, 74.2, 73.9, 72.7, 72.1, 68.3, 65.8, 49.3; IR: ν (cm^{-1}) 3081, 2209, 1297, 1133, 1025, 822, 556, 492; HRESI-MS (MeOH) *m/z* = 480.1159 [**1b**-PF_6]$^+$ (calc. for $C_{30}H_{22}FeN_3$ 480.1159); UV-Vis (acetone) λ_{max} (ε/ L mol^{-1} cm^{-1}): 454 (3100); Anal. Calc. for $C_{30}H_{22}FeN_3PF_6 \bullet H_2O$: C, 56.01; H, 3.76; N, 6.53. Found: C, 55.71; H, 3.84; N, 6.43.

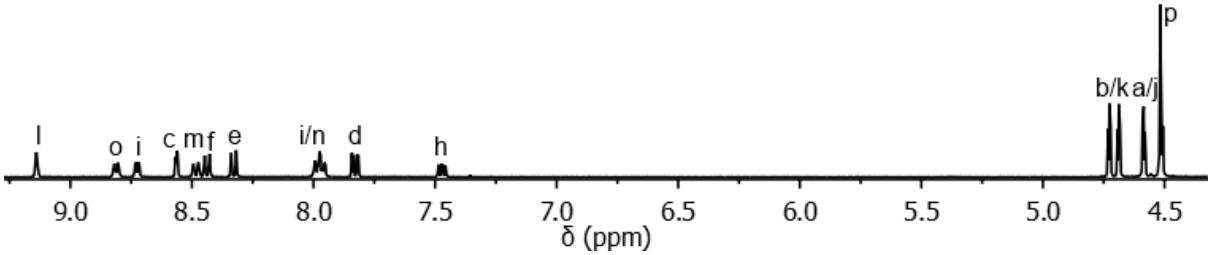

Figure S27 ^{1}H NMR spectrum (400 MHz, d_6-acetone) of **1b**.

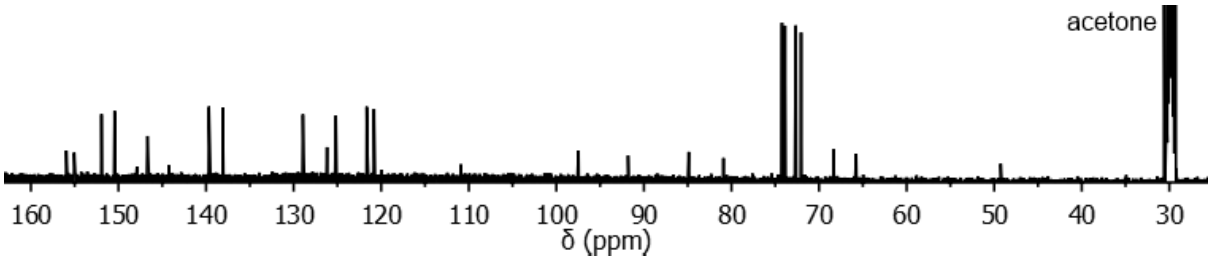

Figure S28 ^{13}C NMR spectrum (125 MHz, d_6-acetone) of **1b**.

1.4 Copper(I) Complexation

1.4.1 [Cu(6,6'-dimesityl-2,2'-bipyridine)(MeCN)$_2$]PF$_6$ ([Cu(3)(CH$_3$CN)$_2$]PF$_6$)

The synthesis of this compound has previously been reported by Schmittel in quantitative yield.[8]

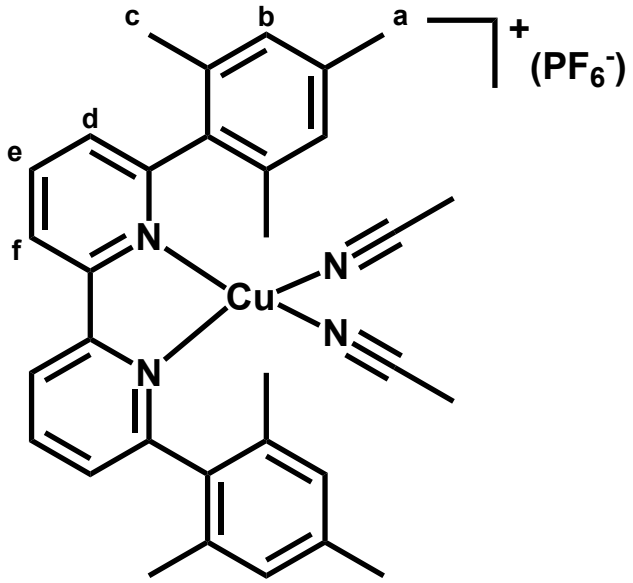

To a solution of [Cu(MeCN)$_4$]PF$_6$ (24 mg, 0.064 mmol, 1.00 eq.) in CD$_3$CN (0.75 mL) was added a solution of **3** (25 mg, 0.064 mmol, 1.00 eq.) in CD$_3$CN (0.75 mL). The mixture was stirred for 15 minutes, the resulting yellow solution subjected to ^{1}H NMR spectroscopy and mass spectrometry, and the complex was found to form in quantitative yield. ^{1}H NMR (400 MHz, CD$_3$CN) δ 8.34 (d, *J* = 8.1 Hz, 2H, H$_f$), 8.15 (t, *J* = 7.8 Hz, 2H, H$_e$), 7.52 (d, *J* = 7.6 Hz, 2H, H$_d$), 6.94 (s, 4H, H$_b$), 2.28 (s, 6H, H$_a$), 1.91 (s, 12H, H$_c$). HRESI-MS (MeOH): *m/z* = 496.1739 [Cu(**3**)(CH$_3$CN)]$^+$ (calc. for C$_{30}$H$_{31}$CuN$_3$ 496.1809), *m/z* = 473.1610 [Cu(**3**)+H$_2$O]$^+$ (calc. for C$_{28}$H$_{30}$OCuN$_2$ 473.1649), *m/z* = 455.1491 [Cu(**3**)]$^+$ (calc. for C$_{28}$H$_{28}$CuN$_2$ 455.1543).

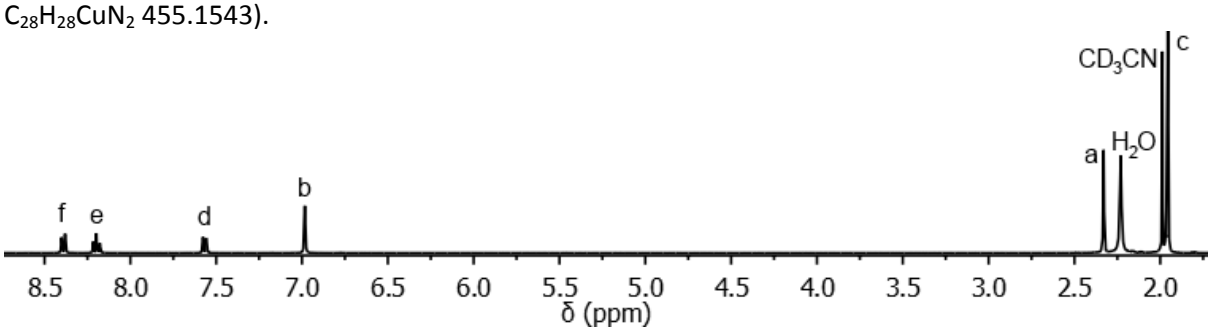

Figure S29 ^{1}H NMR spectrum (400 MHz, CD$_3$CN) of [Cu(**3**)(CH$_3$CN)$_2$]PF$_6$.

1.4.2 [Cu(6,6'-dimesityl-2,2'-bipyridine)(1-(5-yl-ethynyl-2,2'-bipyridine)ferrocene)]PF_6 ([Cu(2a)(3)]PF_6)

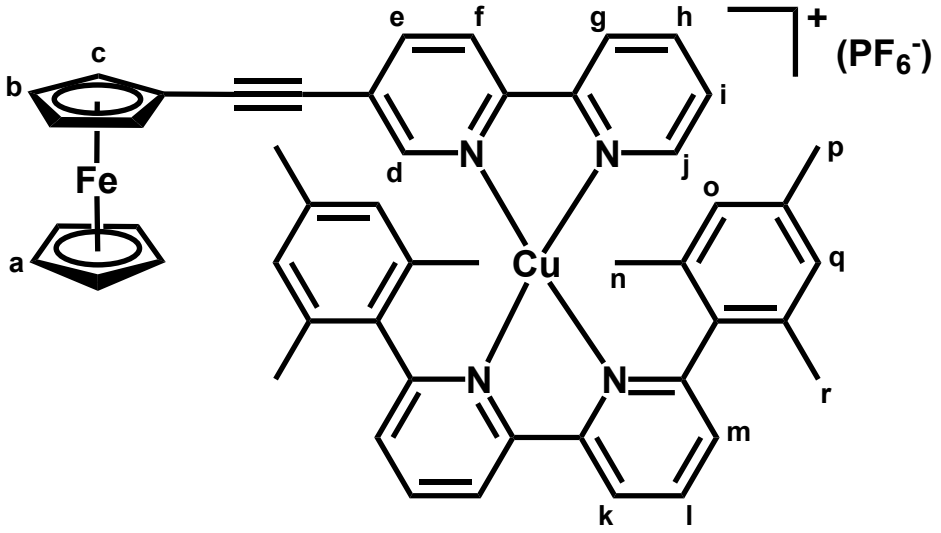

$[Cu(MeCN)_4]PF_6$ (21 mg, 0.055 mmol, 1.00 eq.) was dissolved in acetone (3 mL) and **3** (21 mg, 0.055 mmol, 1.00 eq.), also dissolved in acetone (3 mL), was added. The mixture was stirred for 15 minutes to give a yellow solution. **2a** (20 mg, 0.055 mmol, 1.00 eq.) was dissolved in acetone (3 mL) and added to this solution. The mixture was stirred for a further 15 minutes, then filtered through a cotton wool plug and vapour diffused (acetone/petrol) in order to obtain dark orange crystals (48 mg, 91%). Mp >230 ˚C; ^{1}H NMR (400 MHz, $CDCl_3$) 8.46 (d, *J* = 8.0 Hz, 2H, H_k), 8.22 (t, *J* = 7.8 Hz, 2H, H_l), 8.11 (s, 1H, H_d), 8.09 (d, *J* = 5.7 Hz, 1H, H_j), 7.96-7.91 (m, 2H, $H_{e/h}$), 7.88-7.81 (m, 2H, $H_{f/g}$), 7.52 (d, *J* = 7.5 Hz, 2H, H_m), 7.37 (t, *J* = 5.6 Hz, 1H, H_i), 6.19 (s, 2H, H_q or H_o), 6. 11 (s, 2H, H_q or H_o), 4.55 (t, *J* = 1.8 Hz, 2H, H_c). 4.33 (t, *J* = 1.8 Hz, 2H, H_b), 4.26 (s, 5H, H_a), 1.87 (s, 6H, H_p), 1.80 (s, 6H, H_r or H_n), 1.73 (s, 6H, H_r or H_n); ^{13}C NMR (125 MHz, $CDCl_3$) δ 158.6, 152.1, 150.5, 149.5, 148.6, 147.9, 138.8, 138.5, 138.0, 137.4, 137.2, 134.7, 134.6, 127.5, 127.4, 127.1, 125.3, 123.0, 120.9, 120.3, 116.5, 96.3, 81.3, 71.9, 70.2, 69.8, 63.3, 20.7, 20.2, 2.0; IR: ν (cm^{-1}) 2206, 1559, 1456, 1374, 829, 731, 555; HRESI-MS (MeOH): *m/z* = 819.2242 [Cu(**2a**)(**3**)]$^+$ (calc. for $C_{50}H_{44}CuFeN_4$ 819.2208); UV-Vis ($CHCl_3$) λ_{max} (ε/ L mol^{-1} cm^{-1}): 267 (49700), 316 (51700), 475 (10500); Anal. Calc. for $C_{50}H_{44}CuFeN_4PF_6$: C, 62.21; H, 4.59; N, 5.80. Found: C, 62.29; H, 4.61; N, 5.73.

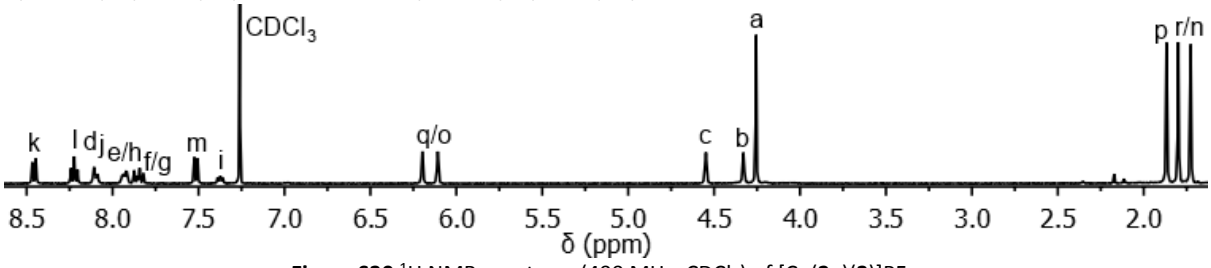

Figure S30 ^{1}H NMR spectrum (400 MHz, $CDCl_3$) of [Cu(**2a**)(**3**)]PF_6.

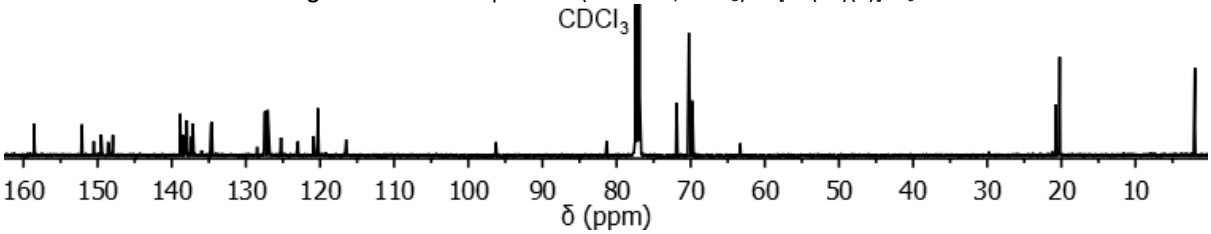

Figure S31 ^{13}C NMR spectrum (125 MHz, $CDCl_3$) of [Cu(**2a**)(**3**)]PF_6.

1.4.3 [Cu(6,6'-dimesityl-2,2'-bipyridine)(1-(5-yl-ethynyl-2,2'-bipyridine)-1'-(N-methyl-3-yl-ethynylpyridine)ferrocene)]$(PF_6)_2$ ([Cu(1b)(3)]$(PF_6)_2$)

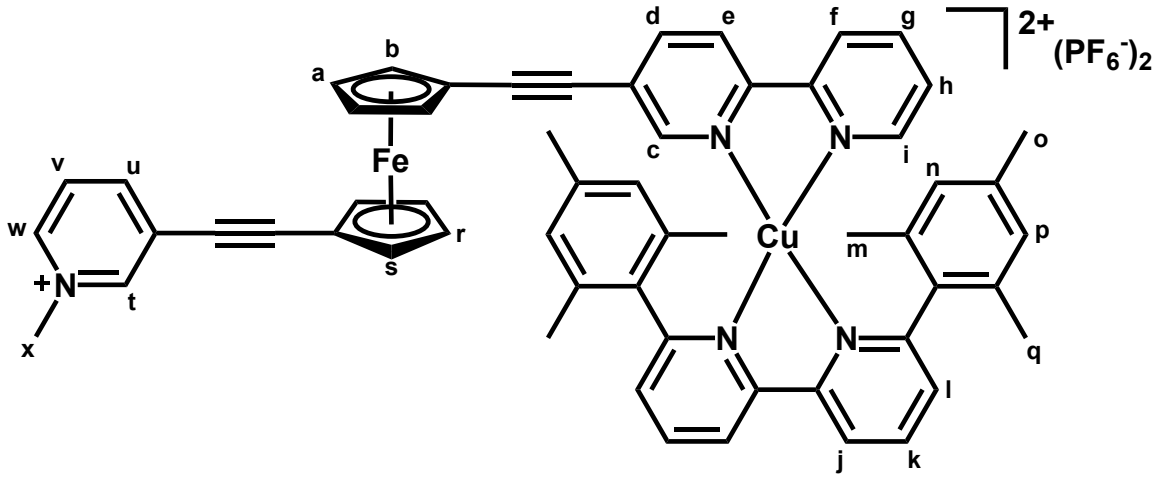

$[Cu(MeCN)_4]PF_6$ (7 mg, 0.016 mmol, 1.00 eq.) was dissolved in acetone (1 mL) and **3** (6 mg, 0.016 mmol, 1.00 eq.), also dissolved in acetone (1 mL), was added. The mixture was stirred for 15 minutes to give a yellow solution. **1b** (10 mg, 0.016 mmol, 1.00 eq.) was dissolved in acetone (1 mL) and added to this solution. The mixture was stirred for 15 minutes, then filtered through a cotton wool plug and the solvent removed *in vacuo* to give the reddish-orange product (20 mg, 100%). Mp 162 ˚C; ^{1}H NMR (400 MHz, d_6-acetone) δ 9.29 (s, 1H, H_t), 9.08 (d, *J* = 6.6 Hz, 1H, H_w), 8.74 (d, *J* = 8.0 Hz, 2H, H_j), 8.63 (d, *J* = 9.3 Hz, 1H, H_u), 8.49 (s, 1H, H_c), 8.42 (d, *J* = 5.2 Hz, 1H, H_i), 8.38 (t, *J* = 7.9 Hz, 2H, H_k), 8.19 (t, *J* = 7.1 Hz, 1H, H_v). 8.16 (t, *J* = 7.8 Hz, 2H, $H_{e/f}$), 8.09-8.05 (m, 2H, $H_{d/g}$), 7.71 (d, *J* = 7.5 Hz, 2H, H_l), 7.58 (t, *J* = 5.3 Hz, 1H, H_h), 6.21 (s, 2H, H_n or H_p), 6.14 (s, 2H, H_n or H_p), 4.73 (s, 2H, H_b or H_s), 4.71 (s, 2H, H_b or H_s), 4.63 (s, 2H, H_a or H_r), 4.54 (s, 3H, H_a or H_r and H_x), 1.85 (s, 12H, H_m or H_q), 1.80 (s, 6H, H_o); ^{13}C NMR (125 MHz, d_6-acetone) δ159.3, 153.3, 151.4, 151.1, 150.3, 149.5, 147.1, 139.7, 139.4, 138.5, 138.2, 138.1, 136.4, 135.7, 135.5, 129.1, 129.0, 128.2, 128.0, 127.9, 126.6, 125.8, 123.2, 121.9, 121.4, 121.1, 97.7, 94.5, 83.2, 80.1, 74.5, 74.3, 73.7, 73.4, 66.3, 64.4, 49.5, 20.8, 20.4, 20.4; IR: ν (cm^{-1}) 2920, 2217, 1611, 1436, 831, 556; HRESI-MS (MeOH): *m/z* = 1080.2277 [Cu(**1b**)(**3**)PF_6]$^+$ (calc. for $C_{58}H_{50}CuFeN_5PF_6$ 1080.2350), *m/z* = 467.6242 [Cu(**1b**)(**3**)]$^{2+}$ (calc. for $C_{58}H_{50}CuFeN_5$ 467.6351); UV-Vis (acetone) λ_{max} (ε/ L mol^{-1} cm^{-1}): 463 (8500); Anal. Calc. for $C_{58}H_{50}CuFeN_5P_2F_{12}$: C, 56.80; H, 4.11; N, 5.71. Found: C, 56.73; H, 4.44; N, 5.78.

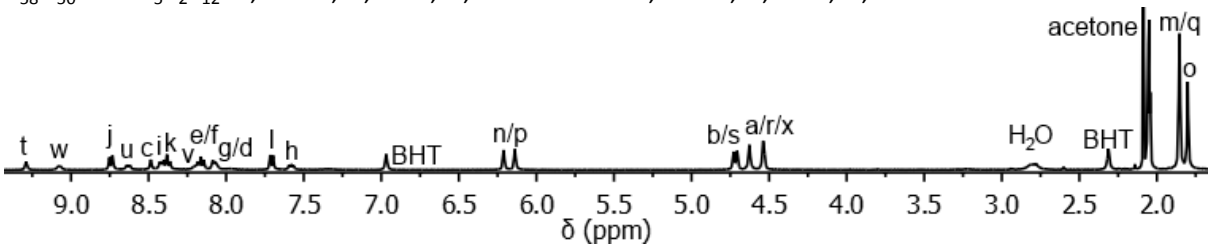

Figure S32 ^{1}H NMR spectrum (400 MHz, d_6-acetone) of [Cu(**1b**)(**3**)]$(PF_6)_2$.

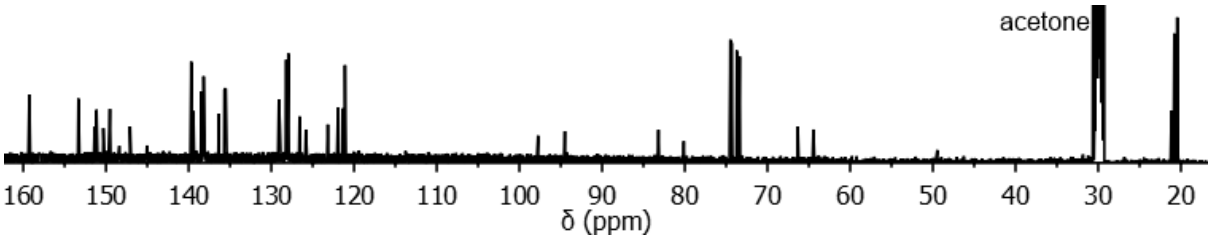

Figure S33 ^{13}C NMR spectrum (125 MHz, d_6-acetone) of [Cu(**1b**)(**3**)]$(PF_6)_2$.

1.4.4 [Cu_2(6,6'-dimesityl-2,2'-bipyridine)$_2$(1,1'-di(5-yl-ethynyl-2,2'-bipyridine)ferrocene)]$(PF_6)_2$ ([Cu_2(**1a**)(**3**)$_2$]$(PF_6)_2$)

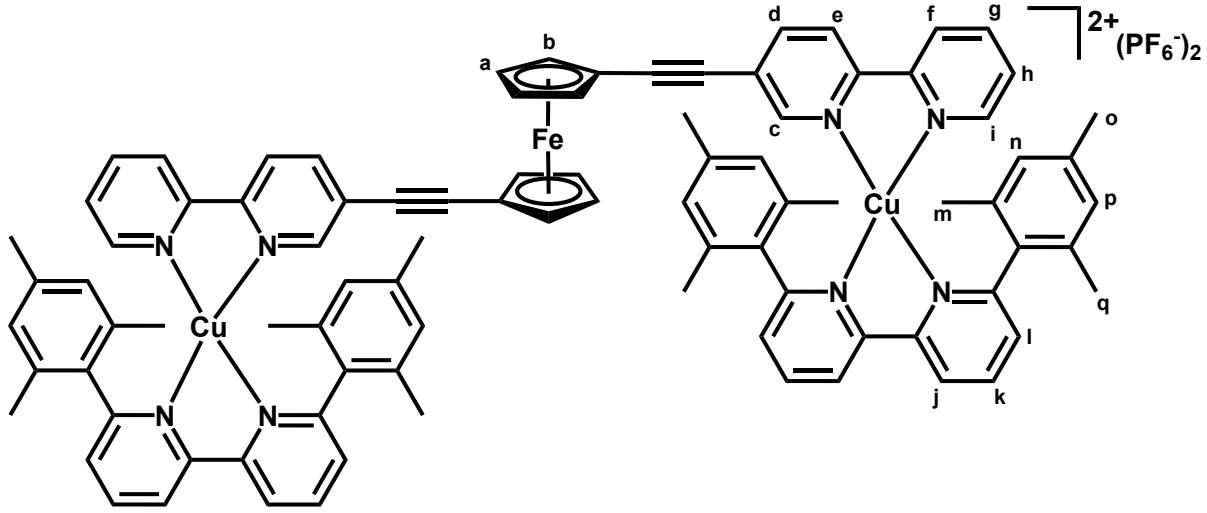

[Cu(MeCN)$_4$]PF_6 (69 mg, 0.184 mmol, 2.00 eq.) was dissolved in acetone (2.5 mL) and **3** (72 mg, 0.184 mmol, 2.00 eq.), also dissolved in acetone (2.5 mL), was added. The mixture was stirred for 15 minutes to give a yellow solution. **1a** (50 mg, 0.092 mmol, 1.00 eq.) was dissolved in acetone (5 mL) and added to this solution. The mixture was stirred for 15 minutes, then filtered through a cotton wool plug and the solvent removed *in vacuo* to give the reddish-orange product (160 mg, 99%). Mp 174 ˚C; ^{1}H NMR (400 MHz, $CDCl_3$) δ 8.48 (d, *J* = 8.0 Hz, 4H, H_j), 8.23 (t, *J* = 7.9 Hz, 4H, H_k), 8.11 (s, 2H, H_c), 8.08-8.04 (m, 4H, $H_{d/i}$), 8.00 (d, *J* = 7.7 Hz, 4H, $H_{e/f}$), 7.92 (t, *J* = 8.0 Hz, 2H, H_g), 7.51 (d, *J* = 7.4 Hz, 4H, H_l), 7.32 (t, *J* = 5.5 Hz, 2H, H_h), 6.15 (s, 4H, H_n or H_p), 6.11 (s, 4H, H_n or H_p), 4.55 (s, 4H, H_b), 4.41 (s, 4H, H_a), 1.85 (s, 12H, H_o), 1.76 (s, 12H, H_m or H_q), 1.74 (s, 12H, H_m or H_q); ^{13}C NMR (100 MHz, $CDCl_3$) δ 158.6, 152.2, 150.8, 149.5, 149.0, 147.8, 139.0, 138.2, 137.3, 137.2, 134.7, 134.6, 128.5, 127.6, 127.5, 127.1, 125.1, 122.7, 121.4, 121.1, 120.4, 94.8, 82.4, 74.0, 72.1, 65.3, 20.8, 20.3, 20.3; IR: ν (cm^{-1}) 2203, 1591, 1561, 1458, 1434, 831, 555; HRESI-MS (MeOH): *m/z* = 727.2211 [Cu_2(**1a**)(**3**)$_2$]$^{2+}$ (calc. for $C_{90}H_{78}Cu_2FeN_8$ 727.2134); UV-Vis ($CHCl_3$) λ_{max} (ε/ L mol^{-1} cm^{-1}): 306 (63200), 476 (12600); Anal. Calc. for $C_{49}H_{46}CuFeN_4PF_6$: C, 61.96; H, 4.51; N, 6.42. Found: C, 61.83; H, 4.39; N, 6.55.

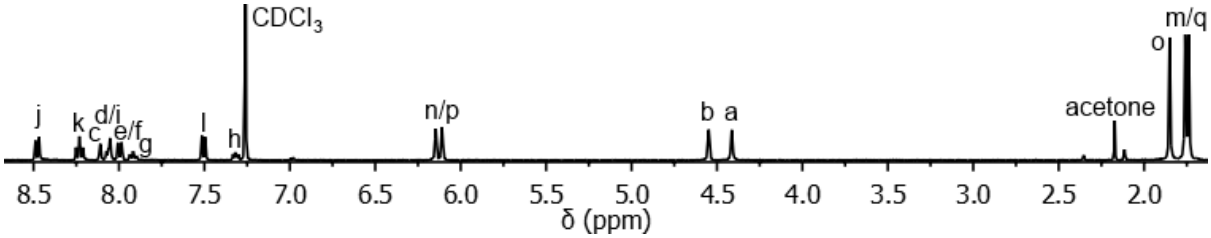

Figure S34 ^{1}H NMR spectrum (400 MHz, $CDCl_3$) of [Cu_2(**1a**)(**3**)$_2$]$(PF_6)_2$.

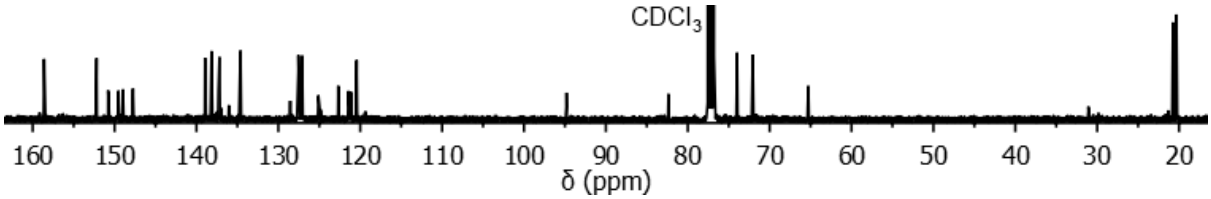

Figure S35 ^{13}C NMR spectrum (100 MHz, $CDCl_3$) of [Cu_2(**1a**)(**3**)$_2$]$(PF_6)_2$.

1.4.1 [Cu(6,6'-dimesityl-2,2'-bipyridine)(2,2':6',2''-terpyridine)]$(PF_6)_2$ ([Cu(5)(3)]$(PF_6)_2$)

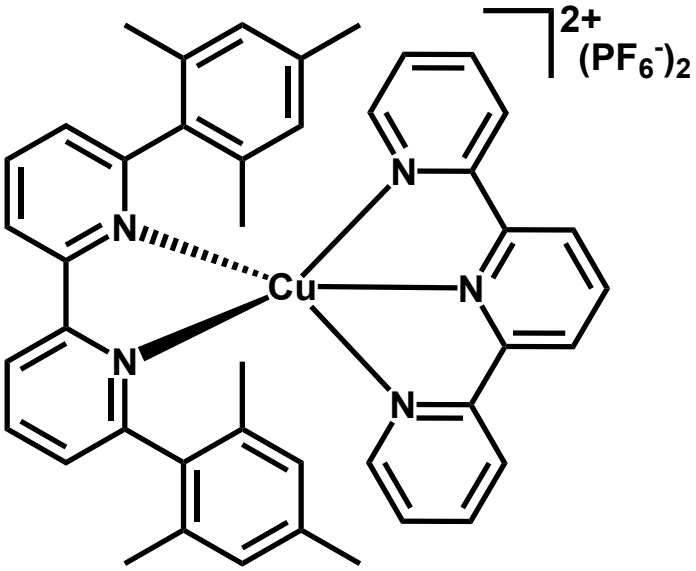

$CuCl_2$ (6.9 mg, 0.051 mmol, 1.00 eq.), $AgPF_6$ (26 mg, 0.102 mmol, 2.00 eq.), 2,2':6',2''-terpyridine (12 mg, 0.051 mmol, 1.00 eq.), and **3** (20 mg, 0.051 mmol, 1.00 eq.) were combined in acetone (5 mL) The mixture was stirred for 15 minutes to give a pale blue solution, then filtered through a cotton wool plug to remove the AgCl precipitate. Vapour diffusion of petroleum ether into the resulting acetone solution gave x-ray quality crystals of the blue product (44 mg, 88%). Mp >230 ˚C; IR: ν (cm^{-1}) 3085, 2923, 1449, 1021, 833, 777, 555; HRESI-MS (MeOH): *m/z* = 344.1222 [Cu(**5**)(**3**)]$^{2+}$ (calc. for $C_{43}H_{39}CuN_5$ 344.1245); UV-Vis (acetone) λ_{max} (ε/ L mol^{-1} cm^{-1}): 342 (13200), 654 (200); Anal. Calc. for $C_{43}H_{39}CuN_5P_2F_{12}$•$1.5H_2O$: C, 51.32; H, 4.21; N, 6.96. Found: C, 51.18; H, 4.05; N, 7.20.

2 ^{1}H NMR Stackplots

2.1 Rotors

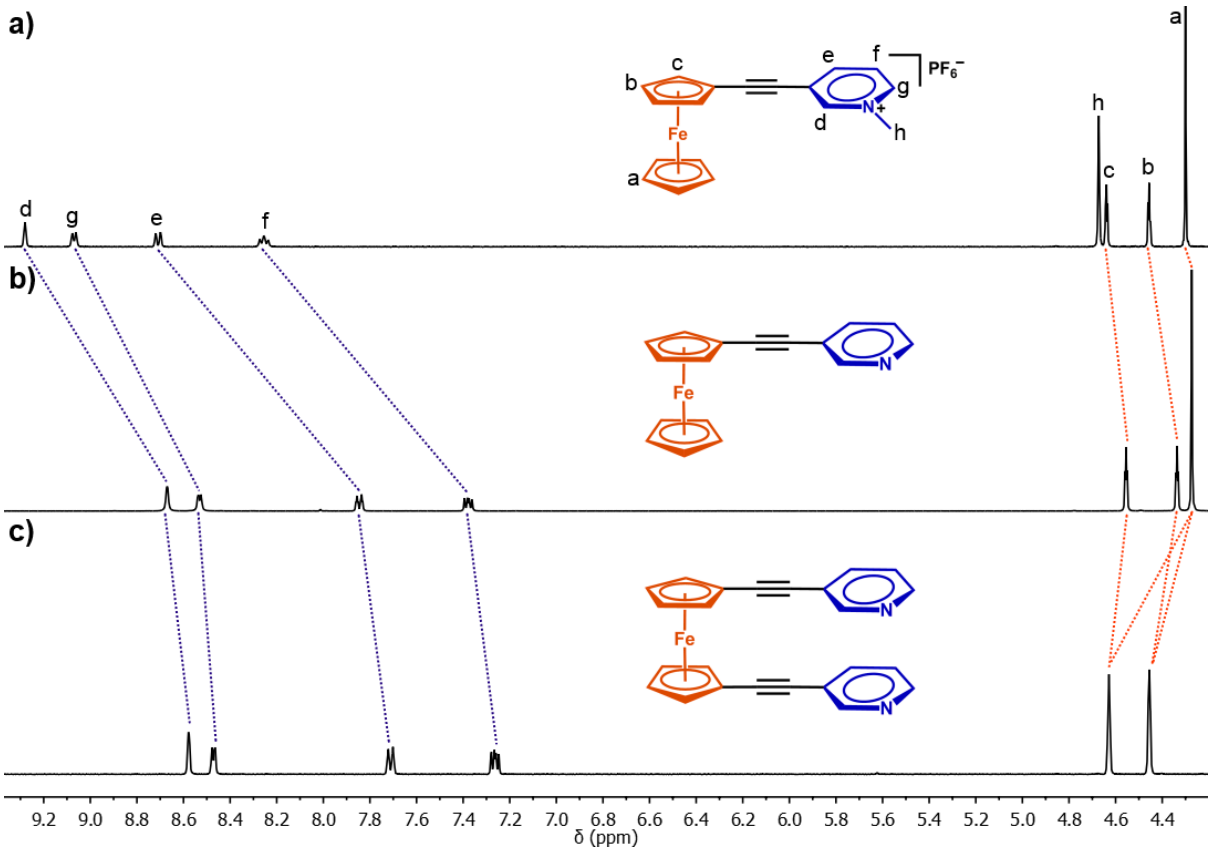

Figure S36 Stacked ^{1}H NMR spectra (d_6-acetone, 298 K) of a) the methylated ligand **2b** and b) the mono-substituted ligand **S9**, and c) the di-substituted ligand **S5**.

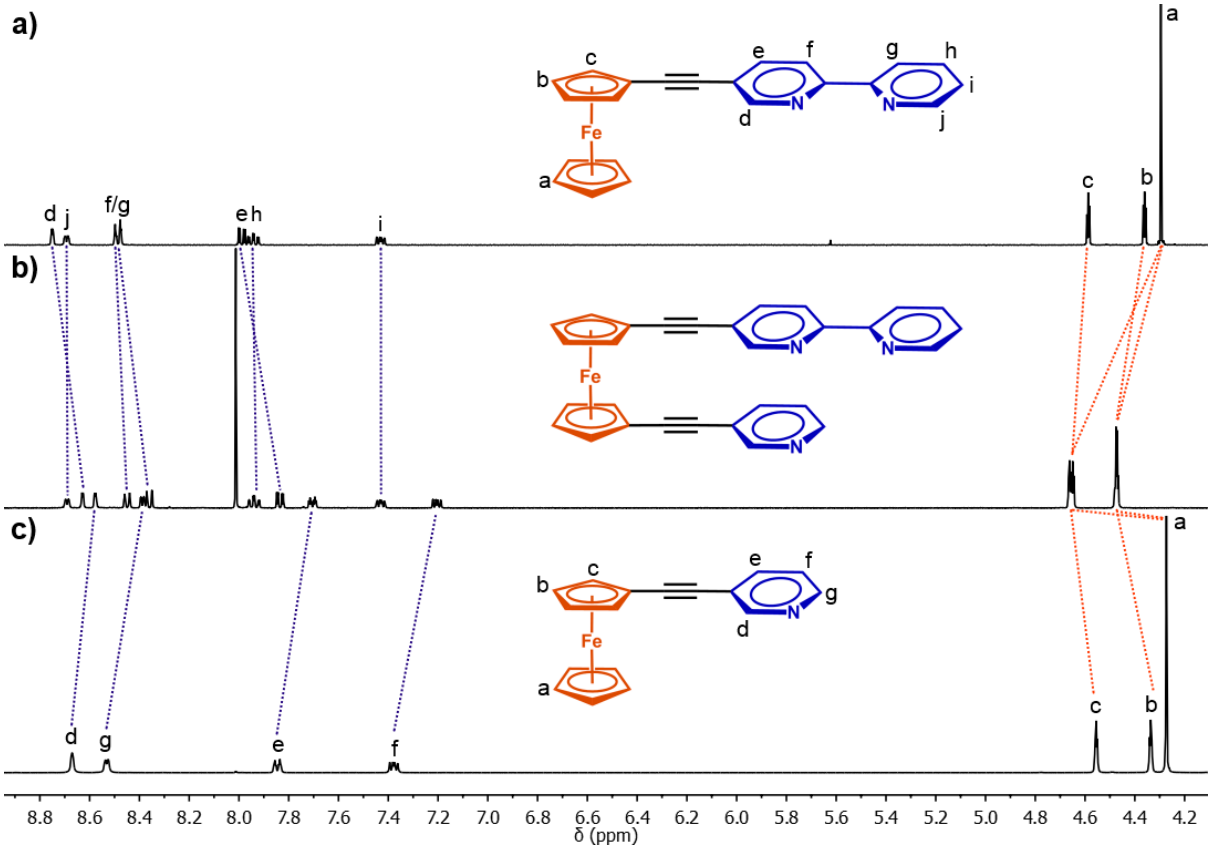

Figure S37 Stacked ^{1}H NMR spectra (d_6-acetone, 298 K) of a) the bipyridine-substituted ligand **2a**, b) the asymmetrically substituted ligand **S8**, and c) the pyridine-substituted ligand **S9**.

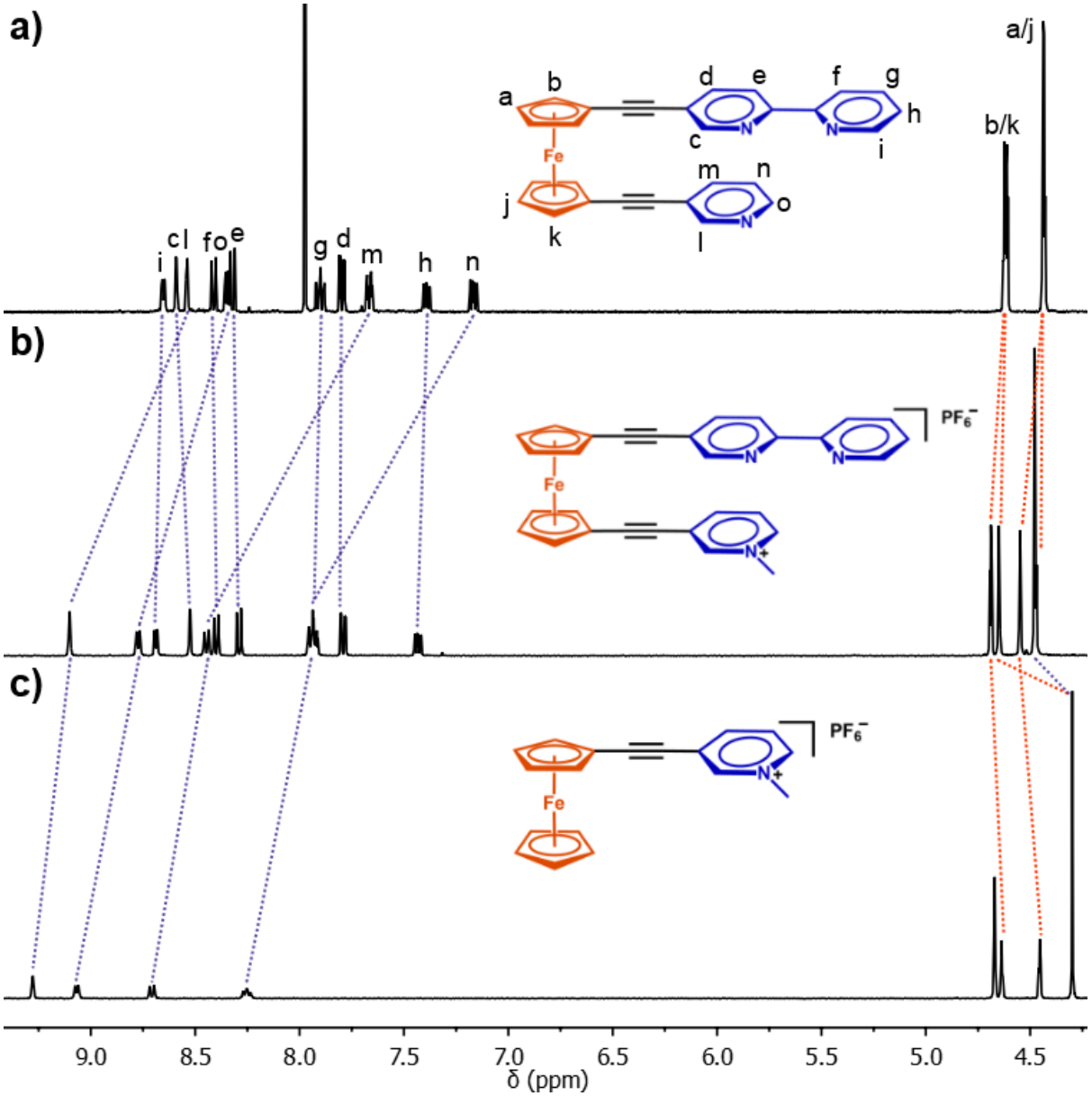

Figure S38 Stacked ^{1}H NMR spectra (d_6-acetone, 298 K) of a) the asymmetrically substituted ligand **S8**, and b) the methylated ligand **1b**, and c) the methylated ligand **2b**.

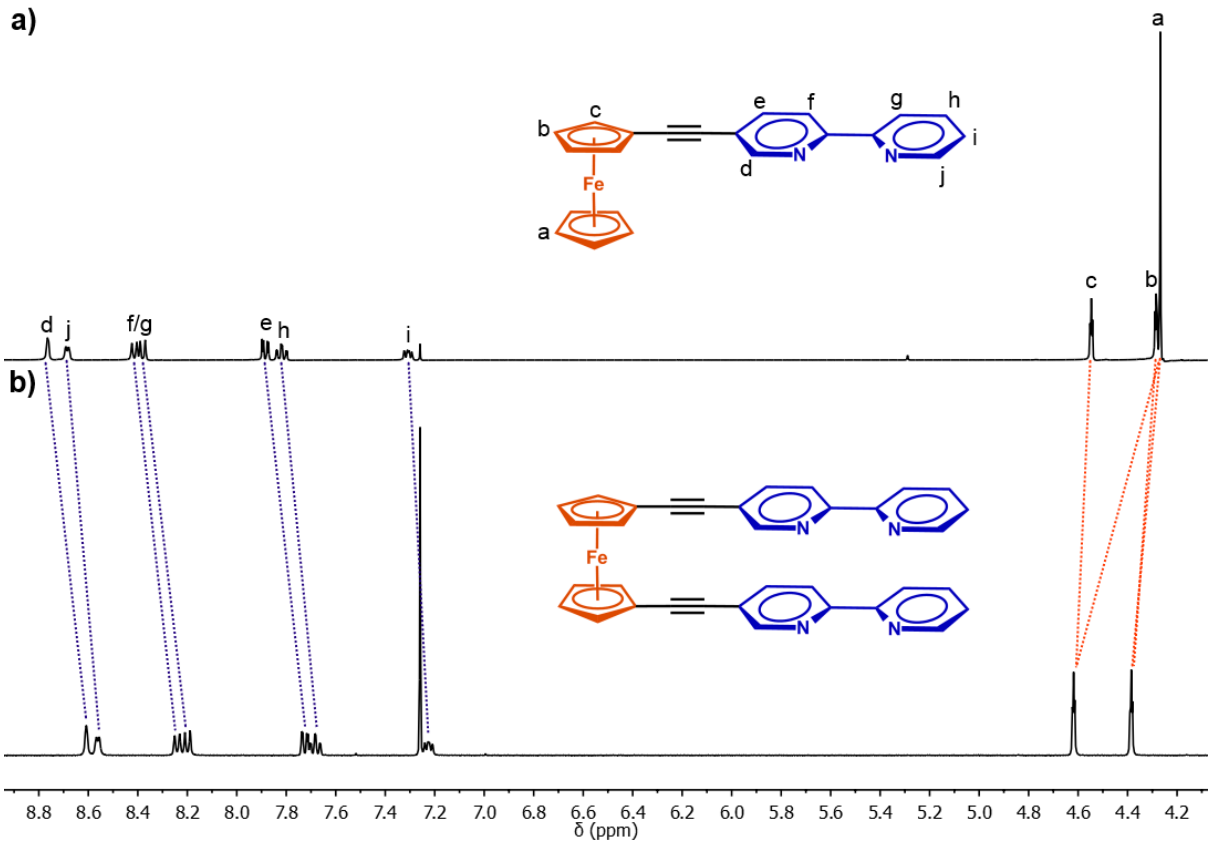

Figure S39 Stacked ^{1}H NMR spectra ($CDCl_3$, 298 K) of a) the mono-substituted ligand **2a**, and b) the di-substituted ligand **1a**.

2.2 Complexes

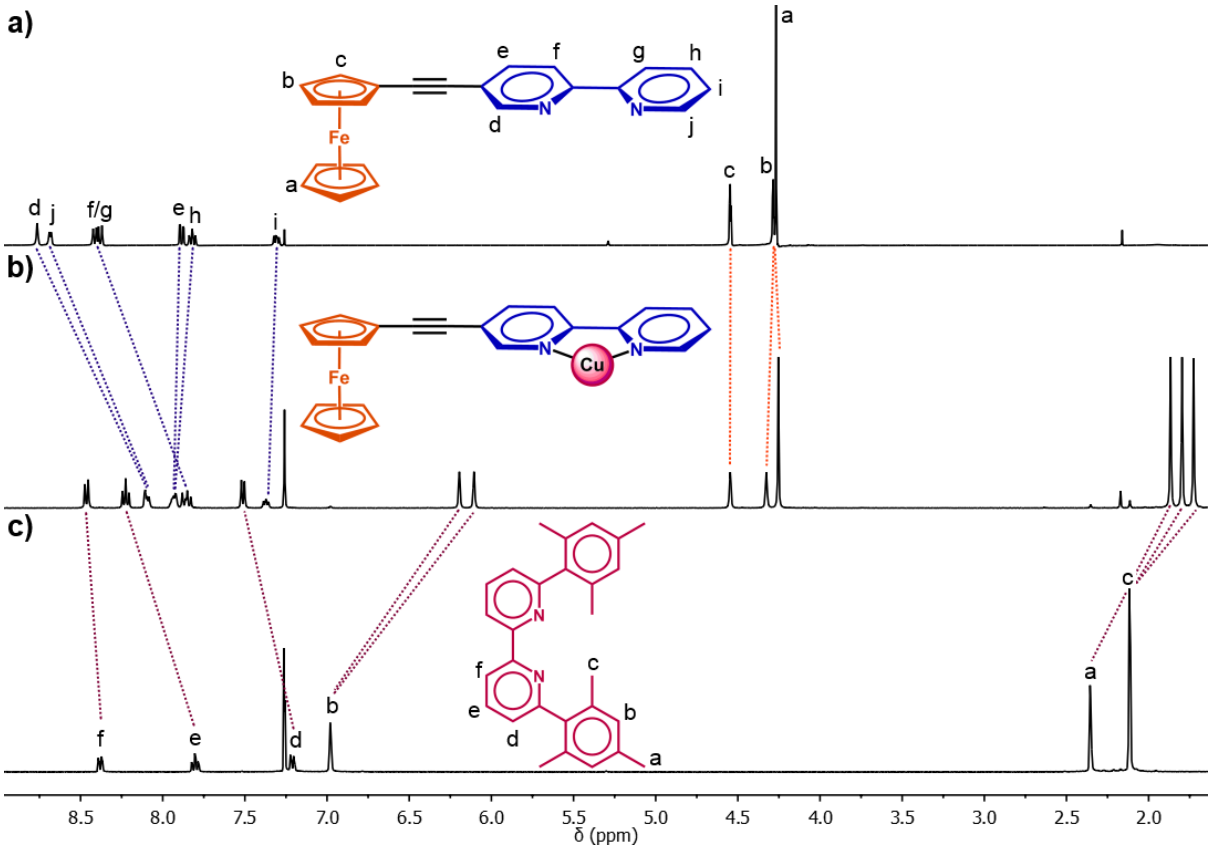

Figure S40 Stacked ^{1}H NMR spectra ($CDCl_3$, 298 K) of a) the mono-substituted ligand **2a**, b) the Cu(I) complex [Cu(**2a**)(**3**)]PF_6, and c) the dimesityl-bipyridine ligand **3**.

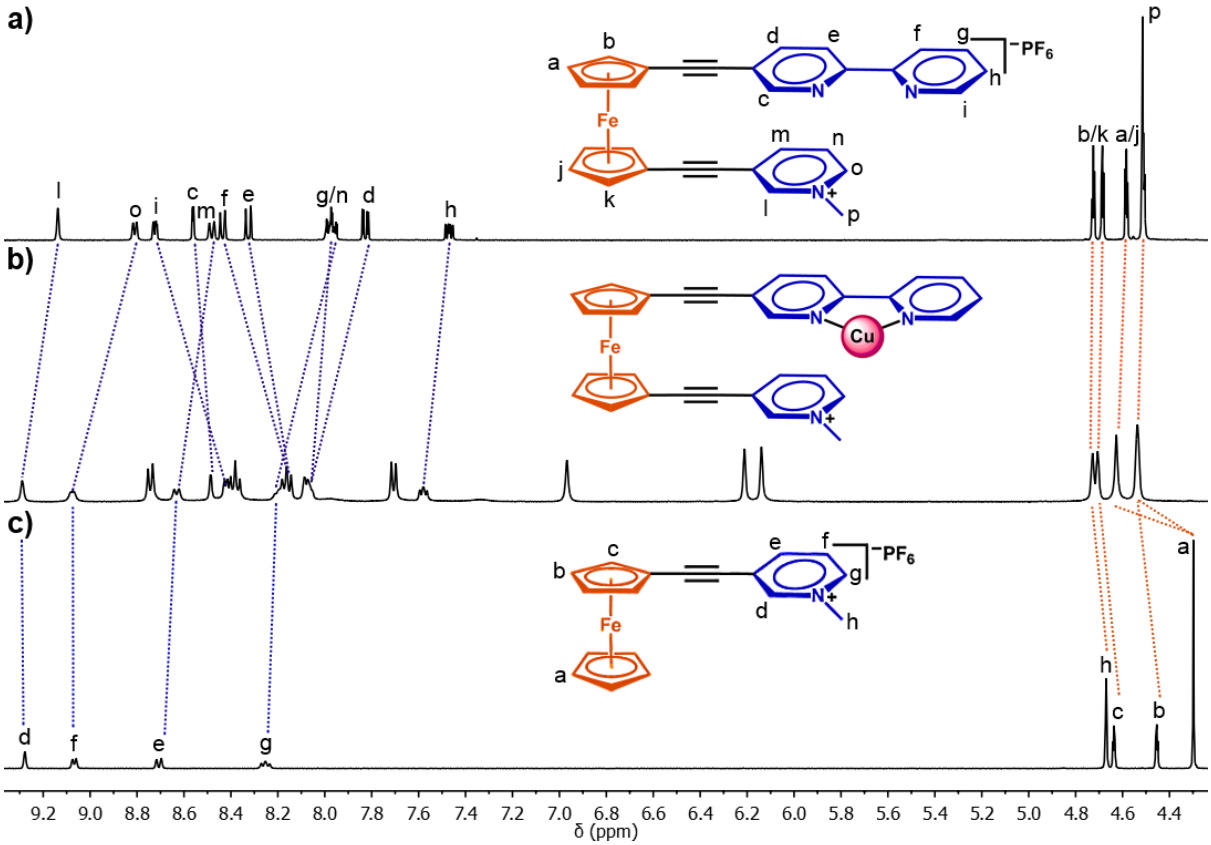

Figure S41 Stacked ^{1}H NMR spectra (d_6-acetone, 298 K) of a) the asymmetrically-substituted ligand **1b**, b) the Cu(I) complex [Cu(**1b**)(**3**)](PF$_6$)$_2$, and c) the mono-substituted ferrocene **2b**.

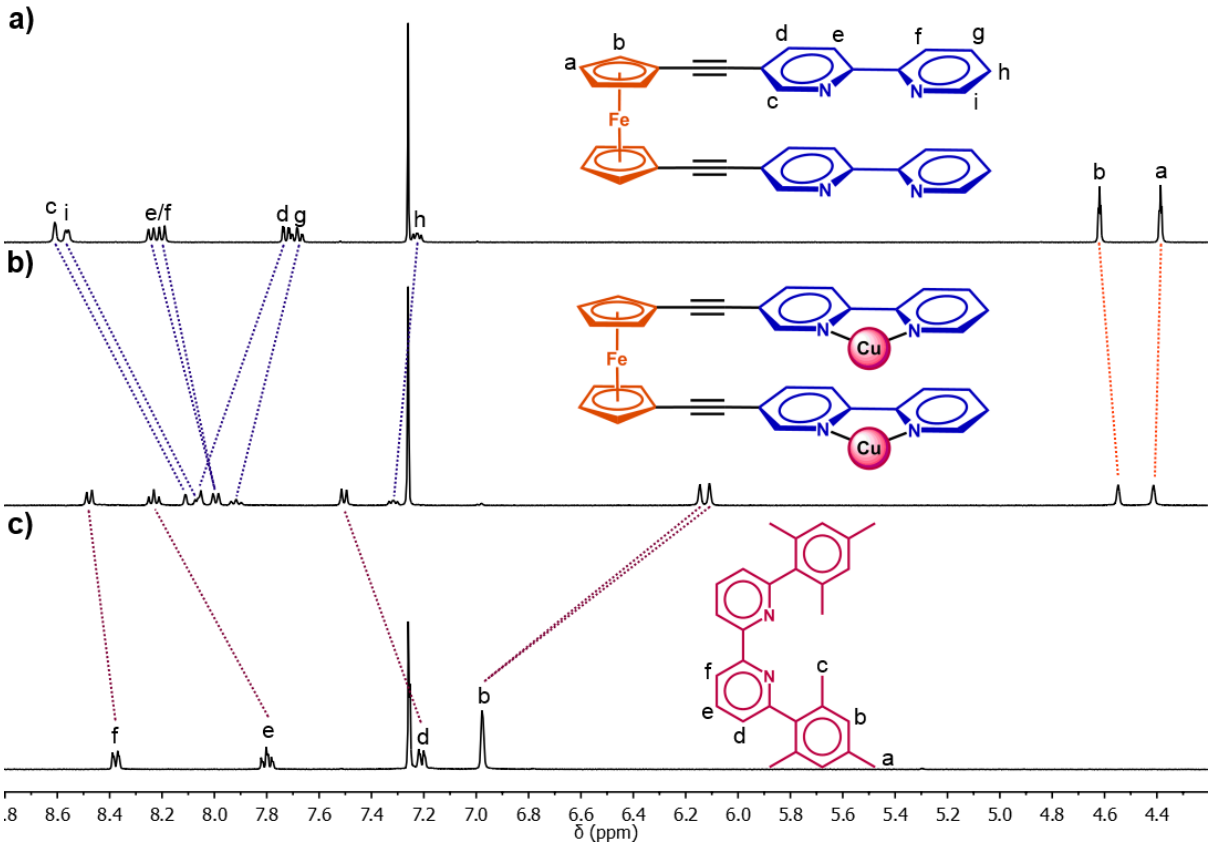

Figure S42 Stacked ^{1}H NMR spectra ($CDCl_3$, 298 K) of a) the di-substituted ligand **1a**, b) the Cu(I) complex [Cu(**1a**)(**3**)$_2$](PF$_6$)$_2$, and c) the dimesityl-bipyridine ligand **3**.

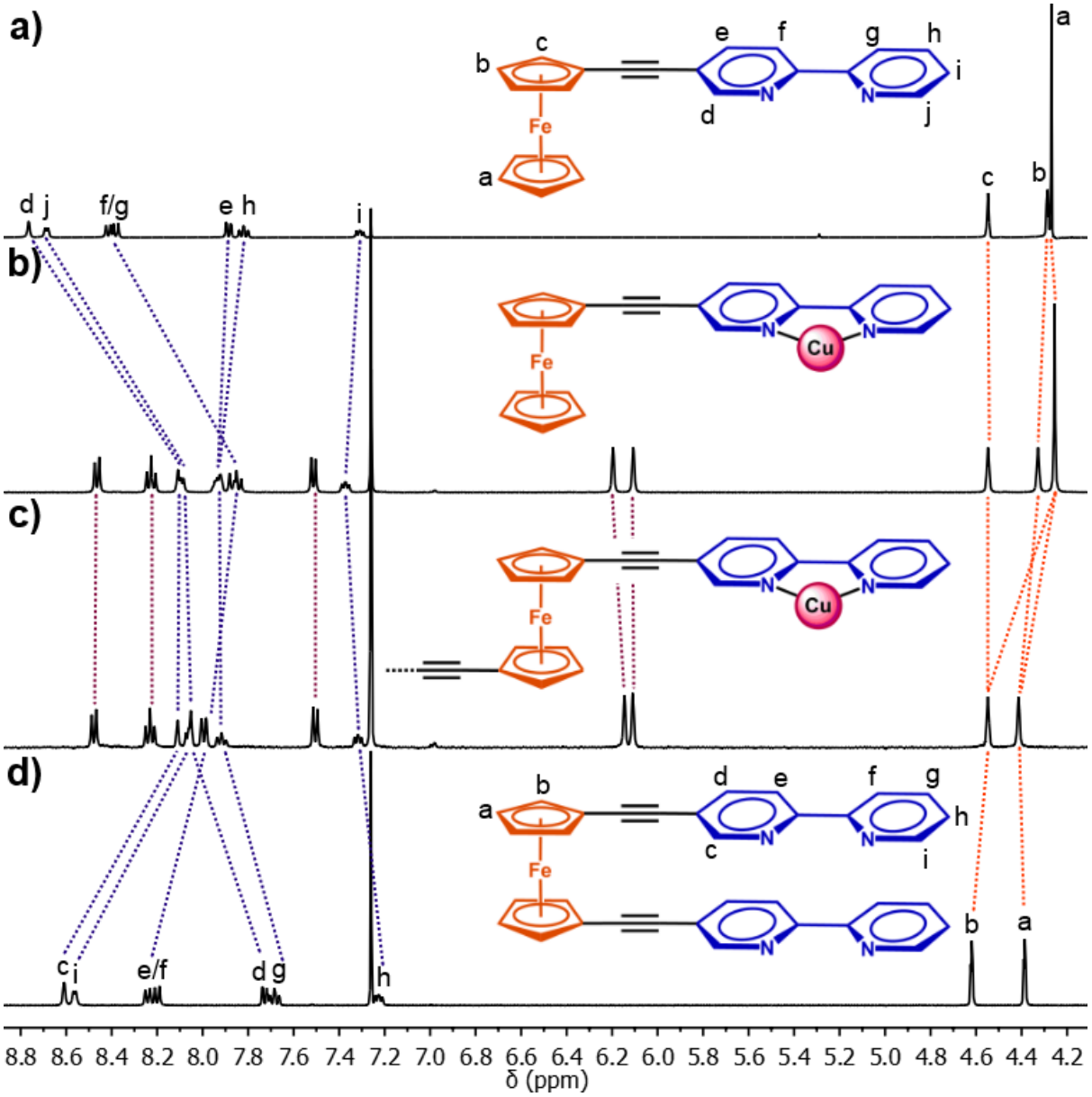

Figure S43 Stacked ^{1}H NMR spectra ($CDCl_3$, 298 K) of a) the mono-substituted ligand **2a**, b) the Cu(I) complex [Cu(**2a**)(**3**)]PF_6, c) the Cu(I) complex [Cu(**1a**)(**3**)$_2$]$(PF_6)_2$, and d) the di-substituted ligand **1a**.

2.3 Switching

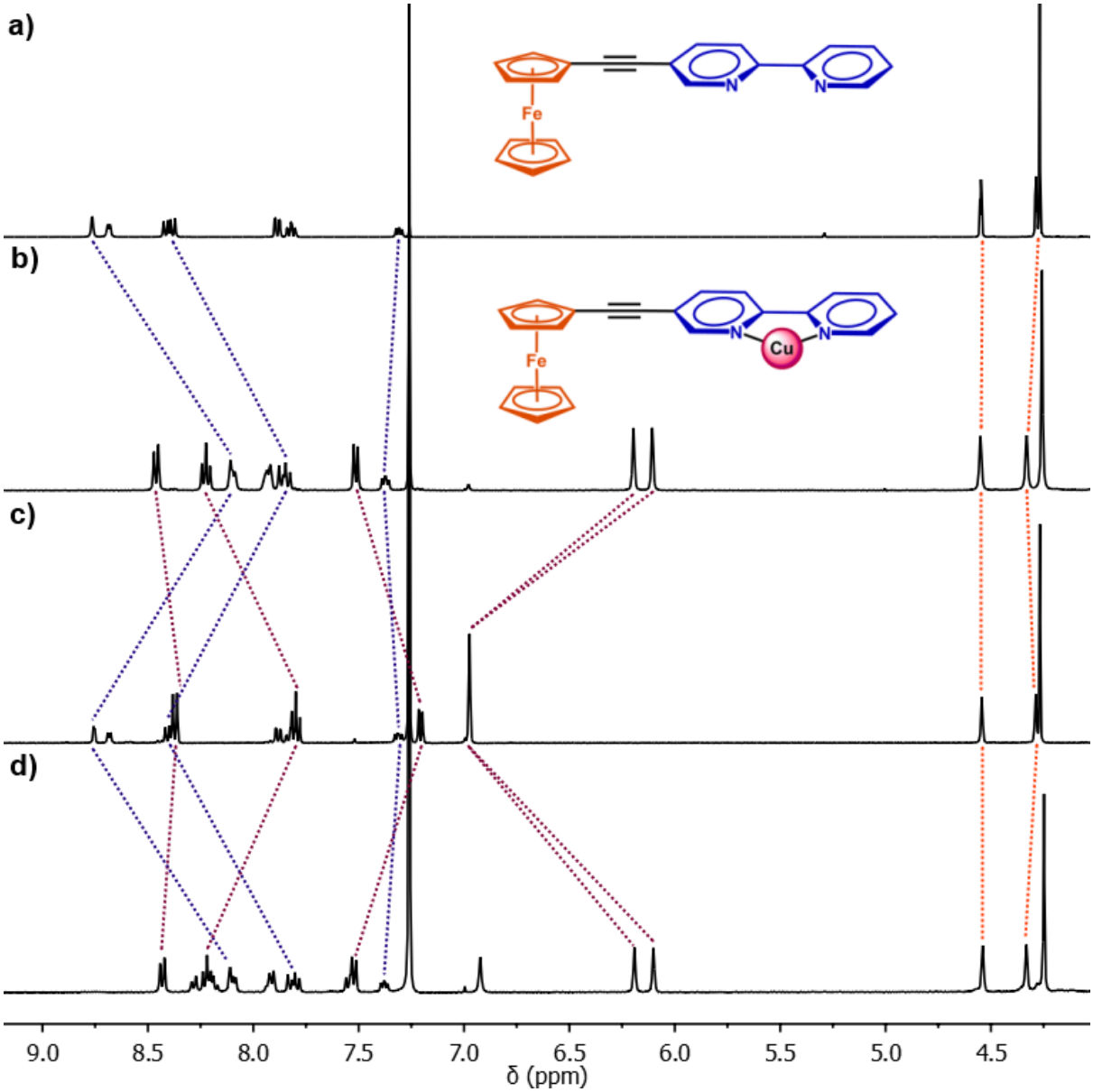

Figure S44 Stacked ^{1}H NMR spectra ($CDCl_3$, 298 K) of a) the mono-substituted ligand **2a**, b) the Cu(I) complex [Cu(**2a**)(**3**)]PF_6, c) [Cu(**2a**)(**3**)]PF_6 after adding 1 eq. of CN^-, and d) [Cu(**2a**)(**3**)]PF_6 after adding 1 eq. of Cu(I).

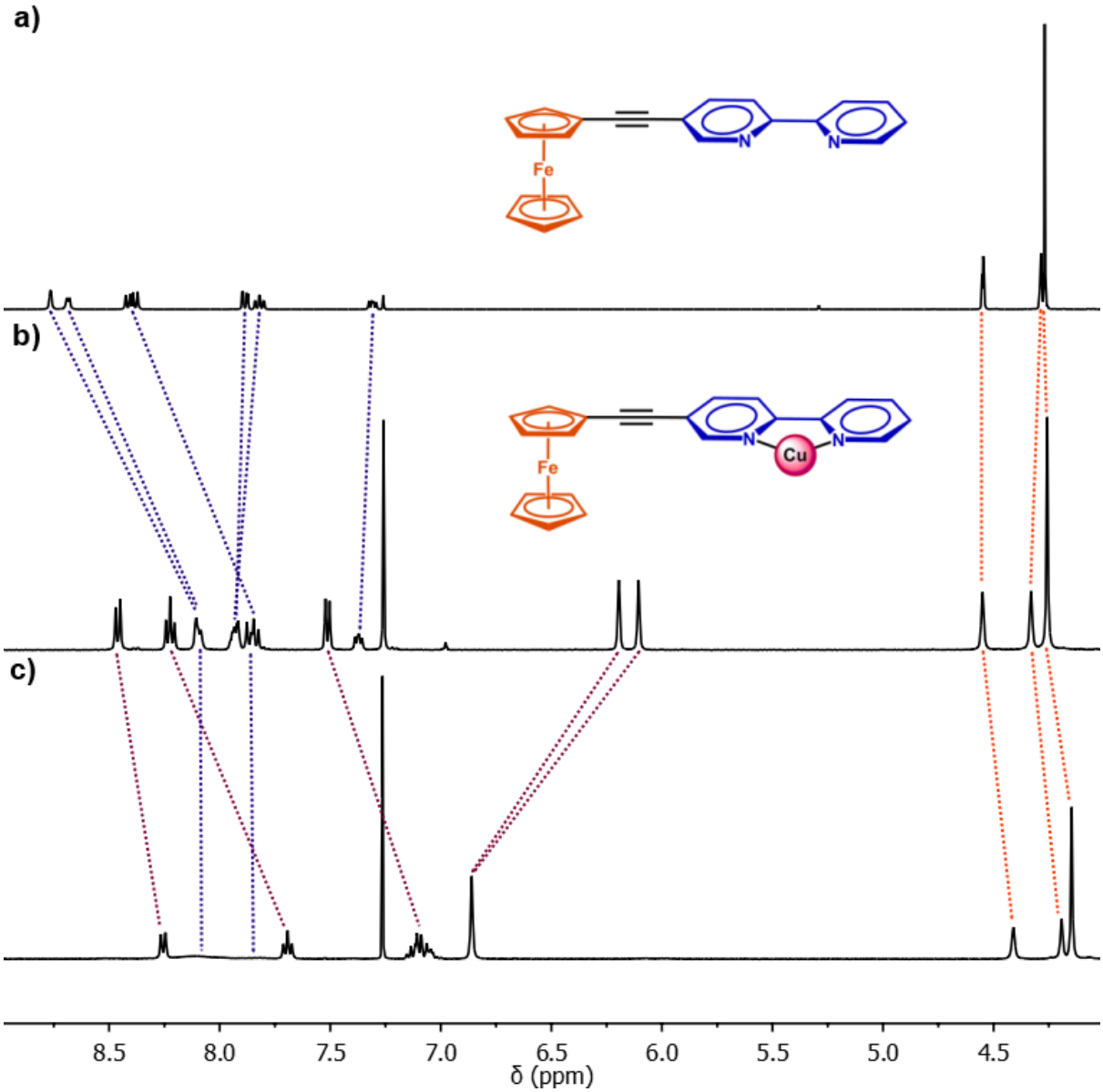

Figure S45 Stacked ^{1}H NMR spectra ($CDCl_3$, 298 K) of a) the mono-substituted ligand **2a**, b) the Cu(I) complex [Cu(**2a**)(**3**)]PF_6, and c) [Cu(**2a**)(**3**)]PF_6 after adding 1 eq. of Cl^-.

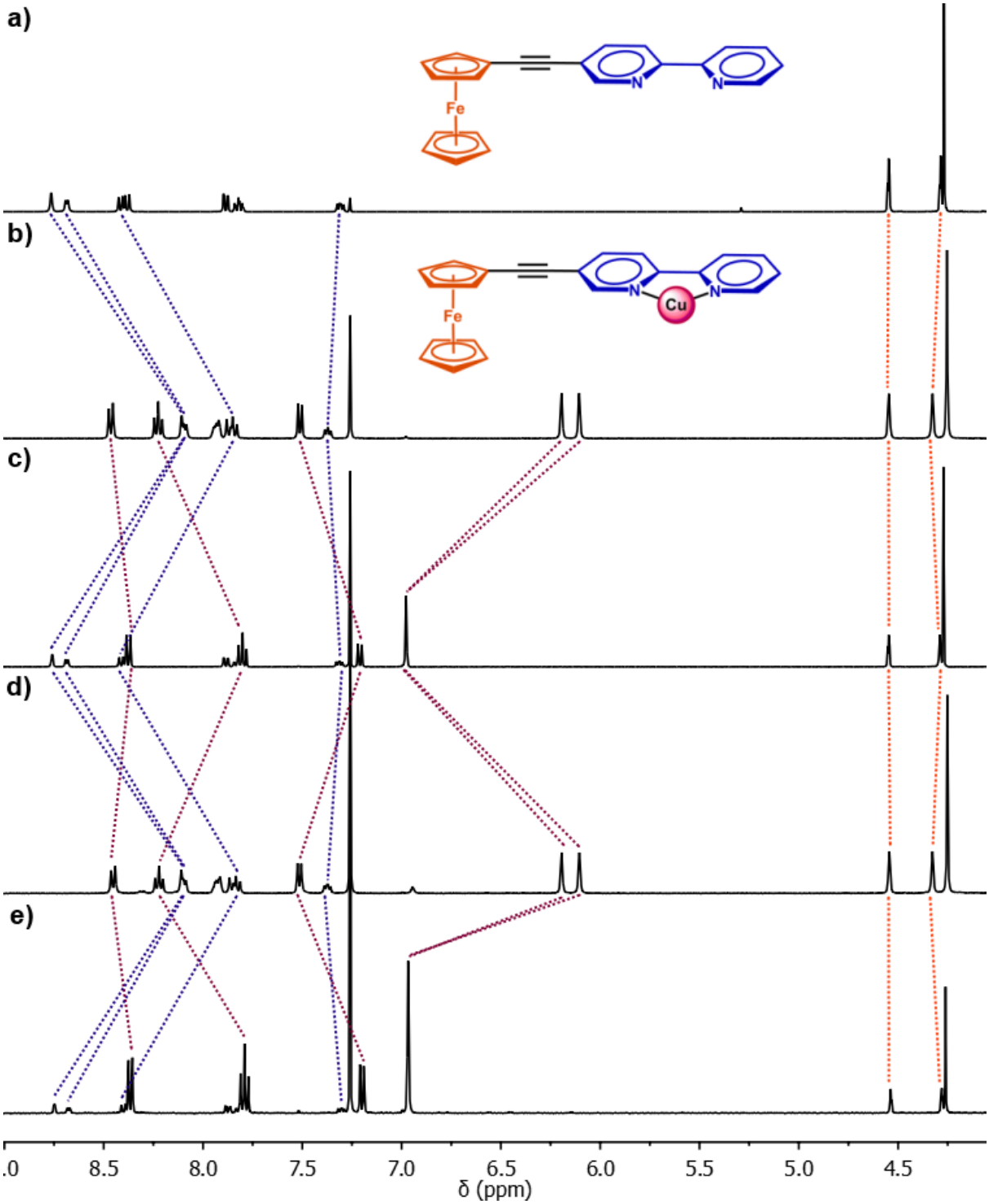

Figure S46 Stacked ^{1}H NMR spectra ($CDCl_3$, 298 K) of a) the mono-substituted ligand **2a**, b) the Cu(I) complex [Cu(**2a**)(**3**)]PF_6, c) [Cu(**2a**)(**3**)]PF_6 after adding 1 eq. of cyclam, d) [Cu(**2a**)(**3**)]PF_6 after adding 1 eq. of Cu(I), and e) [Cu(**2a**)(**3**)]PF_6 after adding a further 1 eq. of cyclam.

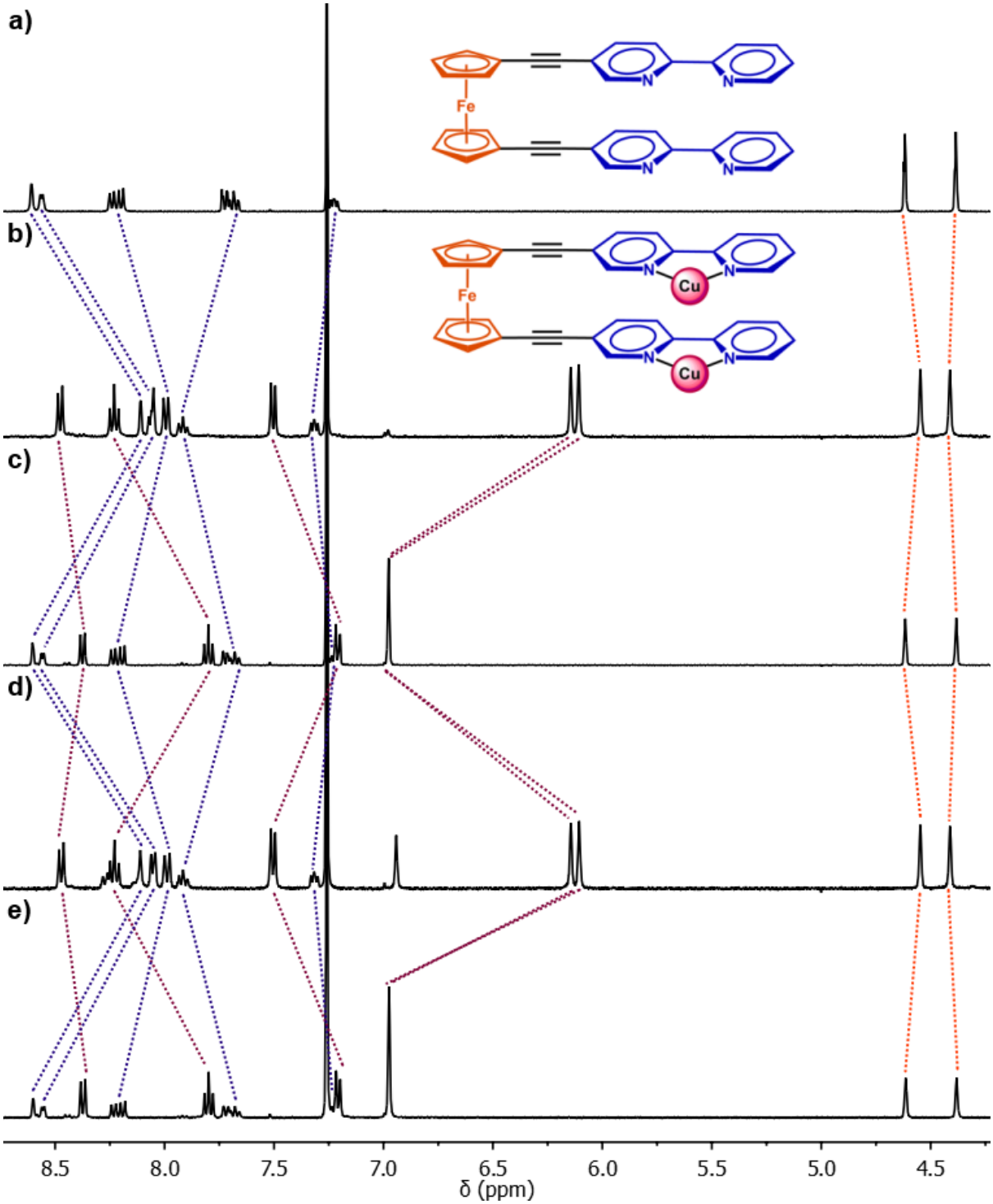

Figure S47 Stacked ^{1}H NMR spectra ($CDCl_3$, 298 K) of a) the di-substituted ligand **1a**, b) the Cu(I) complex [Cu(**1a**)(**3**)$_2$](PF$_6$)$_2$, c) [Cu(**1a**)(**3**)$_2$](PF$_6$)$_2$ after adding 1 eq. of cyclam, d) [Cu(**1a**)(**3**)$_2$](PF$_6$)$_2$ after adding 1 eq. of Cu(I), and e) [Cu(**1a**)(**3**)$_2$](PF$_6$)$_2$ after adding a further 1 eq. of cyclam.

3 Relevant Mass Spectra

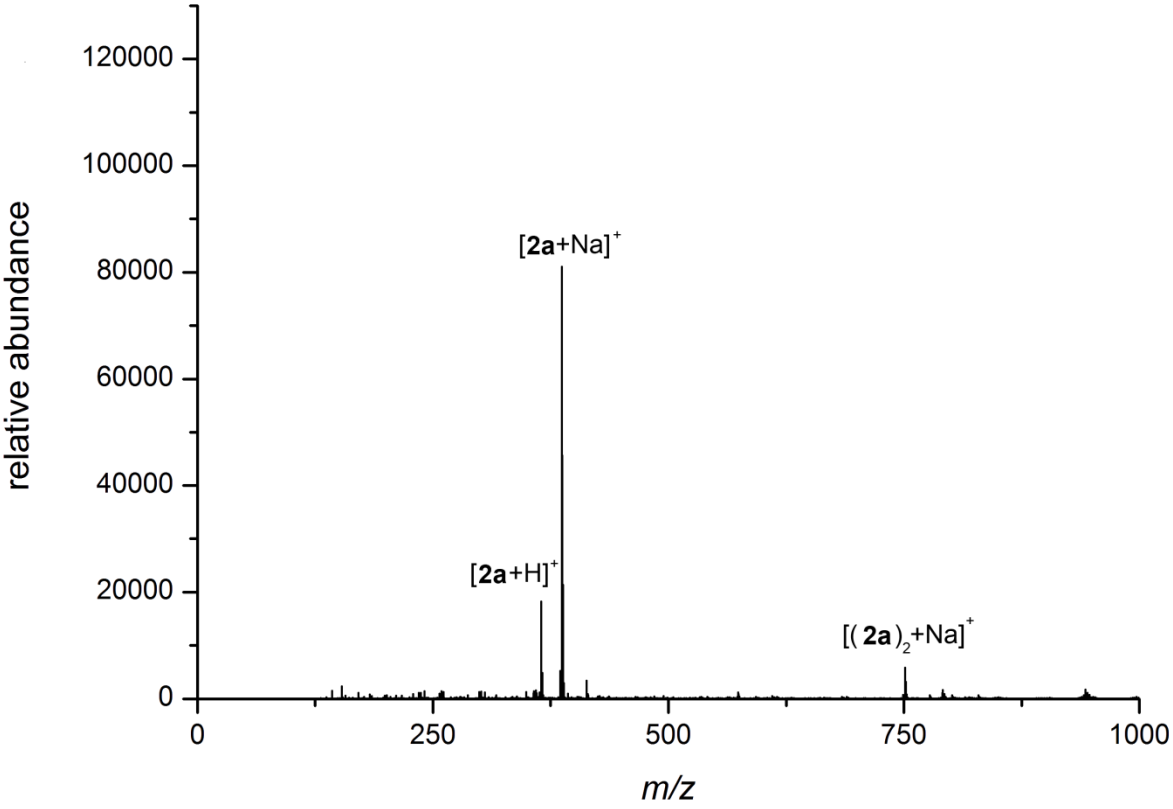

Figure S48 Full mass spectrum (MeOH) of model ligand **2a** with relevant peaks annotated.

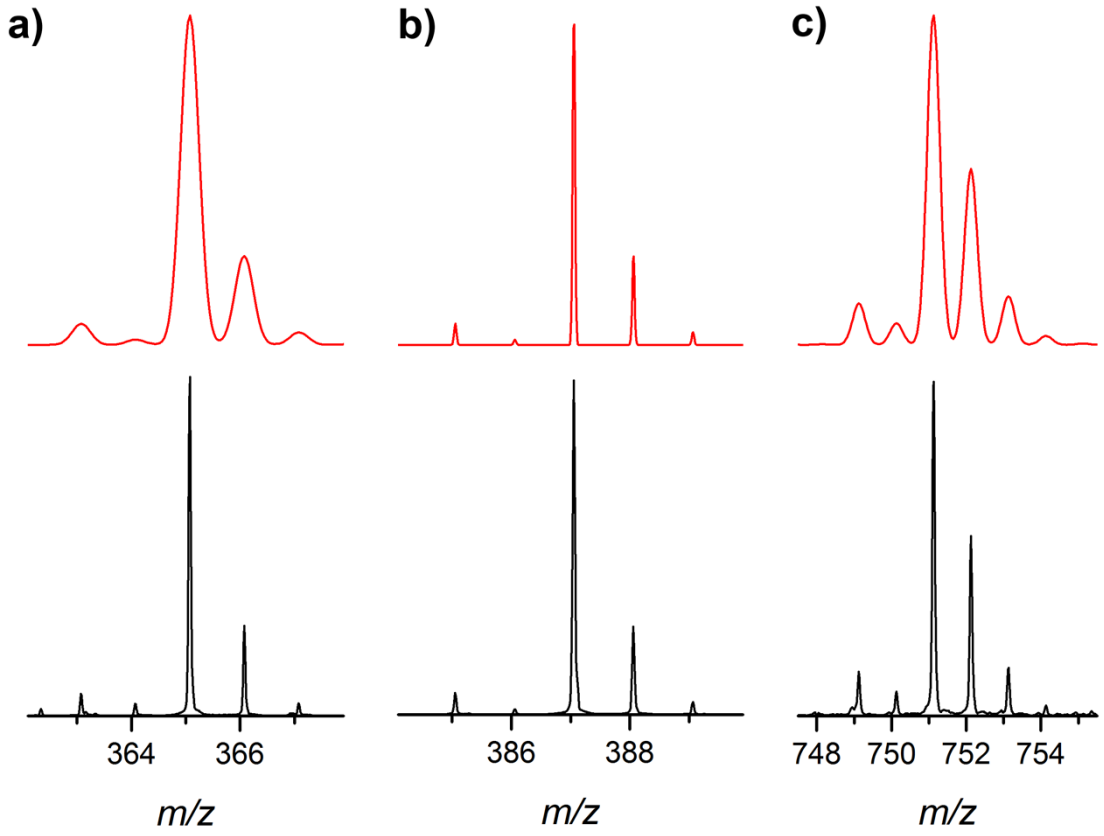

Figure S49 The calculated (red trace) and experimental (black trace) isotope patterns for a) [**2a**+H]$^+$, b) [**2a**+Na]$^+$, and c) [(**2a**)$_2$+Na]$^+$.

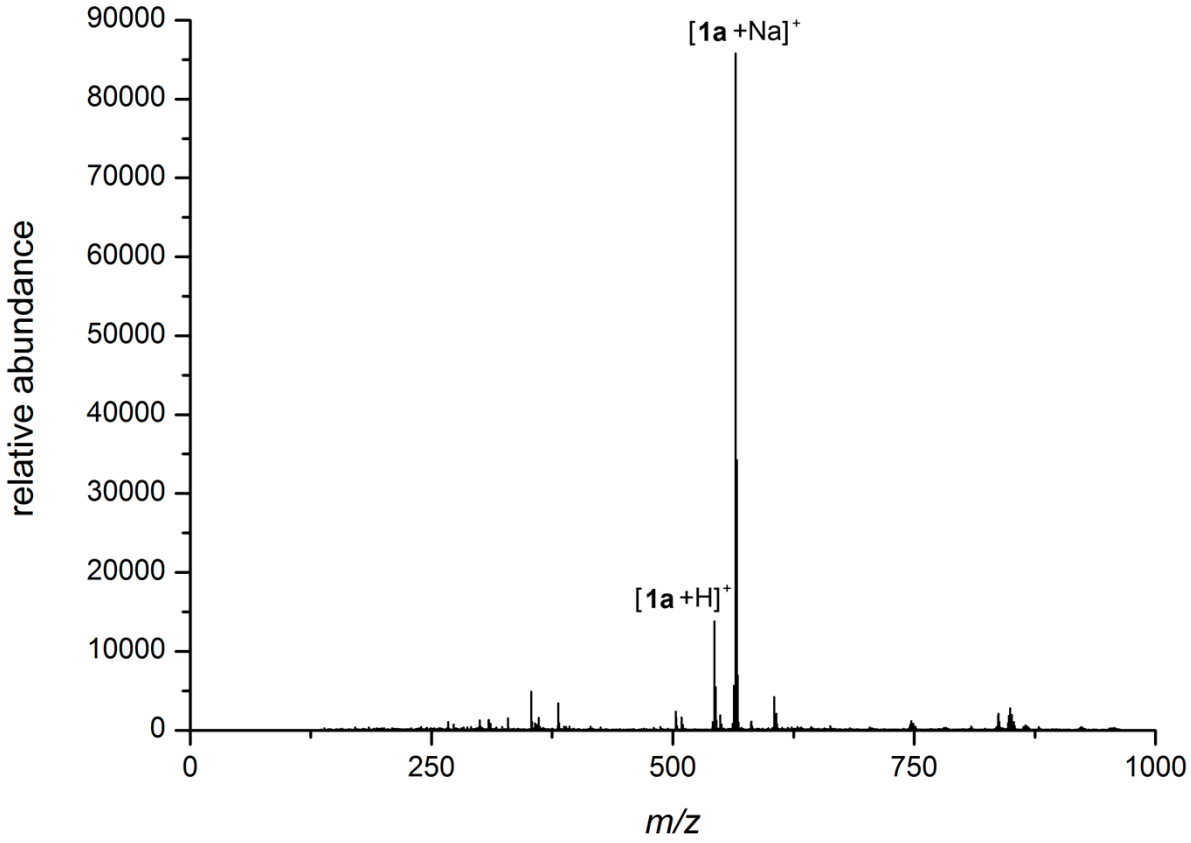

Figure S50 Full mass spectrum (MeOH) of rotor **1a** with relevant peaks annotated.

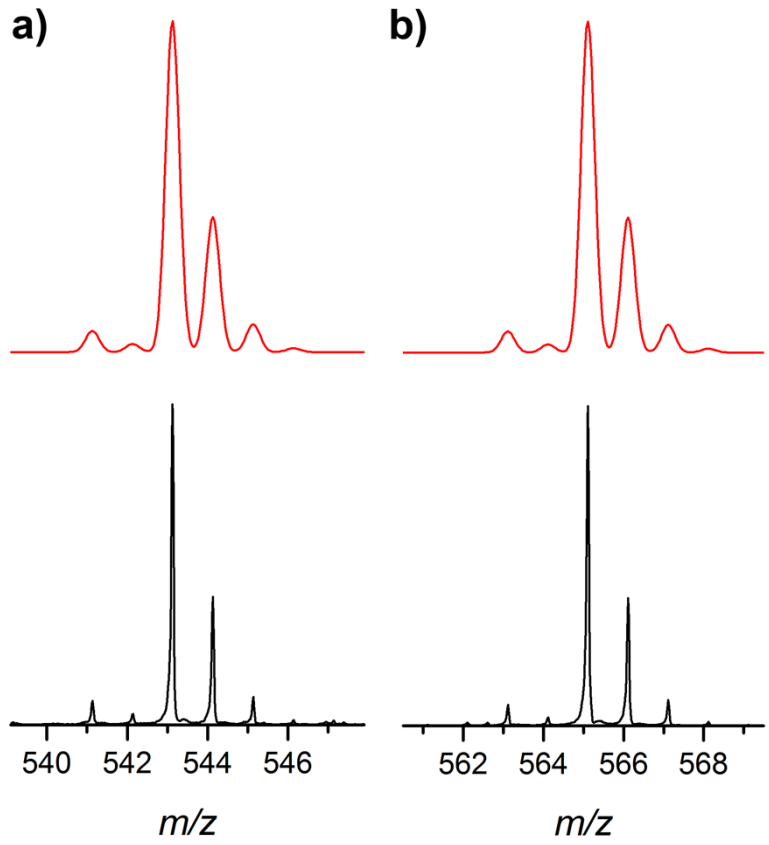

Figure S51 The calculated (red trace) and experimental (black trace) isotope patterns for a) [**1a**+H]$^+$, and b) [**1a**+Na]$^+$.

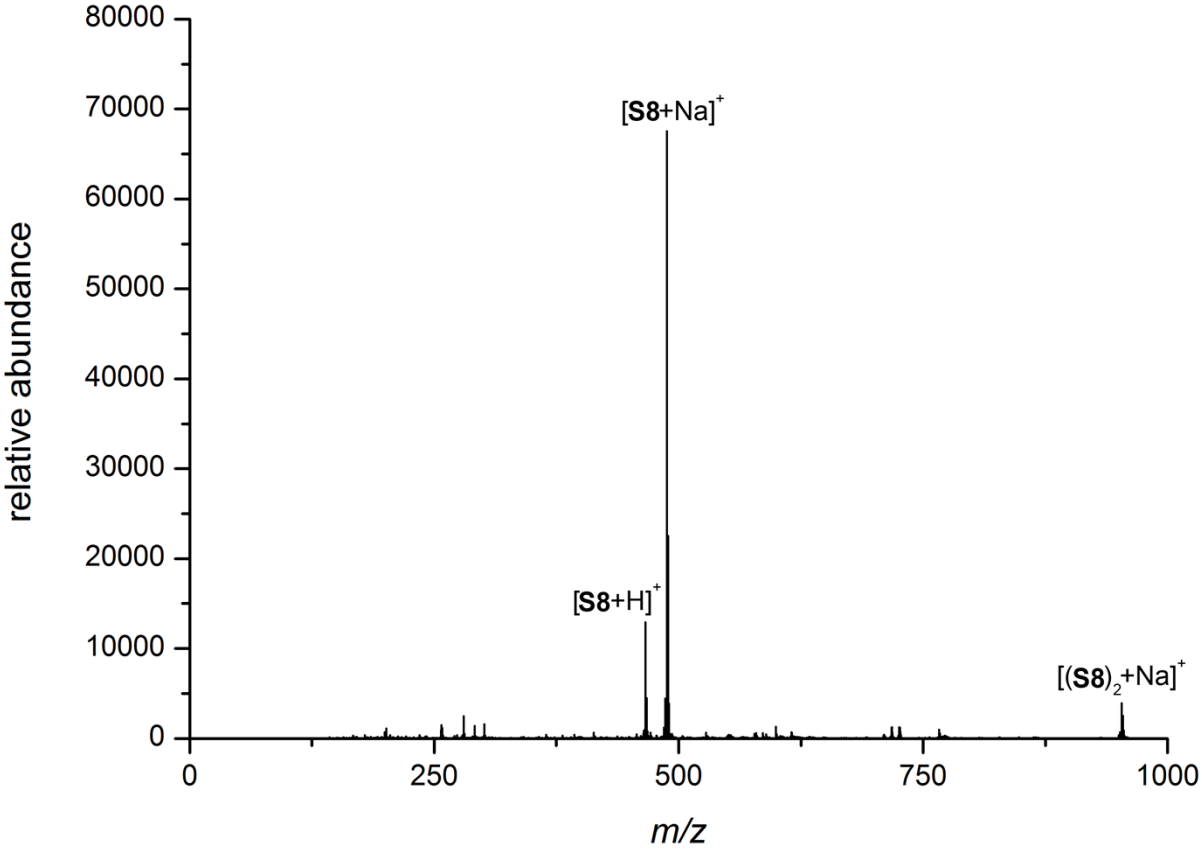

Figure S52 Full mass spectrum (MeOH) of **S8** with relevant peaks annotated.

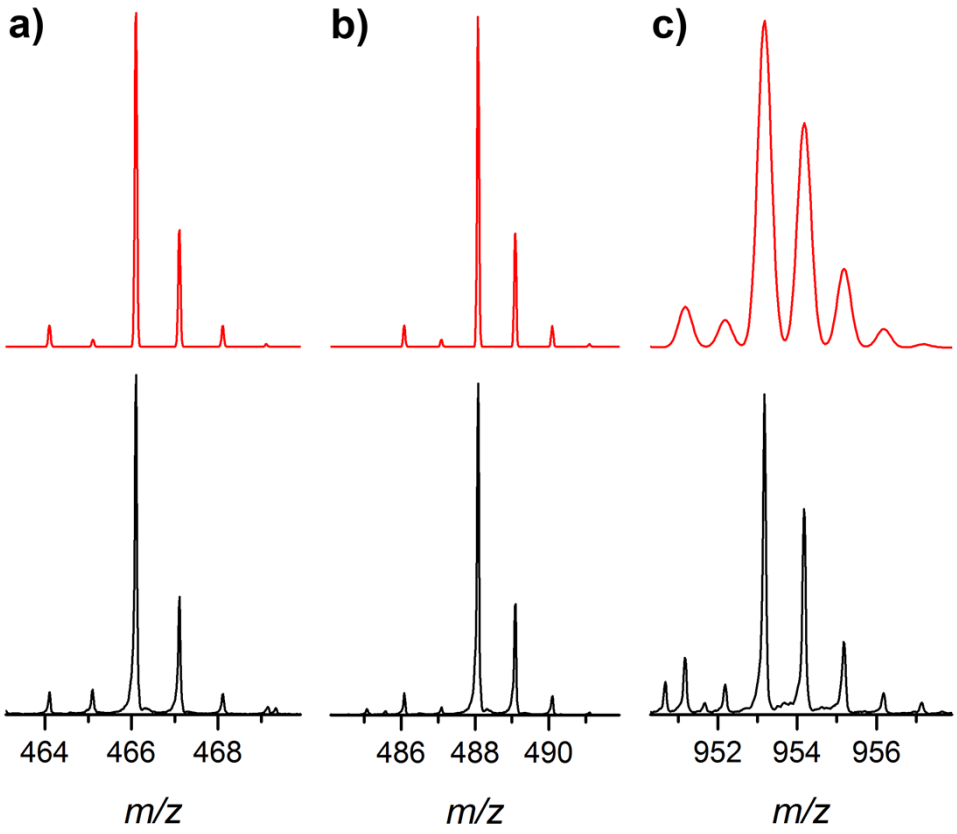

Figure S53 The calculated (red trace) and experimental (black trace) isotope patterns for a) [**S8**+H]$^+$, b) [**S8**+Na]$^+$, and c) [(**S8**)$_2$+Na]$^+$.

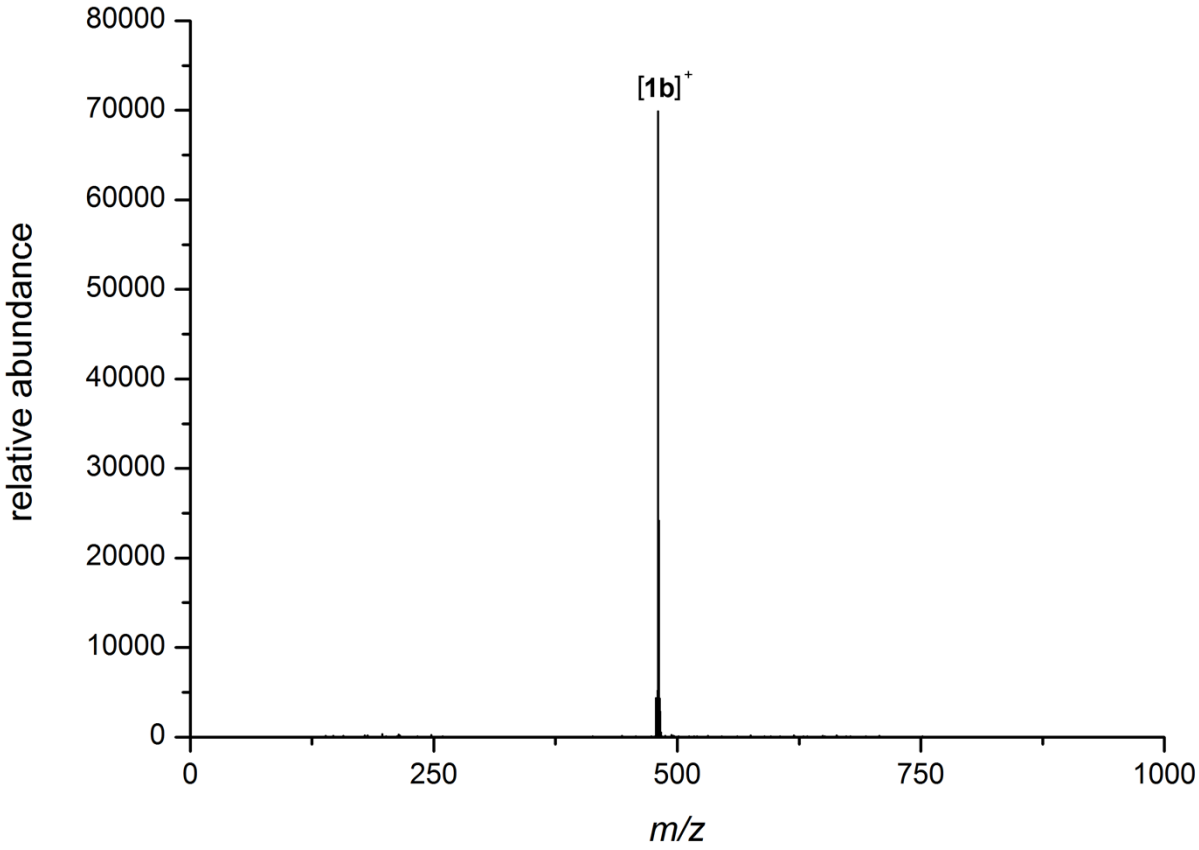

Figure S54 Full mass spectrum (MeOH) of rotor **1b** with relevant peak annotated.

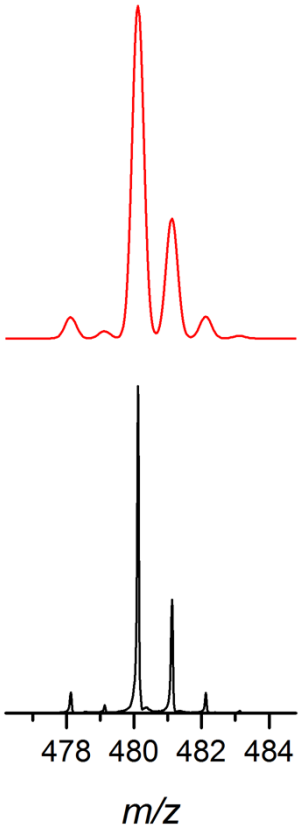

Figure S55 The calculated (red trace) and experimental (black trace) isotope patterns for [**1b**]$^{+}$.

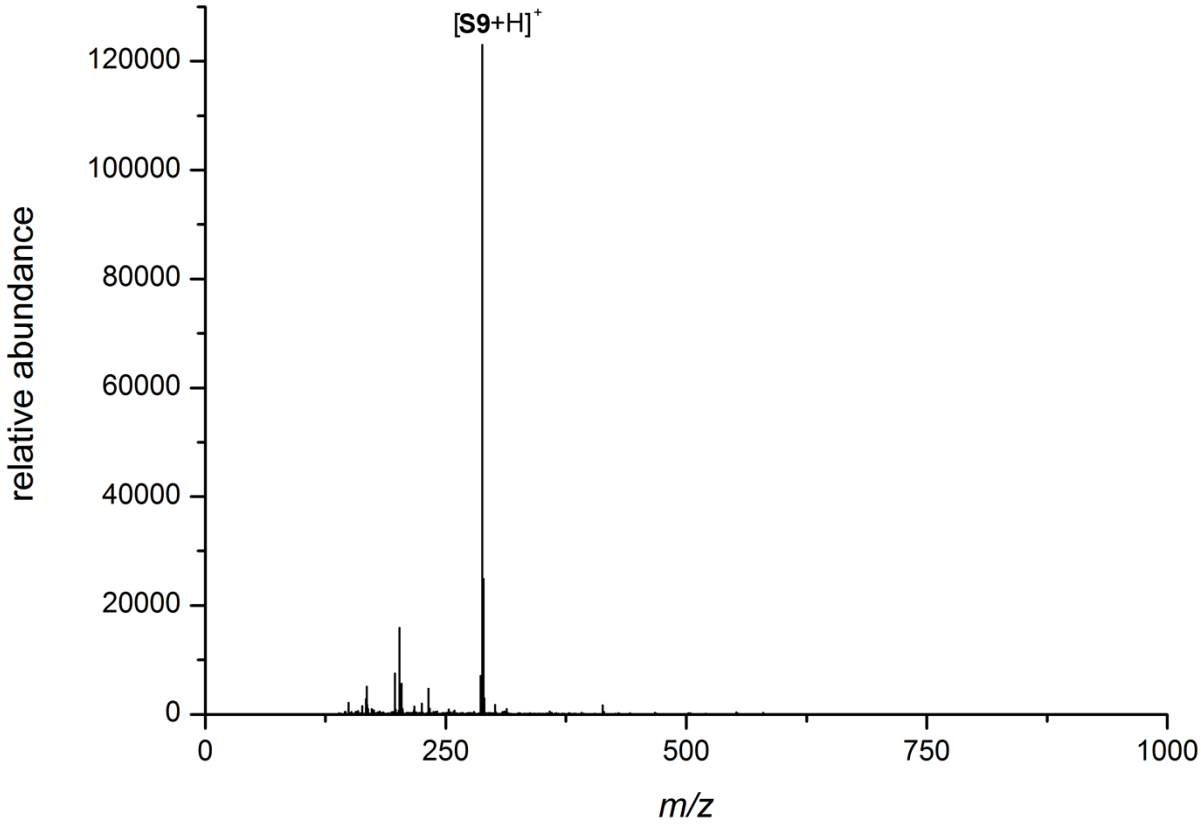

Figure S56 Full mass spectrum (MeOH) of **S9** with relevant peak annotated.

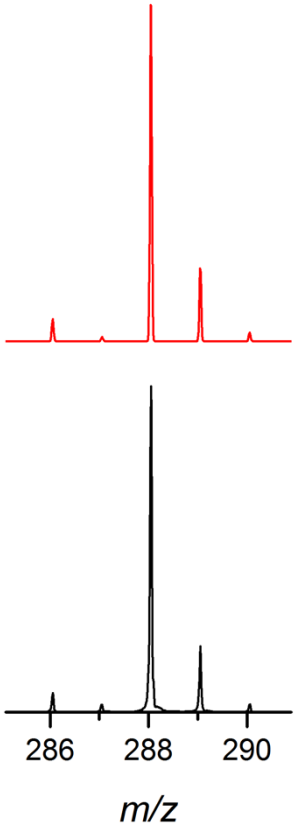

Figure S57 The calculated (red trace) and experimental (black trace) isotope patterns for [**S9**+H]$^+$.

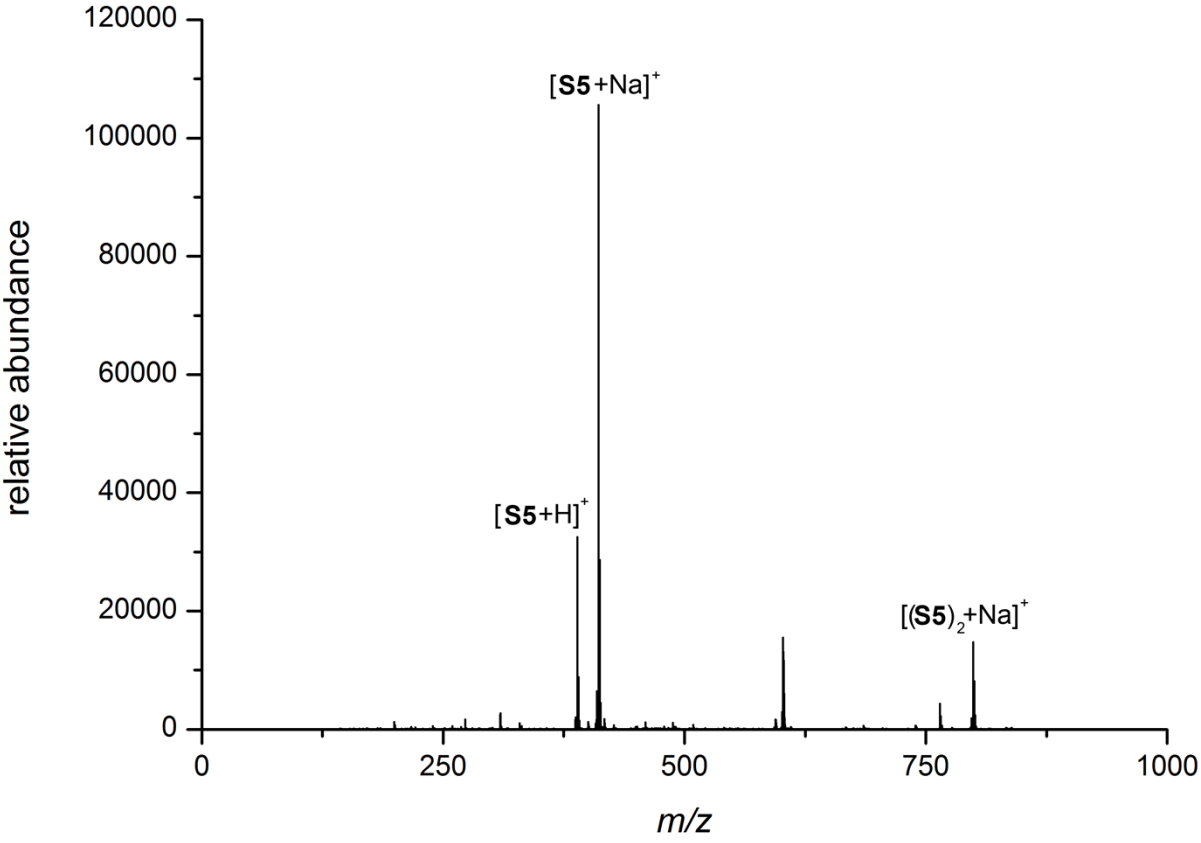

Figure S58 Full mass spectrum (MeOH) of **S5** with relevant peak annotated.

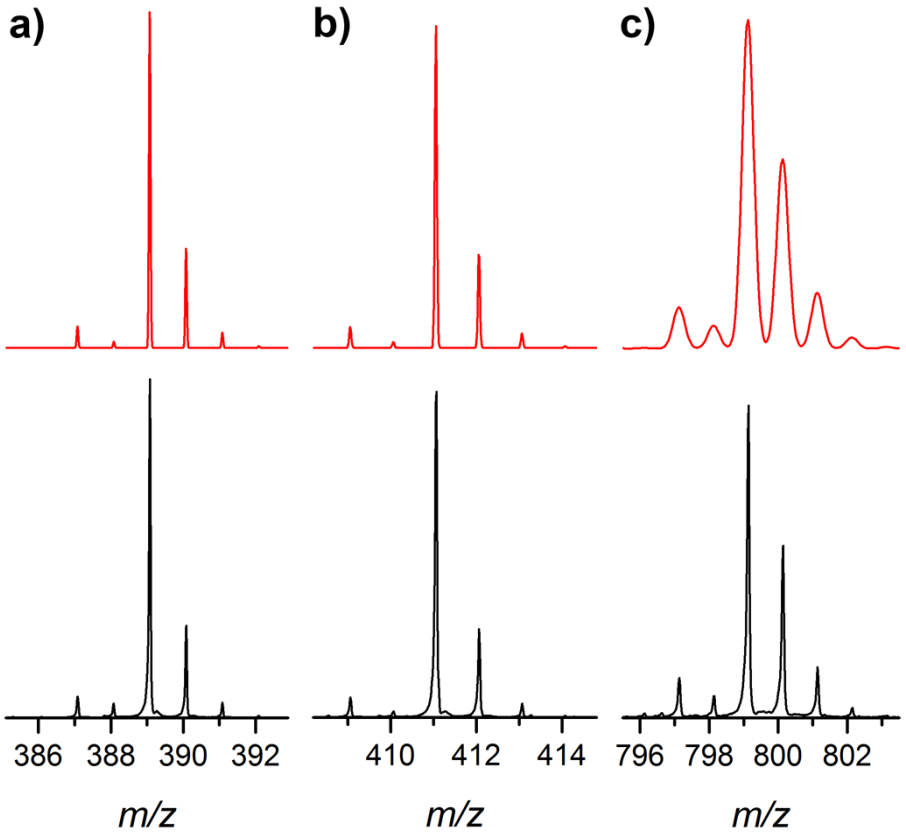

Figure S59 The calculated (red trace) and experimental (black trace) isotope patterns for a) [**S5**+H]$^+$, b) [**S5**+Na]$^+$, and c) [(**S5**)$_2$+Na]$^+$.

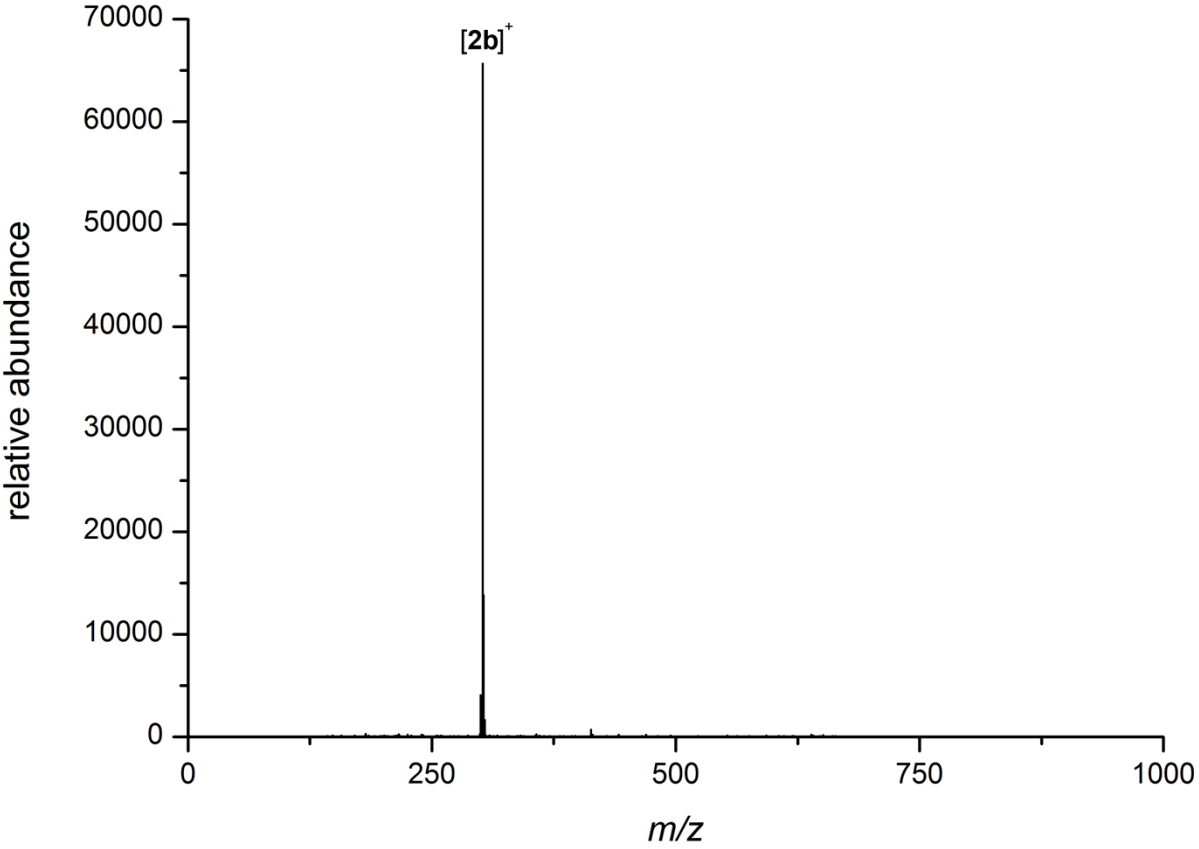

Figure S60 Full mass spectrum (MeOH) of model **2b** with relevant peak annotated.

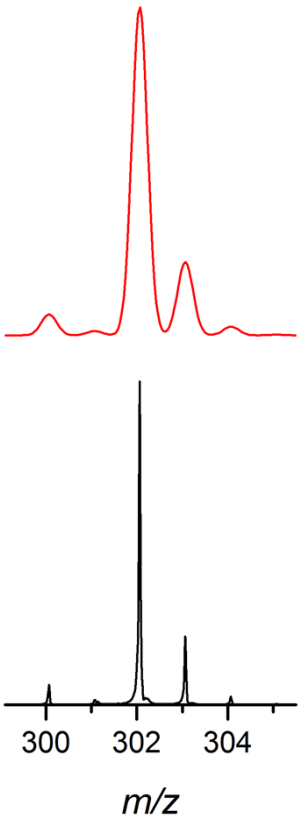

Figure S61 The calculated (red trace) and experimental (black trace) isotope patterns for [**2b**]$^{+}$.

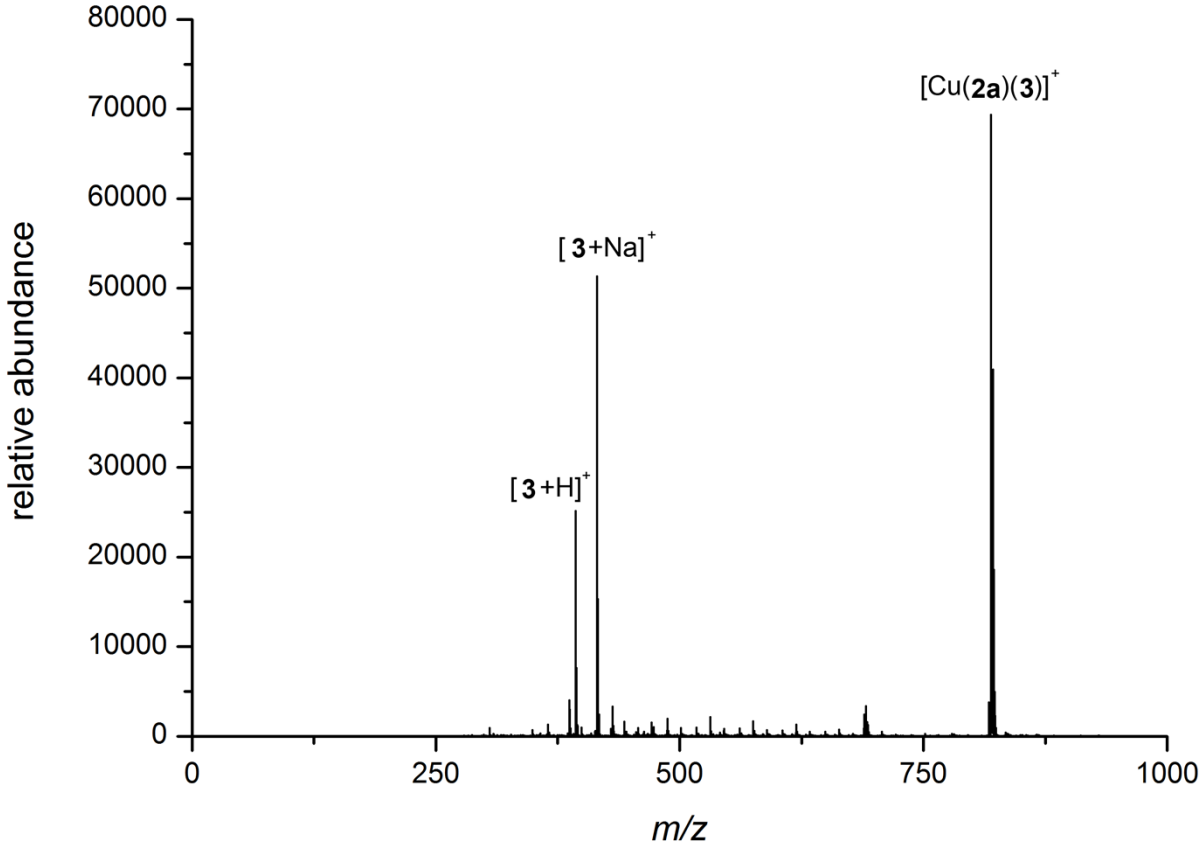

Figure S62 Full mass spectrum (MeOH) of complex [Cu(**2a**)(**3**)]PF_6 with relevant peaks annotated.

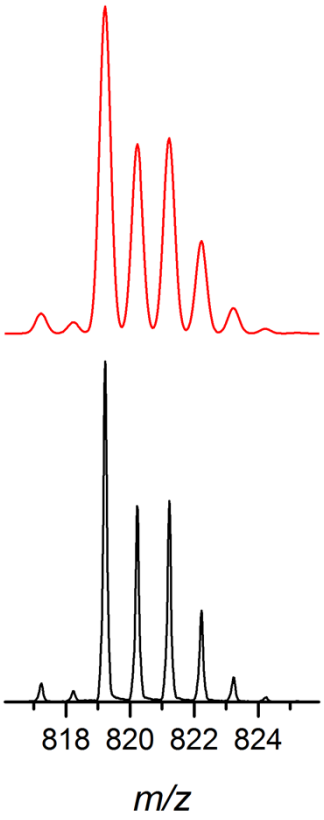

Figure S63 The calculated (red trace) and experimental (black trace) isotope patterns for [Cu(**2a**)(**3**)]$^+$.

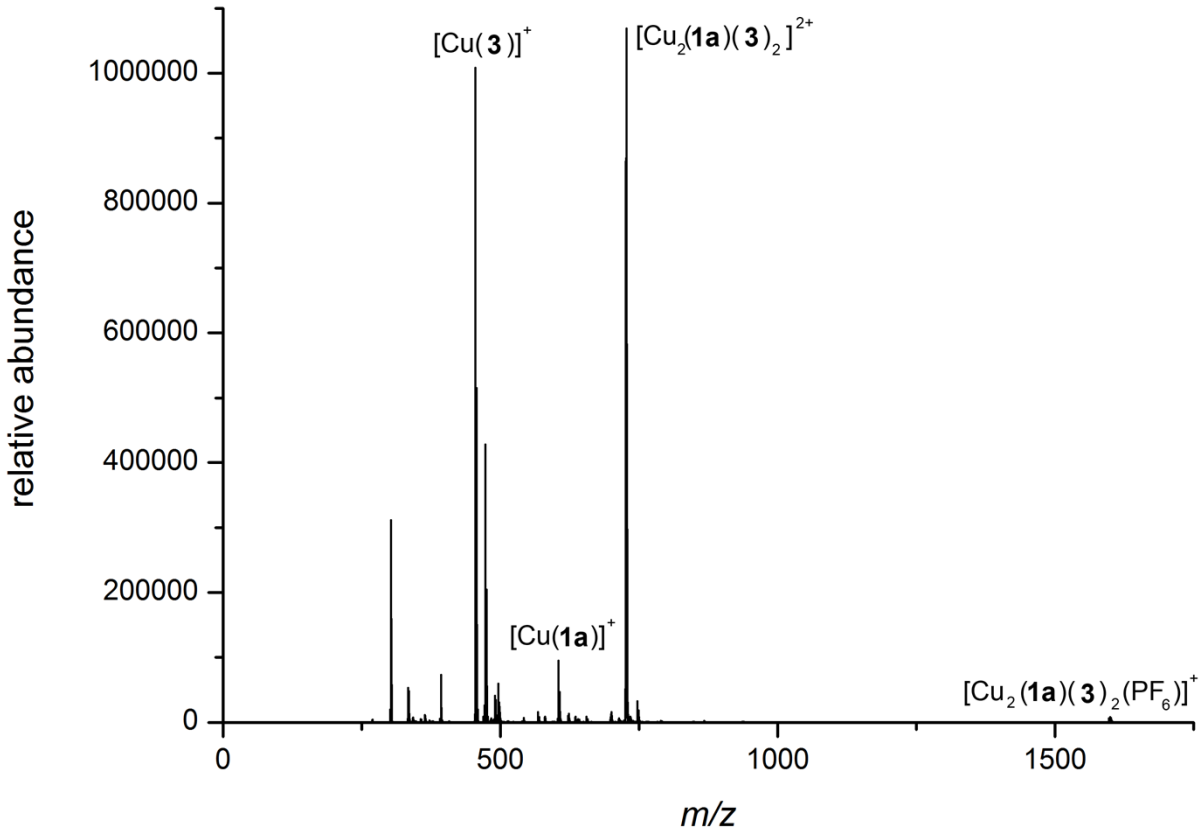

Figure S64 Full mass spectrum (MeOH) of complex $[Cu_2(\mathbf{1a})(\mathbf{3})_2](PF_6)_2$ with relevant peaks annotated.

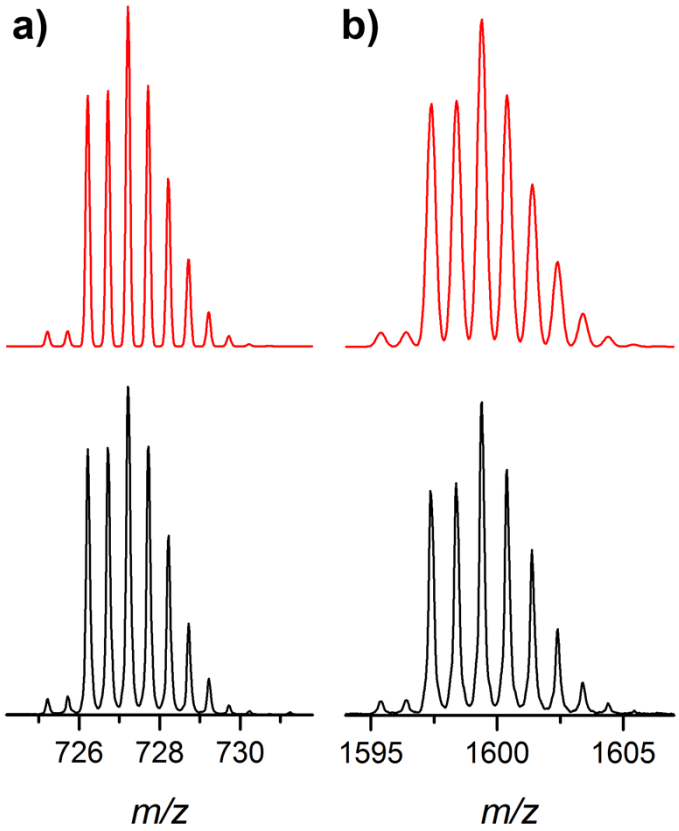

Figure S65 The calculated (red trace) and experimental (black trace) isotope patterns for a) $[Cu_2(\mathbf{1a})(\mathbf{3})_2]^{2+}$, and b) $[Cu_2(\mathbf{1a})(\mathbf{3})_2(PF_6)]^{+}$.

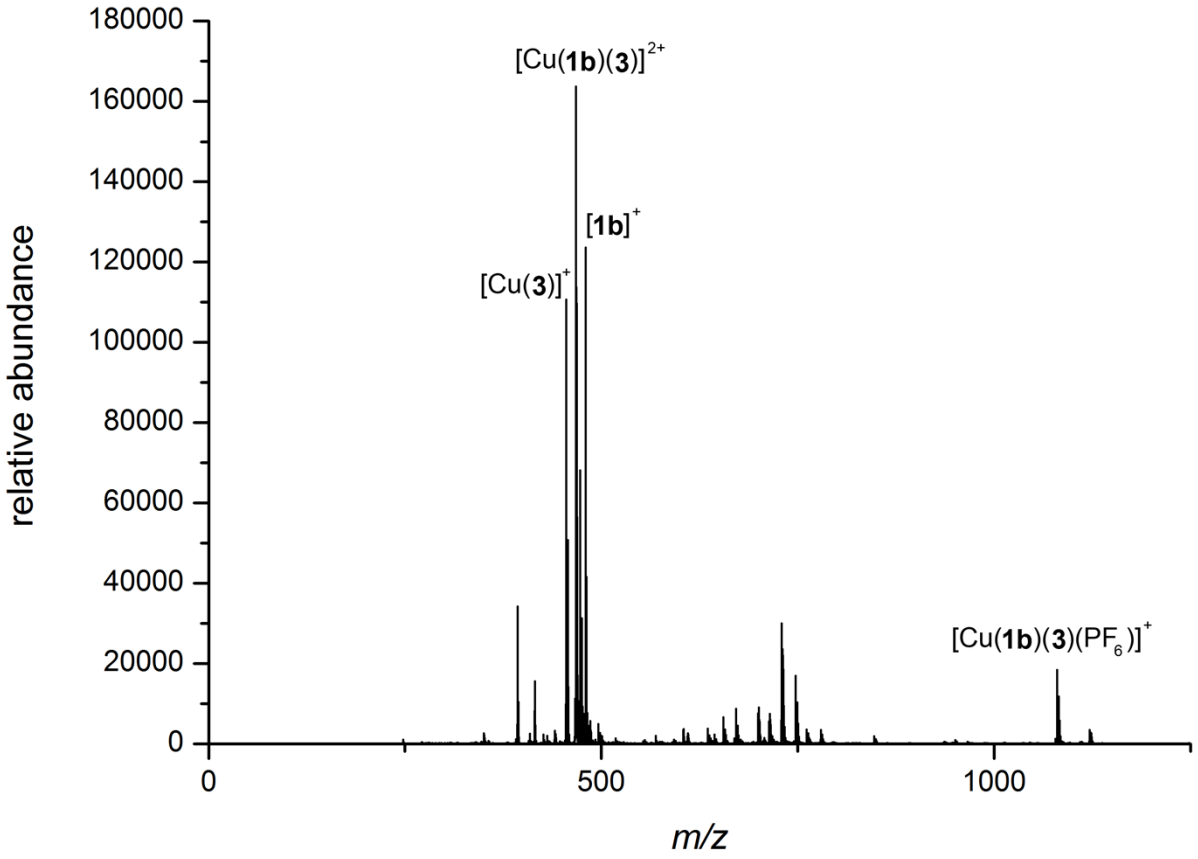

Figure S66 Full mass spectrum (MeOH) of complex [Cu(**1b**)(**3**)]$(PF_6)_2$ with relevant peaks annotated.

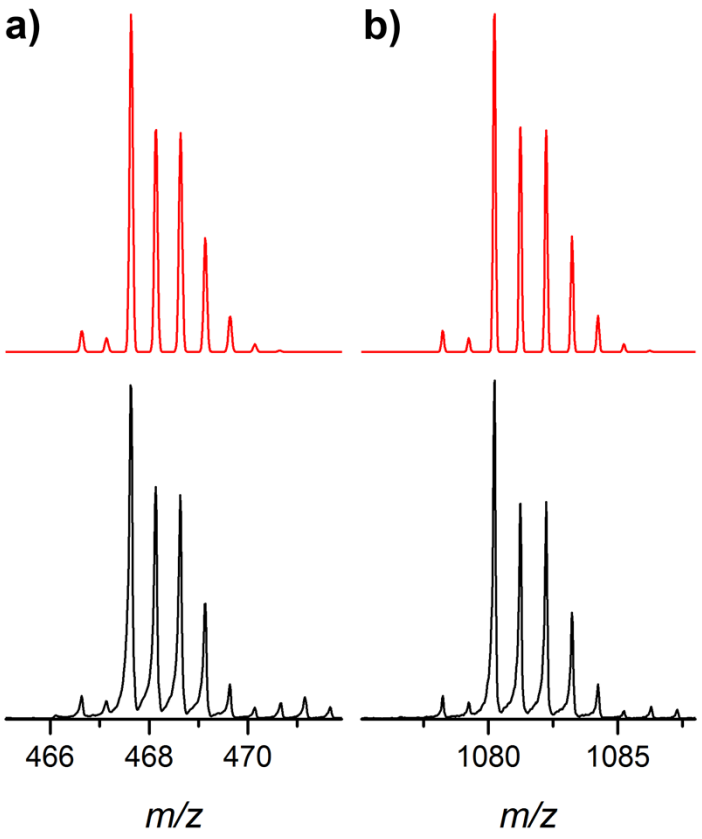

Figure S67 The calculated (red trace) and experimental (black trace) isotope patterns for a) [Cu(**1b**)(**3**)]$^{2+}$, and b) [Cu(**1b**)(**3**)(PF_6)]$^{+}$.

4 UV-Vis Spectra

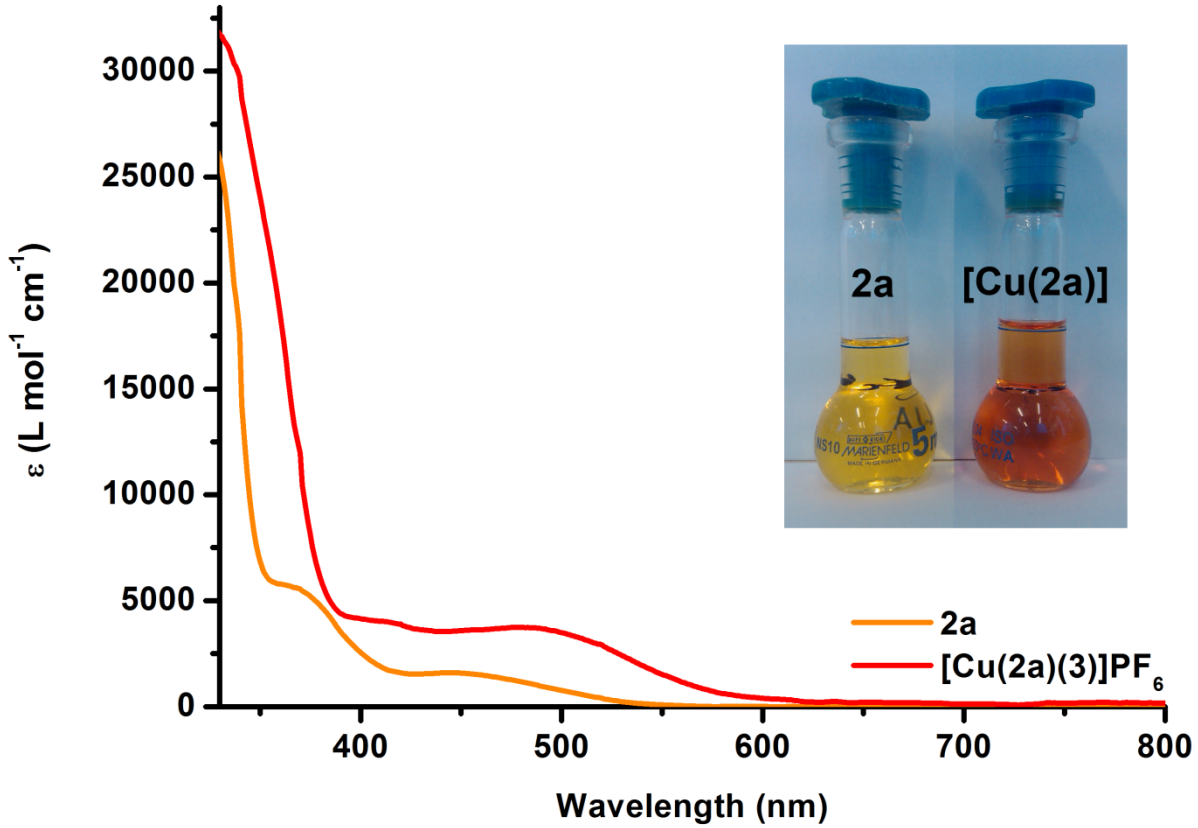

Figure S68 UV-Vis spectra of ligand **2a**, and its Cu(I) complexes [Cu(**2a**)(**3**)]PF_6 in acetone (~1x10^{-5} M). The inset shows the acetone solutions of the relevant compounds (~1x10^{-4} M).

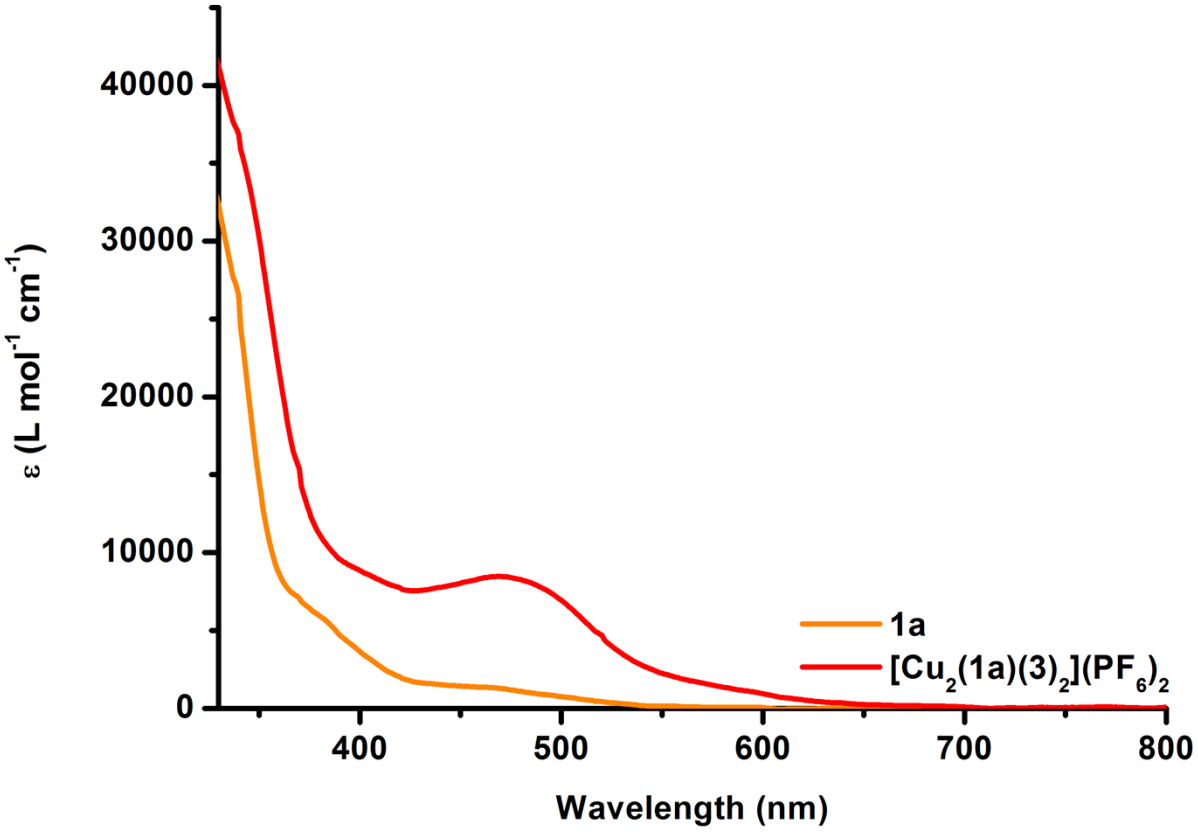

Figure S69 UV-Vis spectra of ligand **1a**, and its Cu(I) complex [Cu_2(**1a**)(**3**)$_2$](PF_6)$_2$ in acetone (~1x10^{-5} M).

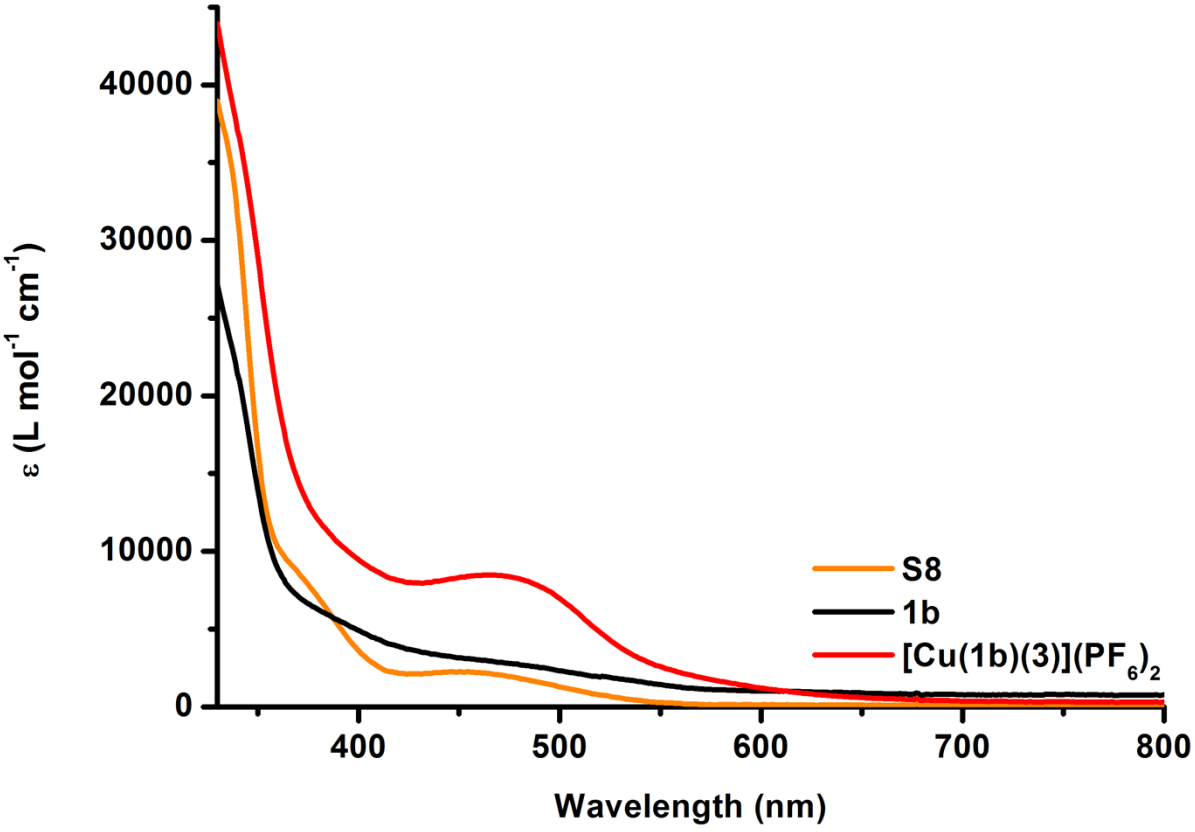

Figure S70 UV-Vis spectra of ligand **S8**, its methylated counterpart **1b**, and the Cu(I) complex [Cu(**1b**)(**3**)]$(PF_6)_2$ in acetone (~1x10^{-5} M).

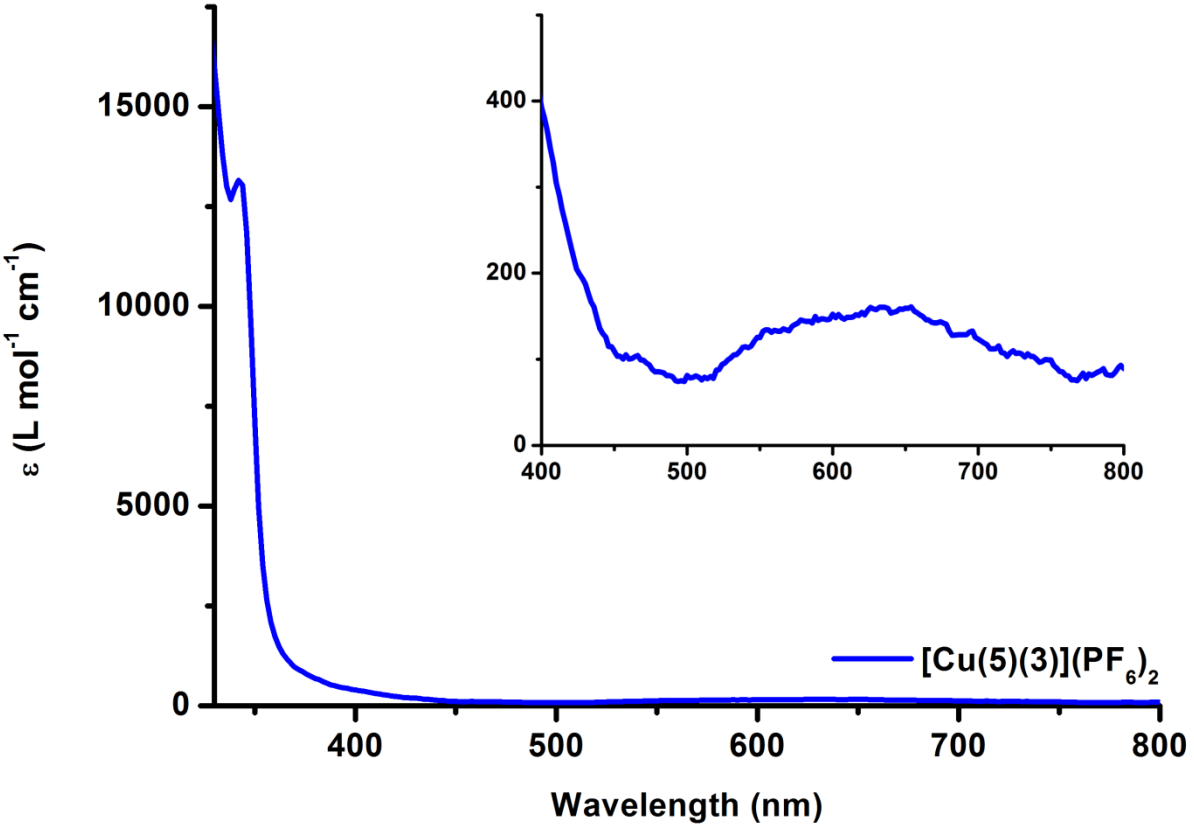

Figure S71 UV-Vis spectrum of Cu(II) complex [Cu(**5**)(**3**)]$(PF_6)_2$ in acetone (~1x10^{-5} M).

5 Electrochemistry

Cyclic voltammetric (CV) experiments in acetone or CH_2Cl_2 were performed at 20 ˚C on solutions degassed with argon. A three-electrode cell was used with Cypress Systems 1.4 mm diameter glassy carbon working, Ag/AgCl reference and platinum wire auxiliary electrodes. The solution was ~10^{-3} M in electroactive material and contained 0.1 M Bu_4NPF_6 as the supporting electrolyte. Voltammograms were recorded with the aid of a Powerlab/4sp computer-controlled potentiostat. Potentials are referenced to the reversible formal potential (taken as $E°$ = 0.00 V) for the decamethylferrocene $[Fc*]^{+/0}$ process.[9] Under the same conditions, $E°$ calculated for $[FcH]^{+/0}$ was 0.49 V (acetone) and 0.55 V (CH_2Cl_2).[10] Bulk electrolysis experiments were undertaken in a three-compartment cell in which the working and auxiliary compartments were separated by two fine frits to minimize mixing of the solutions. The experimental reference electrode was a AgCl-coated Ag wire prepared by anodic electrolysis of the wire in 1 M HCl. Spectroelectrochemical experiments were performed in acetone/0.1 M Bu_4NPF_6 solution in an OTTLE cell (pathlength 0.5 mm) with Pt working and auxiliary, and Ag reference electrodes.

Table S1 Electrochemical data for the mono- and di-armed ferrocene systems (**2a** and **1a**), their Cu(I) complexes, and the Cu(II) complex [Cu(**5**)(**3**)]$(PF_6)_2$.

Compounds	$E°$ (V) (acetone)[a]		$E°$ (V) (CH_2Cl_2)[a]	
	$Cu^{II/I}$	$Fc^{+/0}$	$Cu^{II/I}$	$Fc^{+/0}$
2a	-	0.64	-	0.68
[Cu(**2a**)(**3**)]PF_6	0.61	0.68	0.72	0.79
[Cu(**5**)(**3**)]$(PF_6)_2$	0.00	-	insol.	-
1a	-	insol.	-	0.78
[Cu_2(**1a**)(**3**)$_2$]$(PF_6)_2$	0.64	0.85	0.81	0.85

[a] 1x10^{-3} M in analyte, 0.1 M Bu_4NPF_6, referenced to $[Fc*]^{+/0}$ = 0.00 V.

5.1 Representative Voltammograms

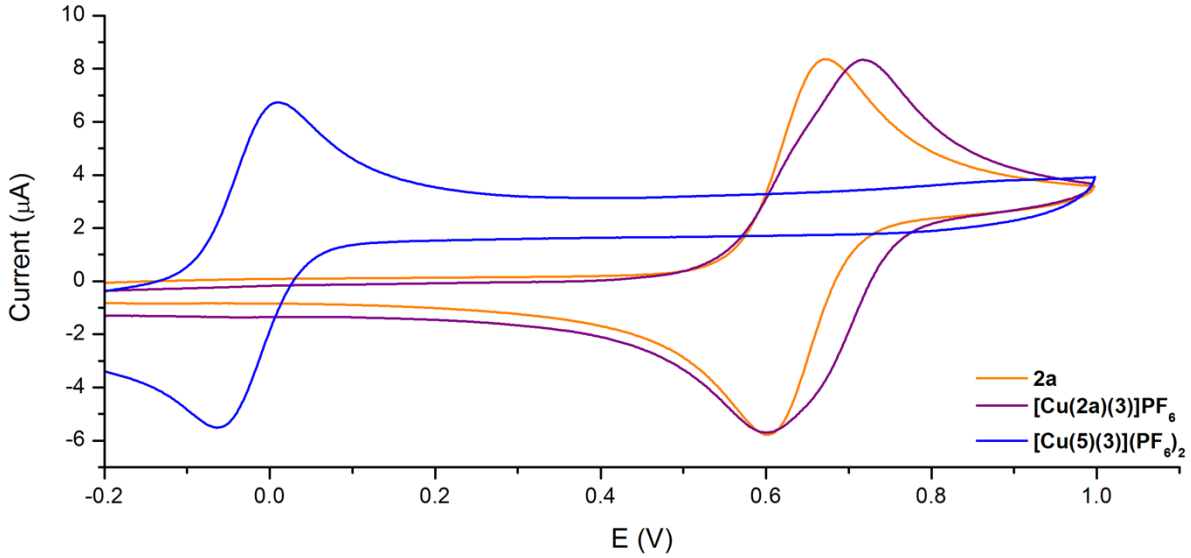

Figure S72 CVs (100 mV s^{-1}) of the model ligand **2a**, its Cu(I) complex [Cu(**2a**)(**3**)]PF_6, and the Cu(II) complex [Cu(**5**)(**3**)]$(PF_6)_2$ in acetone.

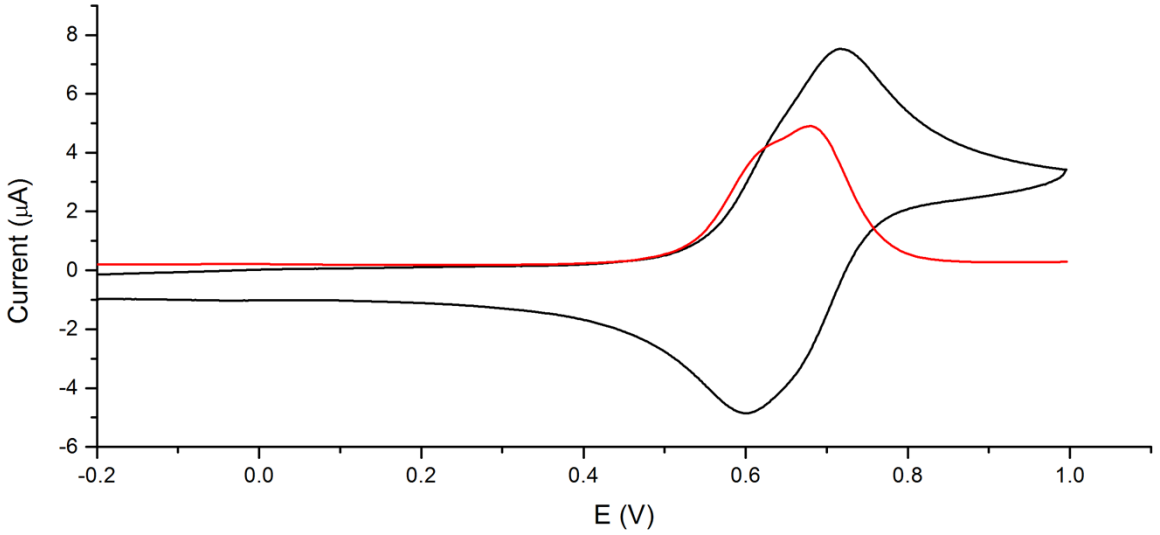

Figure S73 CV (black trace, 100 mV s^{-1}) and DPV (red trace) of the complex [Cu(**2a**)(**3**)]PF_6 in acetone, where the DPV shows the partial resolution of the ferrocene centred and Cu(I) centred oxidations.

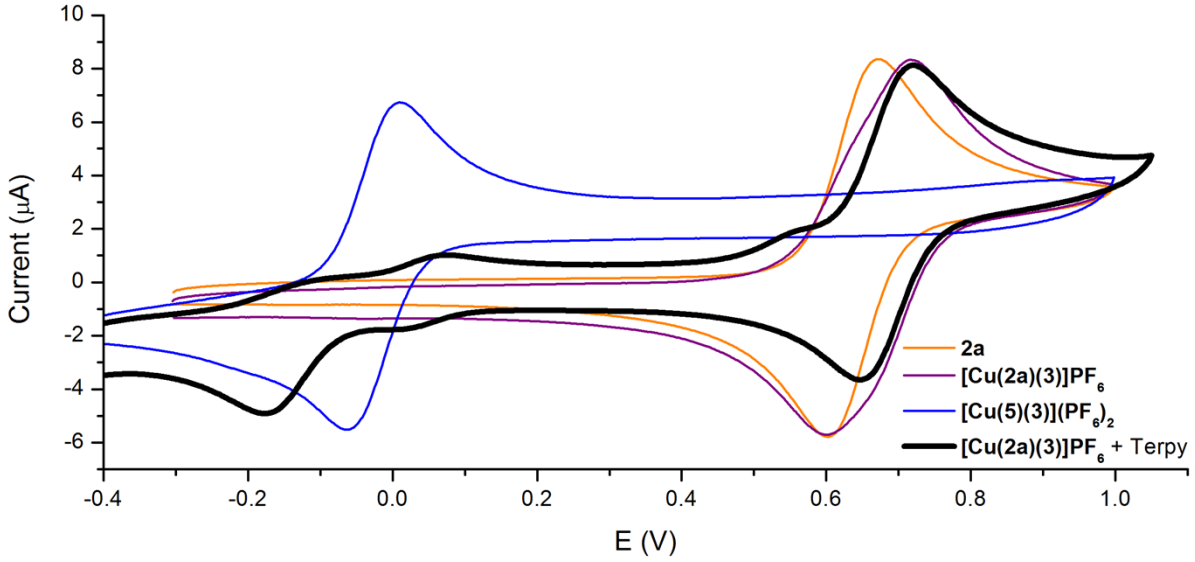

Figure S74 CVs (100 mV s^{-1}) of the model ligand **2a**, its Cu(I) complex [Cu(**2a**)(**3**)]PF_6, the Cu(II) complex [Cu(**5**)(**3**)]$(PF_6)_2$, and [Cu(**2a**)(**3**)]PF_6 in the presence of terpyridine in acetone.

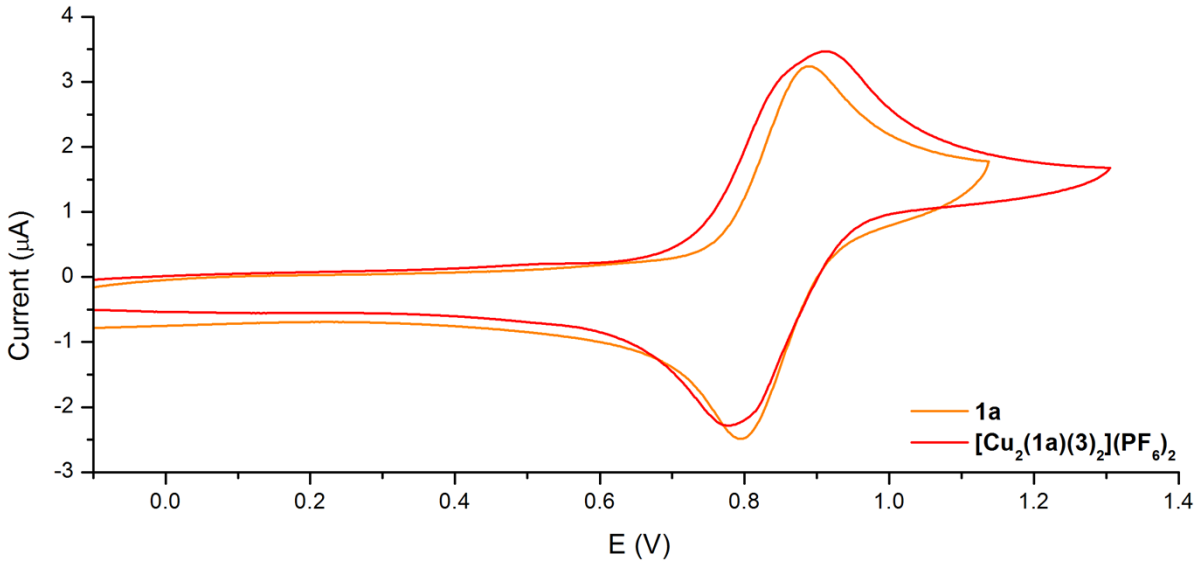

Figure S75 CVs (100 mV s^{-1}) of the di-arm ligand **1a**, and its Cu(I) complex $[Cu_2(\mathbf{1a})(\mathbf{3})_2](PF_6)_2$ in CH_2Cl_2.

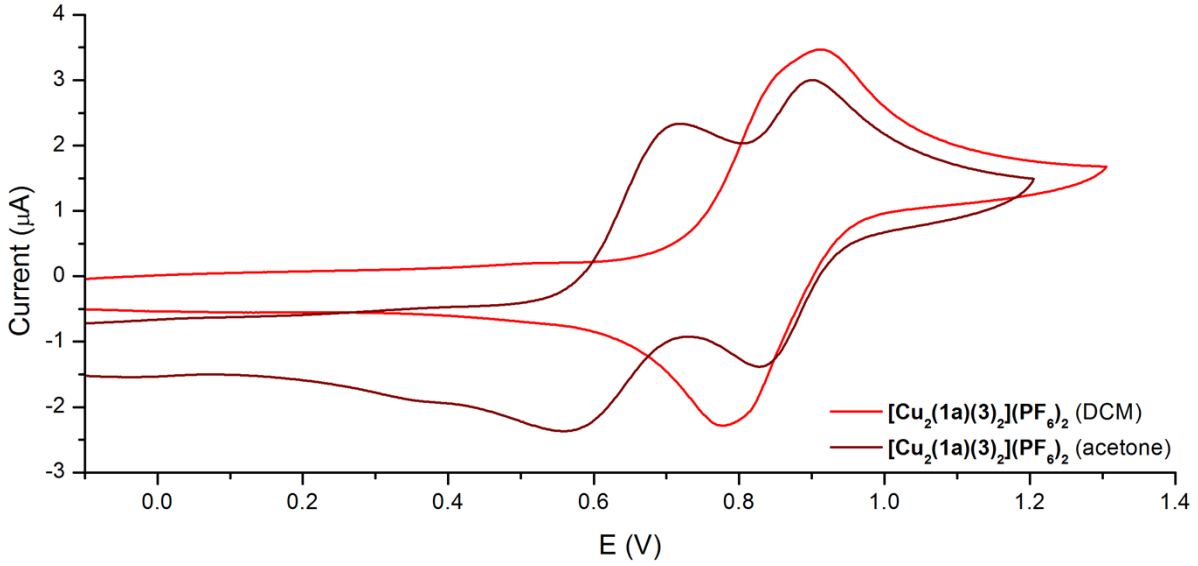

Figure S76 CVs (100 mV s^{-1}) of complex $[Cu_2(\mathbf{1a})(\mathbf{3})_2](PF_6)_2$ in acetone and CH_2Cl_2, illustrating the increased peak resolution attained in acetone.

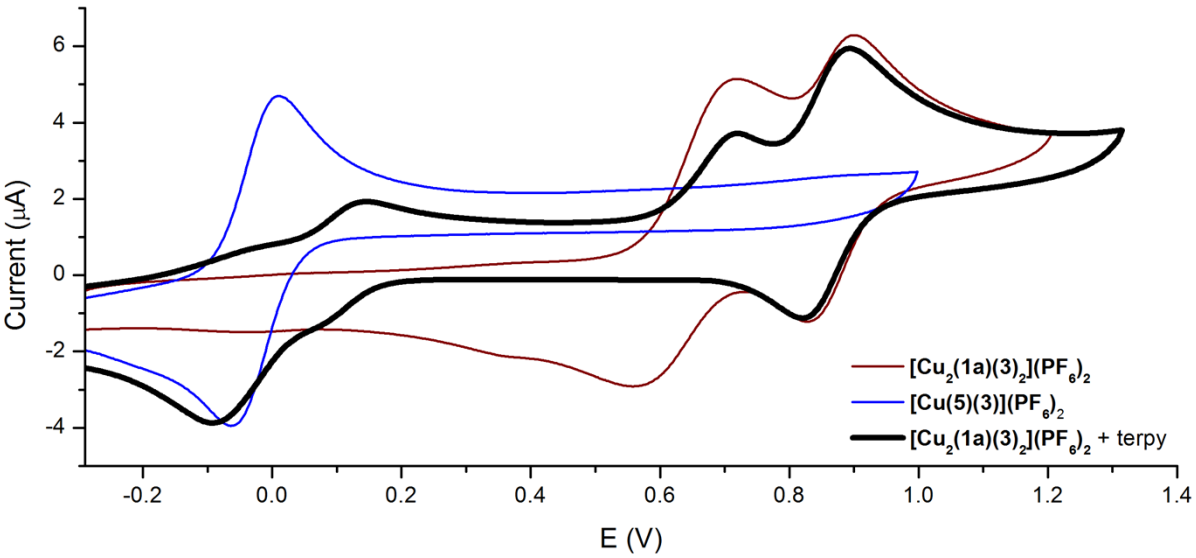

Figure S77 CVs (100 mV s^{-1}) of the Cu(I) complex $[Cu_2(\mathbf{1a})(\mathbf{3})_2](PF_6)_2$, the Cu(II) complex $[Cu(\mathbf{5})(\mathbf{3})](PF_6)_2$, and $[Cu_2(\mathbf{1a})(\mathbf{3})_2](PF_6)_2$ in the presence of terpy in acetone.

5.2 Spectroelectrochemistry Plots

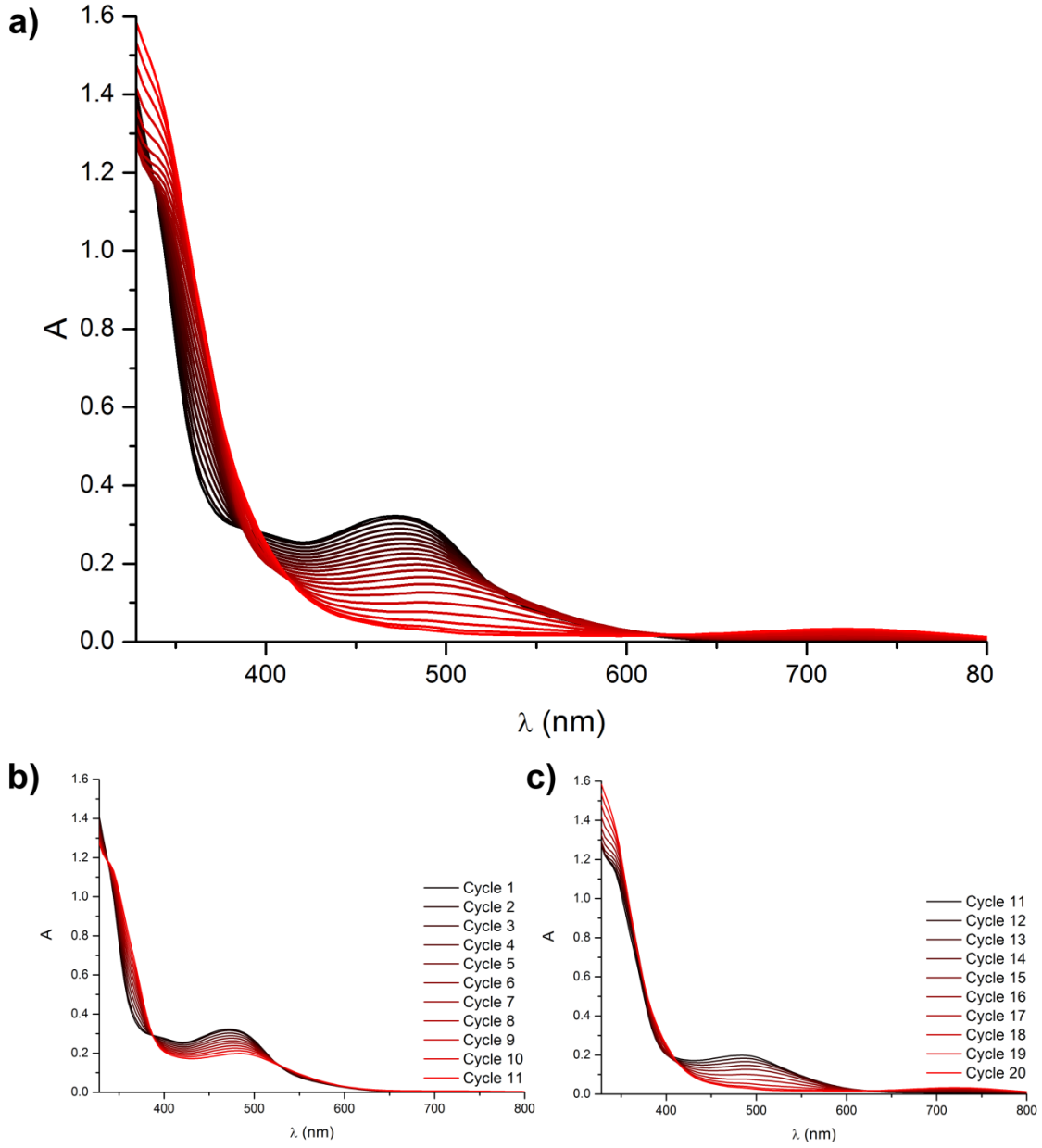

Figure S78 UV-Vis spectra of a) complex [Cu(**2a**)(**3**)]PF_6 as it is fully oxidised over time (time = 0 s in black, each cycle 108 s apart). The oxidation can be split into two separate processes: b) the oxidation of the Cu(I) to Cu(II), and c) the oxidation of the Fc to Fc^+.

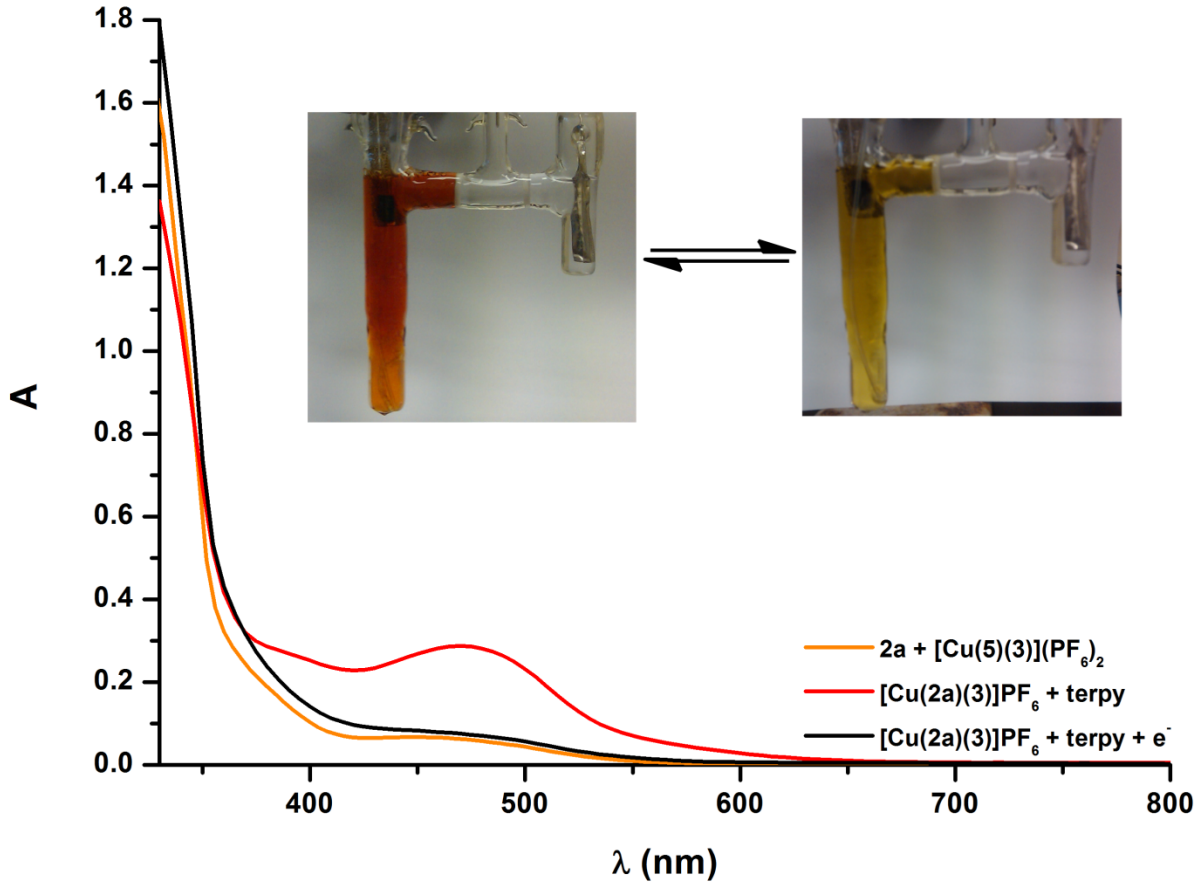

Figure S79 UV-Vis spectra of ligand **2a** in the presence of [Cu(**5**)(**3**)]$(PF_6)_2$, complex [Cu(**2a**)(**3**)]PF_6 in the presence of terpyridine, and the complex [Cu(**2a**)(**3**)]PF_6 in the presence of terpyridine after the oxidation of the Cu(I) to Cu(II), showing the electrochemically induced switching of the model system from the complex [Cu(**2a**)(**3**)]PF_6 to the free ligand **2a** plus complex [Cu(**5**)(**3**)]$(PF_6)_2$. Inset is the colour change seen during bulk electrolysis of a 1 mM solution, wherein the red colour of the complex [Cu(**2a**)(**3**)]PF_6 fades to the yellow of the free ligand **2a** after + 0.5 V has been passed through the solution for ~5 minutes. The colour change is reversed on application of – 0.5 V, as the system is reduced back to the Cu(I) complex [Cu(**2a**)(**3**)]PF_6.

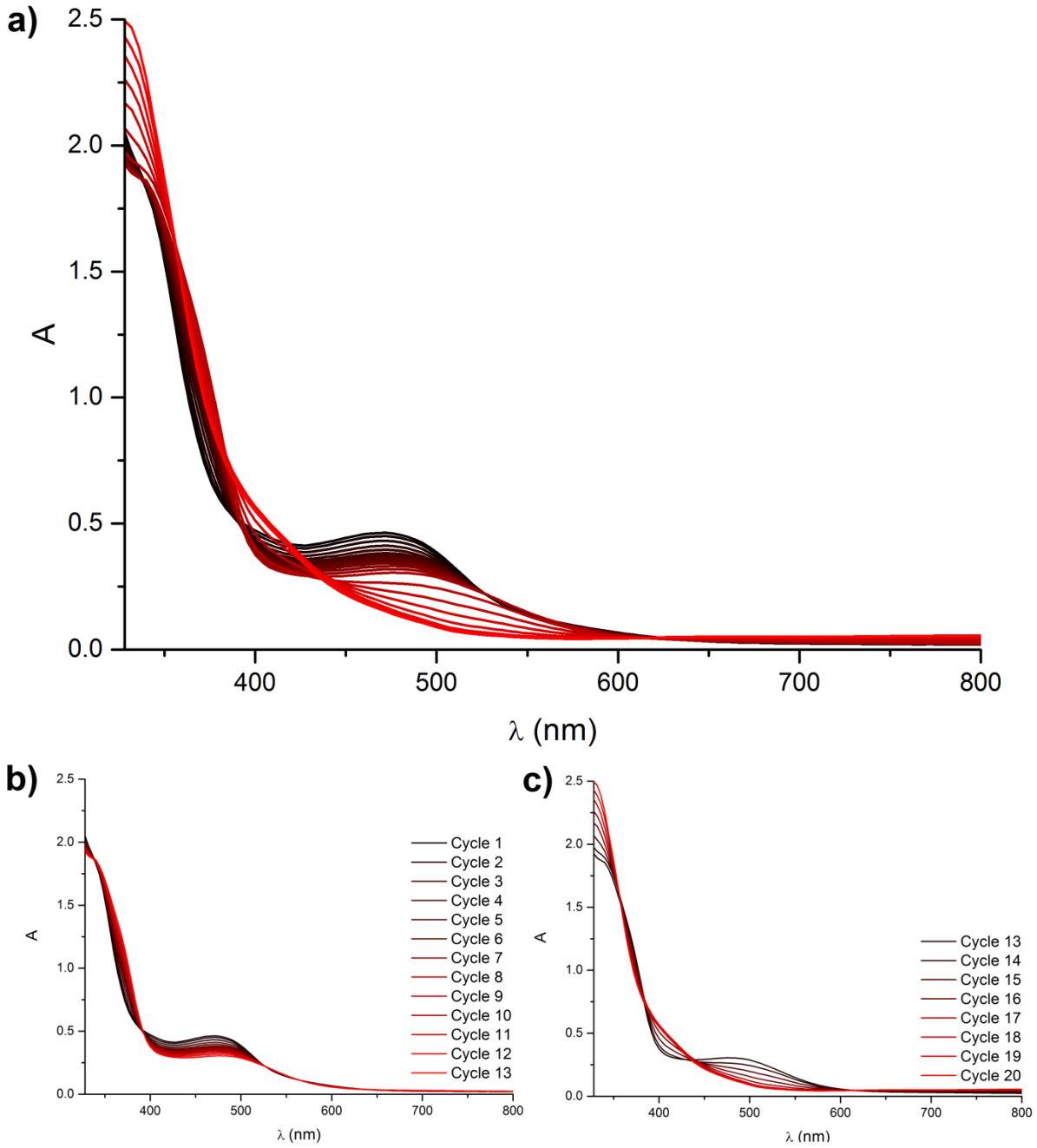

Figure S80 UV-Vis spectra of a) complex $[Cu_2(\mathbf{1a})(\mathbf{3})_2](PF_6)_2$ as it is fully oxidised over time (time = 0 s in black, each cycle 108 s apart). The oxidation can be split into two separate processes: b) the oxidation of the Cu(I) to Cu(II), and c) the oxidation of the Fc to Fc^+.

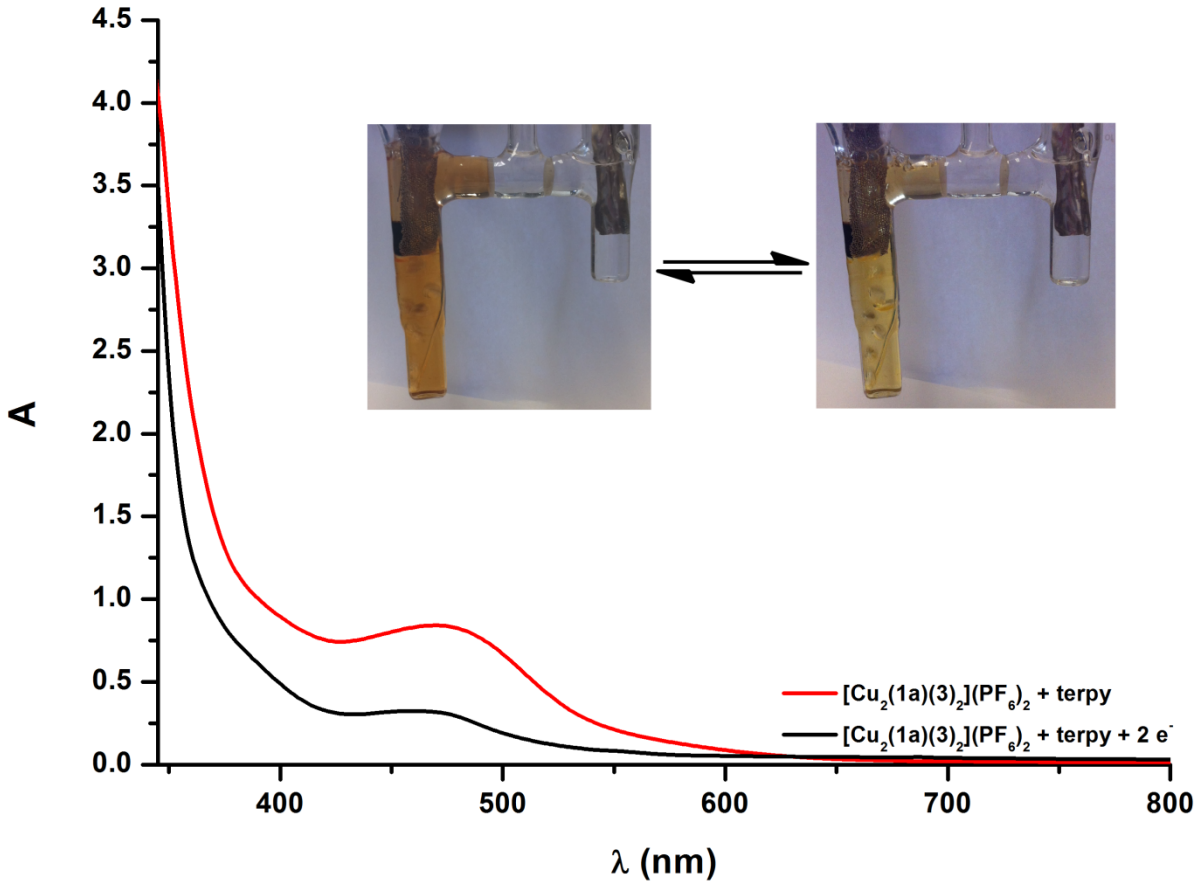

Figure S81 UV-Vis spectra of complex $[Cu_2(\mathbf{1a})(\mathbf{3})_2](PF_6)_2$ in the presence of terpyridine, and the complex $[Cu_2(\mathbf{1a})(\mathbf{3})_2](PF_6)_2$ in the presence of terpyridine after the oxidation of the Cu(I) to Cu(II), showing the electrochemically induced switching of the model system from the complex $[Cu_2(\mathbf{1a})(\mathbf{3})_2](PF_6)_2$ to the free ligand **1a** plus complex $[Cu(\mathbf{5})(\mathbf{3})](PF_6)_2$. The free ligand **1a** was not soluble enough in acetone to allow a separate plot of the free ligand and $[Cu(\mathbf{5})(\mathbf{3})](PF_6)_2$, however, the ligand does stay in solution during the bulk electrolysis due to the presence of the electrolyte keeping the ligand from aggregating and precipitating. Inset is the colour change seen during bulk electrolysis of a 0.1 mM solution, wherein the red colour of the complex $[Cu_2(\mathbf{1a})(\mathbf{3})_2](PF_6)_2$ fades to the yellow of the free ligand **1a** after + 0.5 V has been passed through the solution for ~5 minutes. The colour change is reversed on application of – 0.5 V, as the system is reduced back to the Cu(I) complex $[Cu_2(\mathbf{1a})(\mathbf{3})_2](PF_6)_2$. A time-lapse video of the reversible process is available in the ESI (see publisher's website).

6 Computational Details

Computational modelling was performed with the Gaussian 09 software package[11] using the CAM-B3LYP[12] functional and 6-31G(d) basis set. A DMF solvent field was implemented using an integral equation formalism polarisable continuum model (IEF-PCM) self-consistent reaction field (SCRF)[13] with the default solvent parameters provided by Gaussian. Ligands **1a** and **1b** were modelled in both the open and closed forms while the Cu complexes $[Cu_2(\mathbf{1a})(\mathbf{3})_2](PF_6)_2$ and $[Cu(\mathbf{1b})(\mathbf{3})](PF_6)_2$ were modelled only in the open form. Simulated Raman spectra were generated utilising GaussSum v2.1.6[14] software, with scaling factors of between 0.95 and 0.96. The mean absolute deviation (MAD) between experimental and simulated Raman bands in the alkyne systems were reasonable at between 7 and 13 cm^{-1}. The GaussView[15] v5.0.8 and Molden[16] software packages allowed visualisation of the molecular orbitals and vibrational modes respectively. The potential energy surface scan of the ferrocene dihedral angle (α) was accomplished by freezing the dihedral angle at various values and allowing the rest of the molecule to relax to its lowest energy configuration. The structure at which α = 180° was taken to be the zero energy point (as this could be calculated for all systems) and the energy of the other dihedrals was calculated relative to this to allow Figure S81, Figure S83, Figure S85, and Figure S87 to be produced.

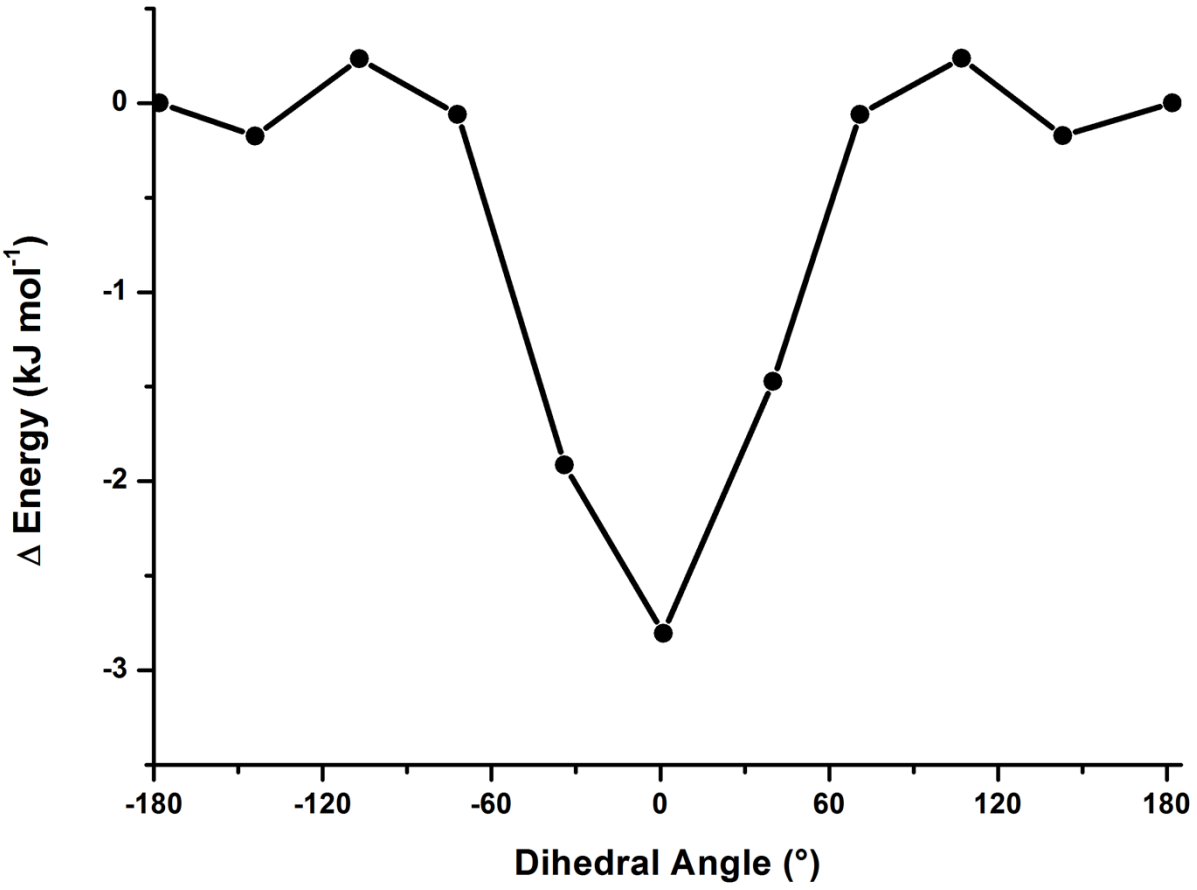

Figure S82 Relative energy of ligand **1a** across a range of possible dihedral angles.

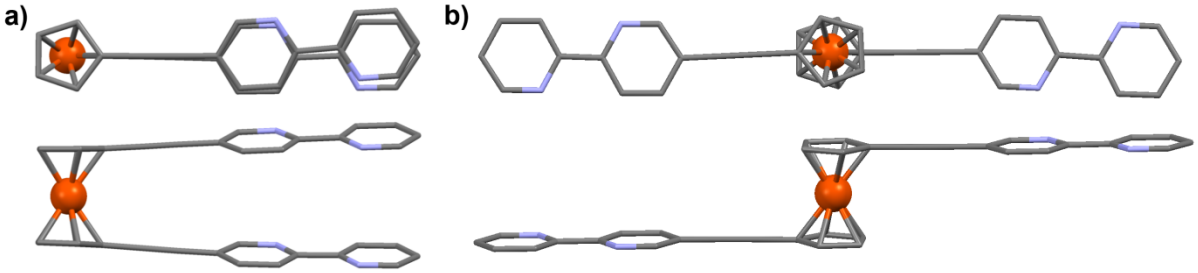

Figure S83 Energy minimised structures of the ligand **1a** with the dihedral angle between the two "arms" constrained to a) 0° and b) 180°.

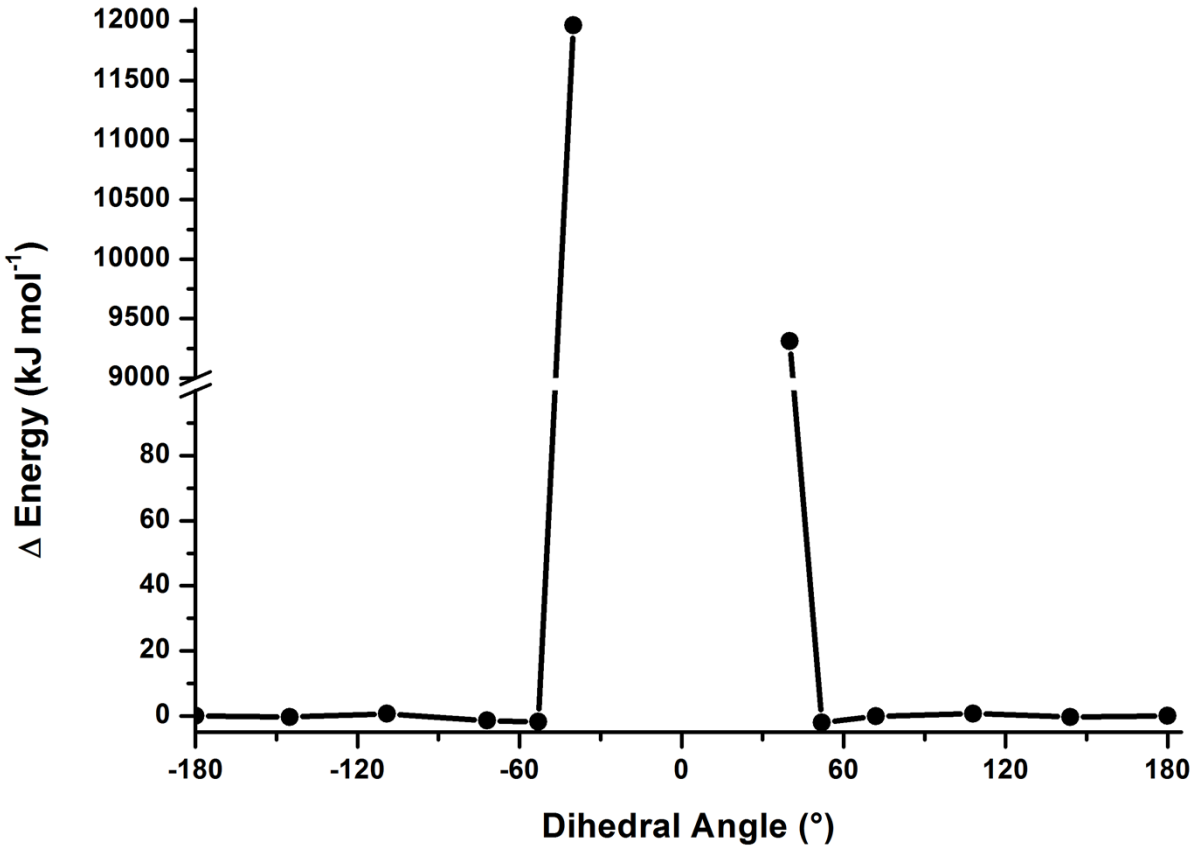

Figure S84 Relative energy of complex $[Cu_2(\mathbf{1a})(\mathbf{3})_2](PF_6)_2$ across a range of possible dihedral angles.

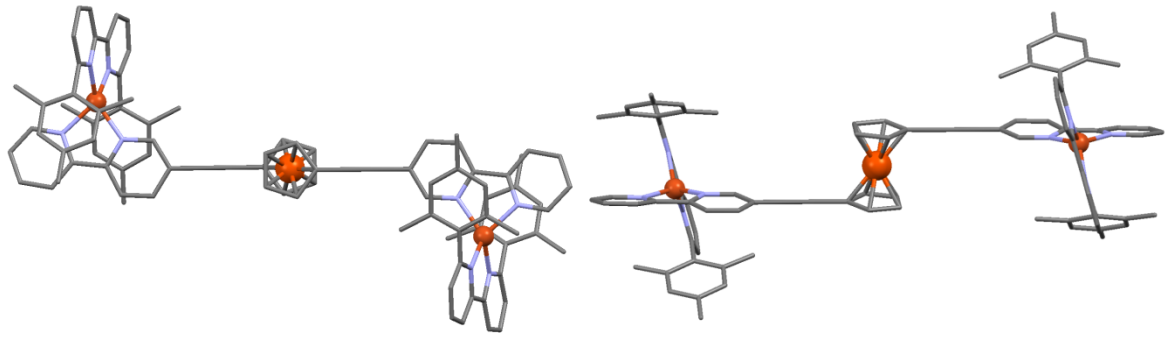

Figure S85 Energy minimised structure of the complex $[Cu_2(\mathbf{1a})(\mathbf{3})_2](PF_6)_2$ with the dihedral angle between the two "arms" constrained to 180°.

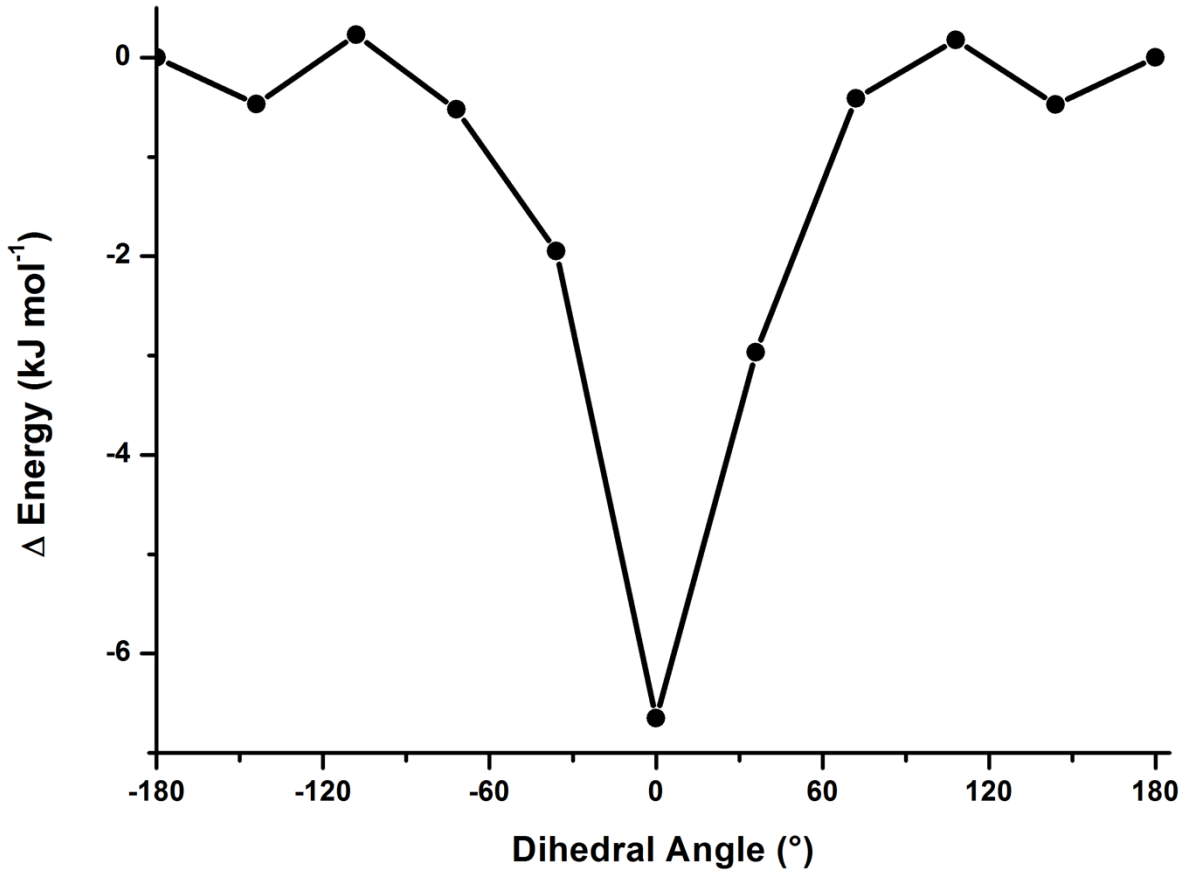

Figure S86 Relative energy of methylated ligand **1b** across a range of possible dihedral angles.

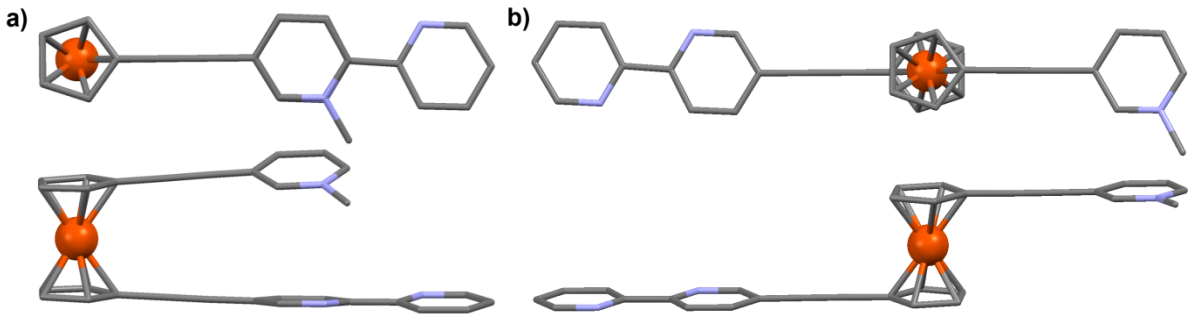

Figure S87 Energy minimised structures of the methylated ligand **1b** with the dihedral angle between the two "arms" constrained to a) 0° and b) 180°.

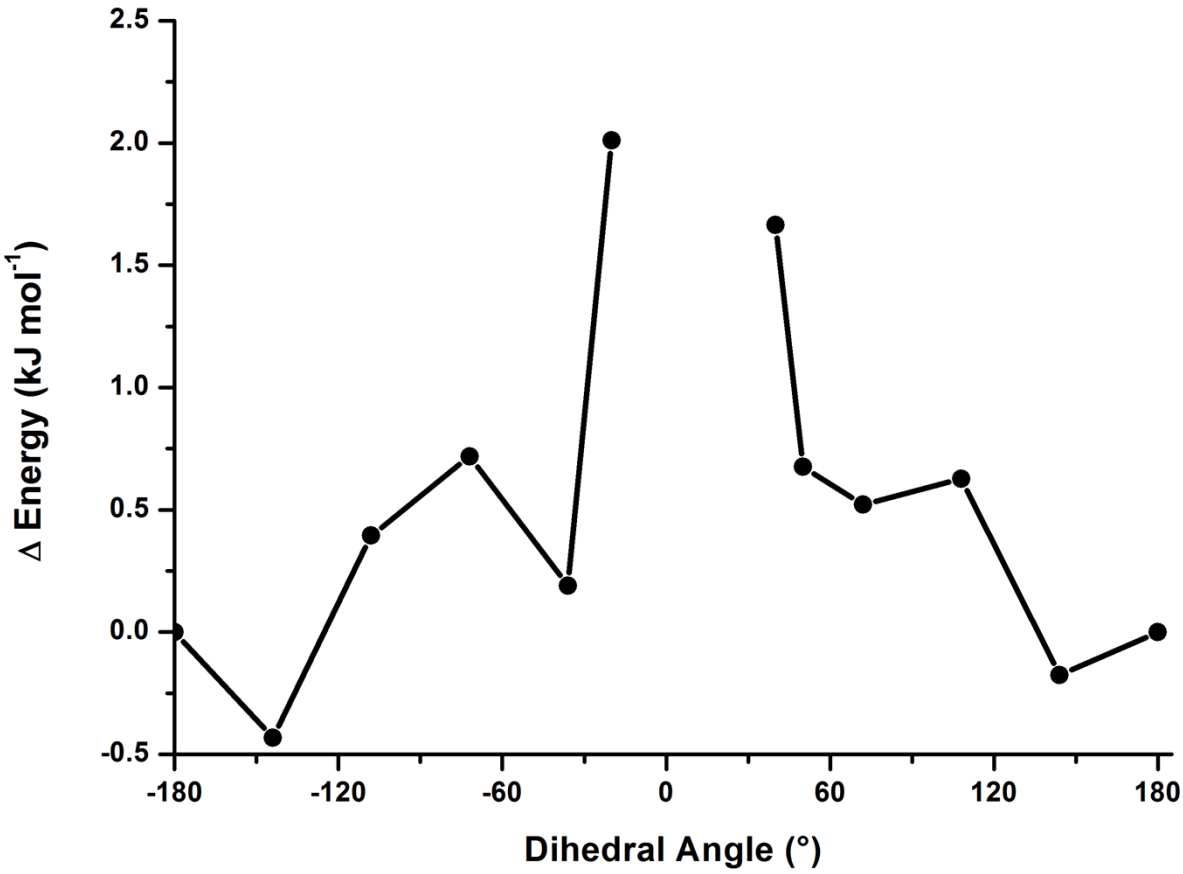

Figure S88 Relative energy of complex [Cu(**1b**)(**3**)]$(PF_6)_2$ across a range of possible dihedral angles.

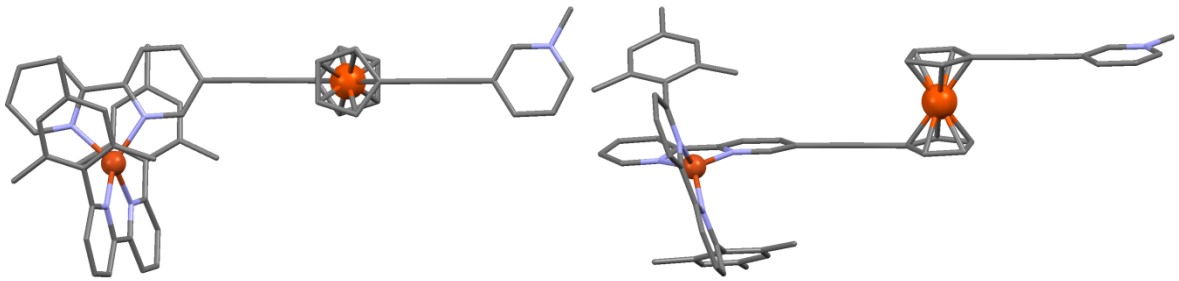

Figure S89 Energy minimised structure of the complex [Cu(**1b**)(**3**)]$(PF_6)_2$ with the dihedral angle between the two "arms" constrained to 180°.

7 X-ray Data

7.1 Crystallographic Data Tables

Compound	**2a**		**2b**		[Cu(**5**)(**3**)](PF$_6$)$_2$	
CCDC	1046341		1046342		1046336	
Empirical formula	$C_{22}H_{16}FeN_2$		$C_{18}H_{16}F_6FeNP$		$C_{43}H_{39}CuF_{12}N_5P_2$	
Formula weight	364.22		447.14		979.27	
Temperature	100.01(13) K		100.01(10) K		100.01(10) K	
Wavelength	1.54184 Å		1.54184 Å		1.54184 Å	
Crystal system	Orthorhombic		Monoclinic		Monoclinic	
Space group	*Pna*2$_1$		*P*12$_1$1		*P*12$_1$/*n*1	
Unit cell dimensions	a = 23.8585(13) Å	α = 90˚	a = 7.3960(2) Å	α = 90.0˚	a = 12.70025(10) Å	α = 90˚
	b = 6.8313(4) Å	β = 90˚	b = 10.9122(2) Å	β = 104.382(3)˚	b = 21.30927(15) Å	β = 93.2975(6)˚
	c = 10.0250(6) Å	γ = 90˚	c = 11.2342(3) Å	γ = 90.0˚	c = 15.21998(10) Å	γ = 90˚
Volume	1633.92(16) Å^3		878.26(4) Å^3		4112.21(5) Å^3	
Z	4		2		4	
Density (calculated)	1.481 Mg/m^3		1.691 Mg/m^3		1.582 Mg/m^3	
Absorption coefficient	7.426 mm^{-1}		8.351 mm^{-1}		2.331 mm^{-1}	
F(000)	752		452		1996	
Crystal size	0.175 x 0.091 x 0.029 mm^3		0.2002 x 0.1101 x 0.0638 mm^3		0.5591 x 0.3735 x 0.3089 mm^3	
Theta range for data collection	3.71 to 76.73˚		4.06 to 76.60˚		3.57 to 76.90˚	
Index ranges	-29<=h<=21, -8<=k<=4, -12<=l<=11		-8<=h<=9, -13<=k<=13, -14<=l<=13		-15<=h<=14, -26<=k<=26, -12<=l<=19	
Reflections collected	4765		9675		34019	
Independent reflections	2572 [R(int) = 0.0350]		3563 [R(int) = 0.0482]		8565 [R(int) = 0.0258]	
Completeness	98.0% (theta = 76.73˚)		98.9% (theta = 76.60˚)		98.7% (theta = 76.90˚)	
Max. and min. transmission	1.00000 and 0.65066		1.00000 and 0.65316		1.00000 and 0.66150	
Data / restraints / parameters	2572 / 1 / 226		3563 / 1 / 245		8565 / 0 / 574	
Goodness-of-fit on F^2	1.177		1.054		1.033	
Final R indices [I>2sigma(I)]	R1 = 0.0389, wR2 = 0.1055		R1 = 0.0355, wR2 = 0.0890		R1 = 0.0449, wR2 = 0.1197	
R indices (all data)	R1 = 0.0450, wR2 = 0.1087		R1 = 0.0386, wR2 = 0.0910		R1 = 0.0465, wR2 = 0.1234	
Largest diff. peak and hole	0.517 and -0.325 e.Å^{-3}		0.785 and -0.440 e.Å^{-3}		1.131 and -0.789 e.Å^{-3}	

Compound	**1a**		$[Cu_2(\mathbf{1a})(\mathbf{3})_2](ClO_4)_2$		**S7**	
CCDC	1046340		1046337		1046339	
Empirical formula	$C_{34}H_{22}FeN_4$		$C_{90}H_{78}N_8O_8FeCu_2Cl_2$		$C_{22}H_{15}FeIN_2$	
Formula weight	542.41		1653.46		490.11	
Temperature	99.98(14) K		100(2) K		100(2) K	
Wavelength	1.54184 Å		1.54184 Å		1.54184 Å	
Crystal system	Monoclinic		Monoclinic		Monoclinic	
Space group	$P2_1/n$		$P12_1/n1$		$P12_1/c1$	
Unit cell dimensions	a = 15.622(5) Å	α = 90.0˚	a = 18.1611(2) Å	α = 90˚	a = 5.82160(10) Å	α = 90˚
	b = 9.169(5) Å	β = 102.084(5)˚	b = 52.0625(9) Å	β = 106.0870(10)˚	b = 15.6040(4) Å	β = 91.300(2)˚
	c = 17.531(5) Å	γ = 90.0˚	c = 20.5495(3) Å	γ = 90˚	c = 19.8079(4) Å	γ = 90˚
Volume	2455.5(17) $Å^3$		18669.0(5) $Å^3$		1798.89(7) $Å^3$	
Z	4		8		4	
Density (calculated)	1.467 Mg/m^3		1.177 Mg/m^3		1.810 Mg/m^3	
Absorption coefficient	0.647 mm^{-1}		2.716 mm^{-1}		20.242 mm^{-1}	
F(000)	1120		6848		960	
Crystal size	0.2697 x 0.1400 x 0.0396 mm^3		0.4910 x 0.4185 x 0.2881 mm^3		0.4125 x 0.2212 x 0.1068 mm^3	
Theta range for data collection	1.59 to 26.64˚		3.00 to 68.25˚		3.61 to 77.40˚	
Index ranges	-19<=h<=19, -7<=k<=11, -22<=l<=20		-21<=h<=21, -62<=k<=62, -24<=l<=24		-7<=h<=7, -19<=k<=19, -24<=l<=23	
Reflections collected	20754		217551		22565	
Independent reflections	5100 [R(int) = 0.0736]		34176 [R(int) = 0.0989]		3773 [R(int) = 0.1027]	
Completeness	98.9% (theta = 26.64˚)		100.0% (theta = 68.25˚)		98.8% (theta = 77.40˚)	
Max. and min. transmission	1.00000 and 0.65112		0.5084 and 0.3490		1.00000 and 0.10736	
Data / restraints / parameters	5100 / 0 / 325		34176 / 186 / 2023		3773 / 0 / 235	
Goodness-of-fit on F^2	1.051		1.071		1.035	
Final R indices [I>2sigma(I)]	R1 = 0.0698, wR2 = 0.1822		R1 = 0.1085, wR2 = 0.2930		R1 = 0.0513, wR2 = 0.1417	
R indices (all data)	R1 = 0.0801, wR2 = 0.1907		R1 = 0.1182, wR2 = 0.3008		R1 = 0.0533, wR2 = 0.1451	
Largest diff. peak and hole	1.439 and -0.782 e.$Å^{-3}$		3.286 and -1.694 e.$Å^{-3}$		2.333 and -1.266 e.$Å^{-3}$	

7.2 Crystal Structures and Relevant Notes

All structures were collected on an Agilent Technologies SuperNova diffractometer with an Atlas detector using Cu Kα radiation at low temperature (100 K). SADABS[17] was used for absorption correction. The structures was solved by direct methods using either SIR-97[18] or X-Seed[19] and refined against F^2 using anisotropic thermal displacement parameters for all non-hydrogen atoms using SHELXL-97[20] software. Hydrogen atoms were placed in calculated positions and refined using a riding model.

Due to the extent of disordered solvent in the crystal lattice of $[Cu_2(\mathbf{1a})(\mathbf{3})_2](PF_6)_2$, the SQUEEZE routine within PLATON was implemented. SQUEEZE details are listed below, beneath the relevant structures.

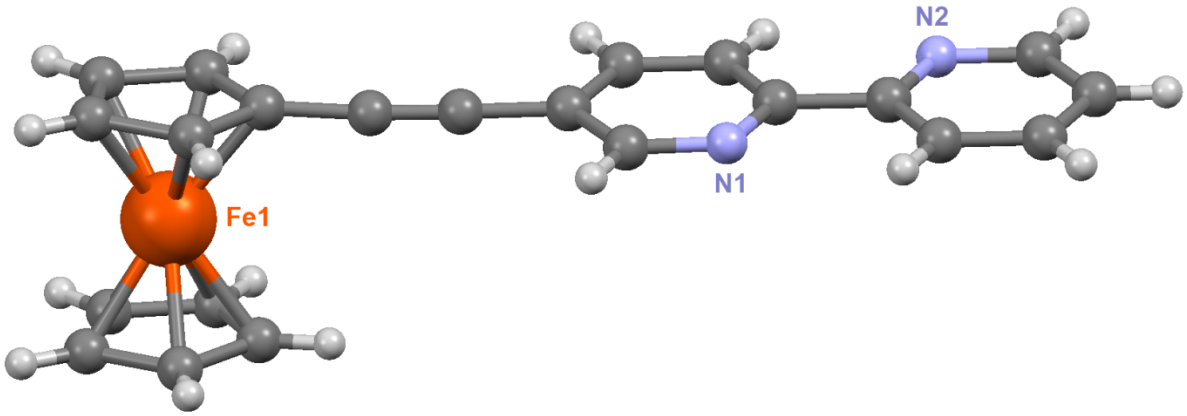

Figure S90 Mercury ball-and-stick plot of **2a**.

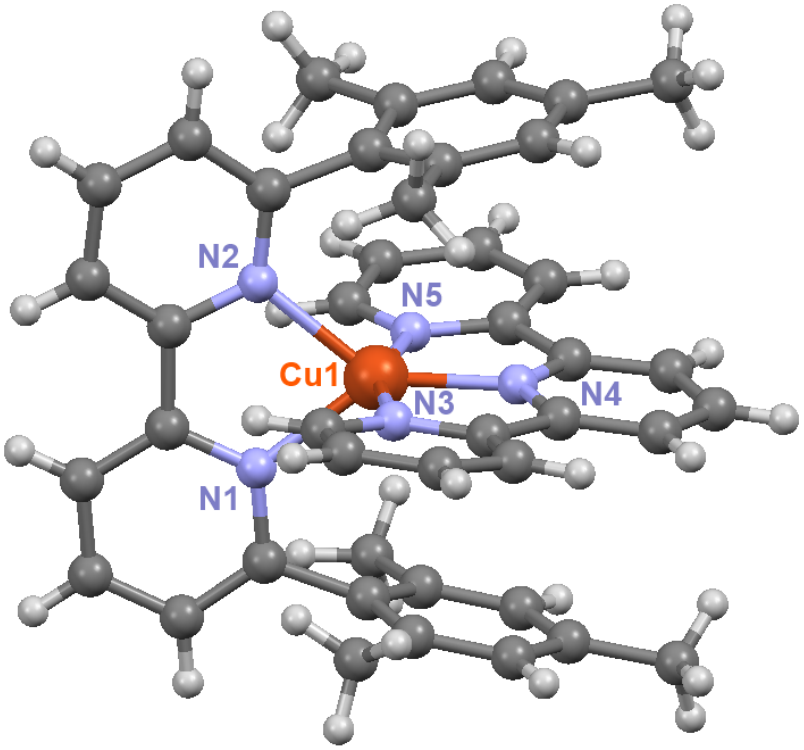

Figure S95 Mercury ball-and-stick plot of $[Cu(\mathbf{5})(\mathbf{3})](PF_6)_2$. Counterions omitted for clarity.

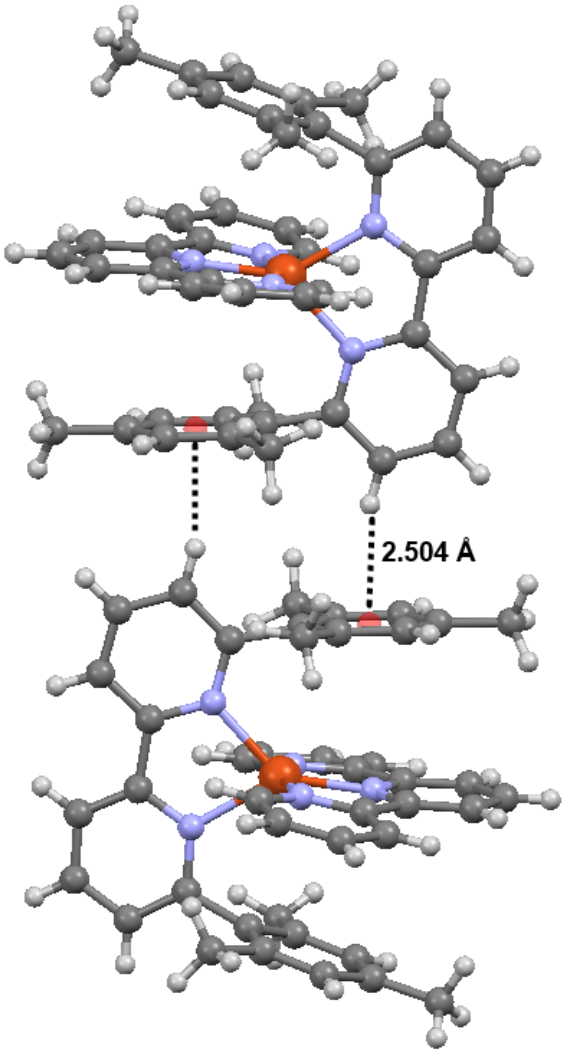

Figure S96 Vertical stacking observed within the packing of [Cu(**5**)(**3**)]$(PF_6)_2$, with the relevant centroid-H distance labelled. Counterions omitted for clarity.

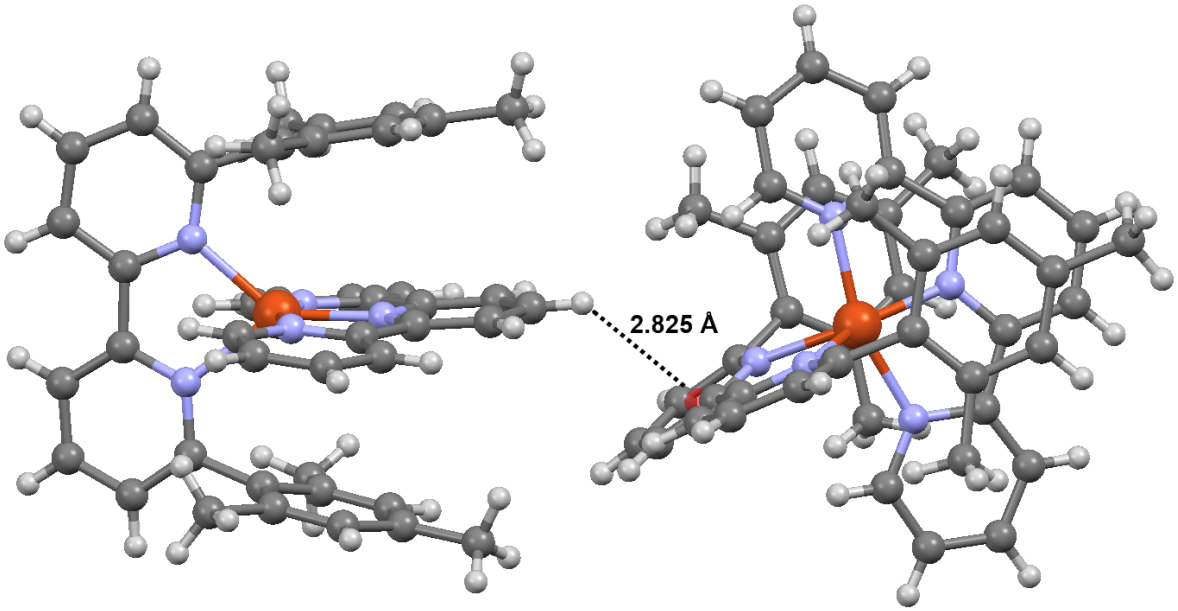

Figure S97 H-π interaction observed within the packing of [Cu(**5**)(**3**)]$(PF_6)_2$, with the relevant centroid-H distance labelled. Counterions omitted for clarity.

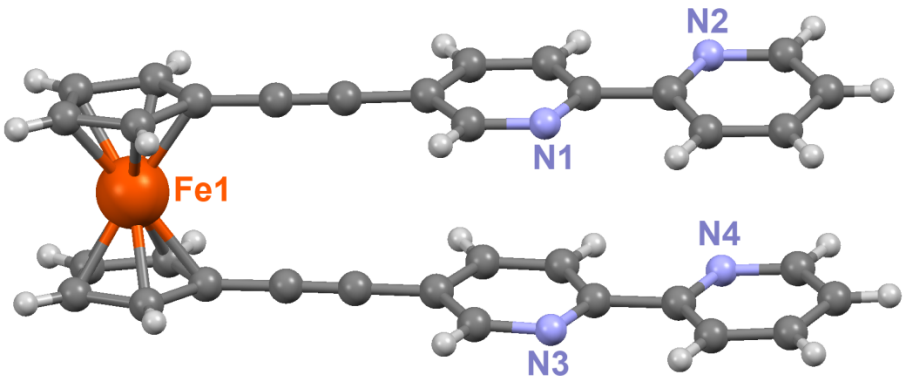

Figure S98 Mercury ball-and-stick plot of **1a**.

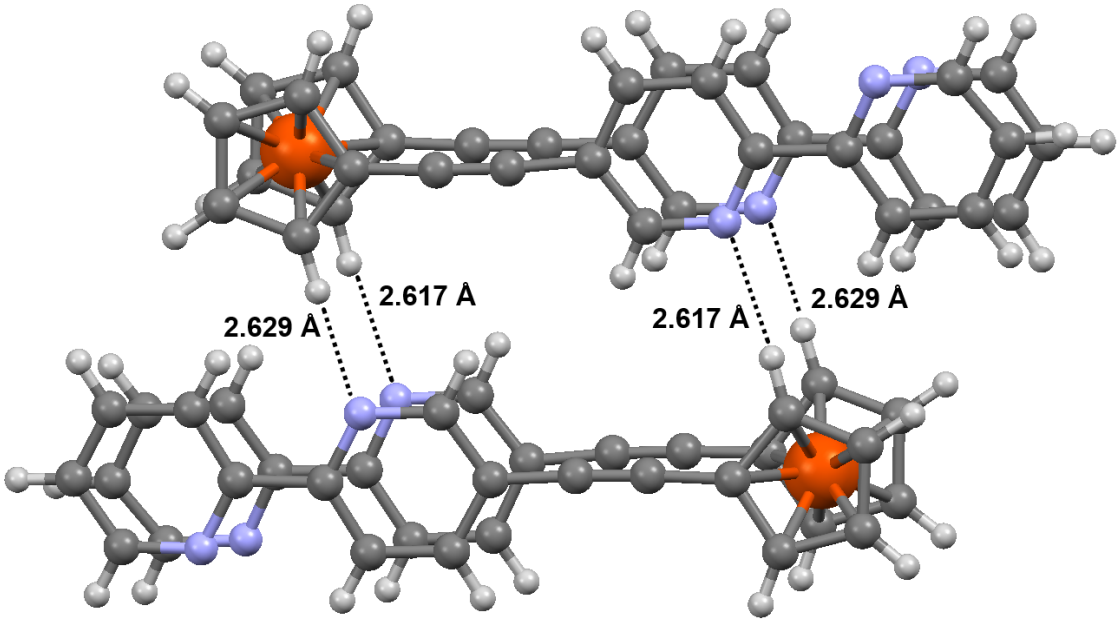

Figure S99 Hydrogen bonding between adjacent molecules within the packing of **1a**, with the N-H bonds labelled.

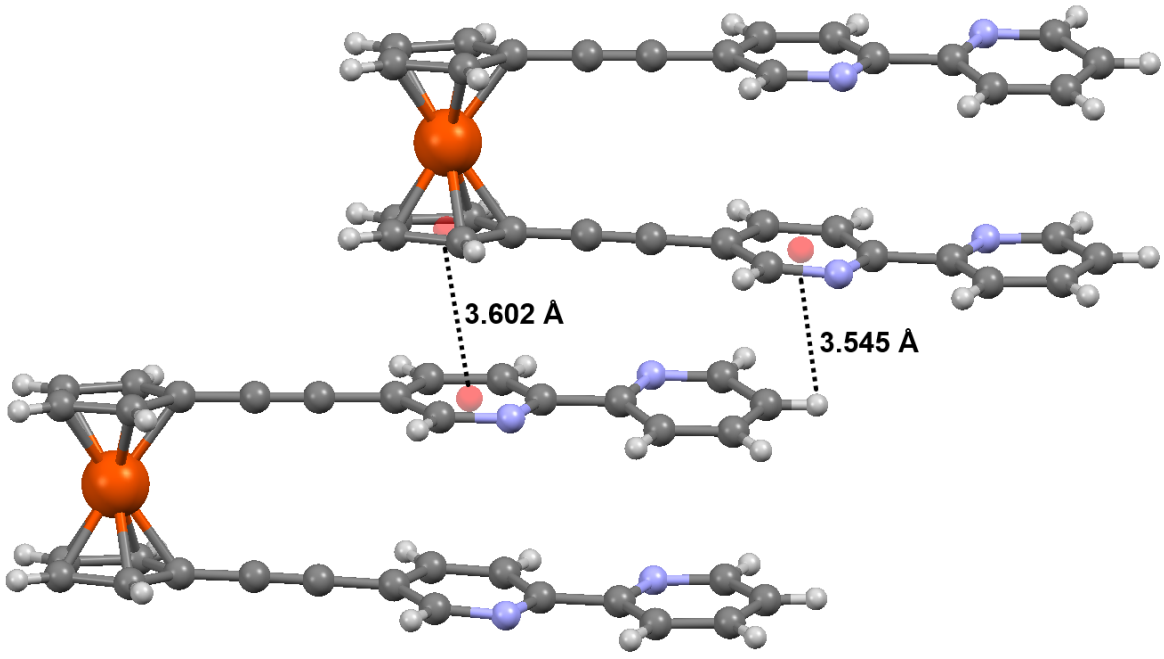

Figure S100 H-π and π-π stacking within the packing of **1a**, with the centroid-centroid and centroid-H distances labelled.

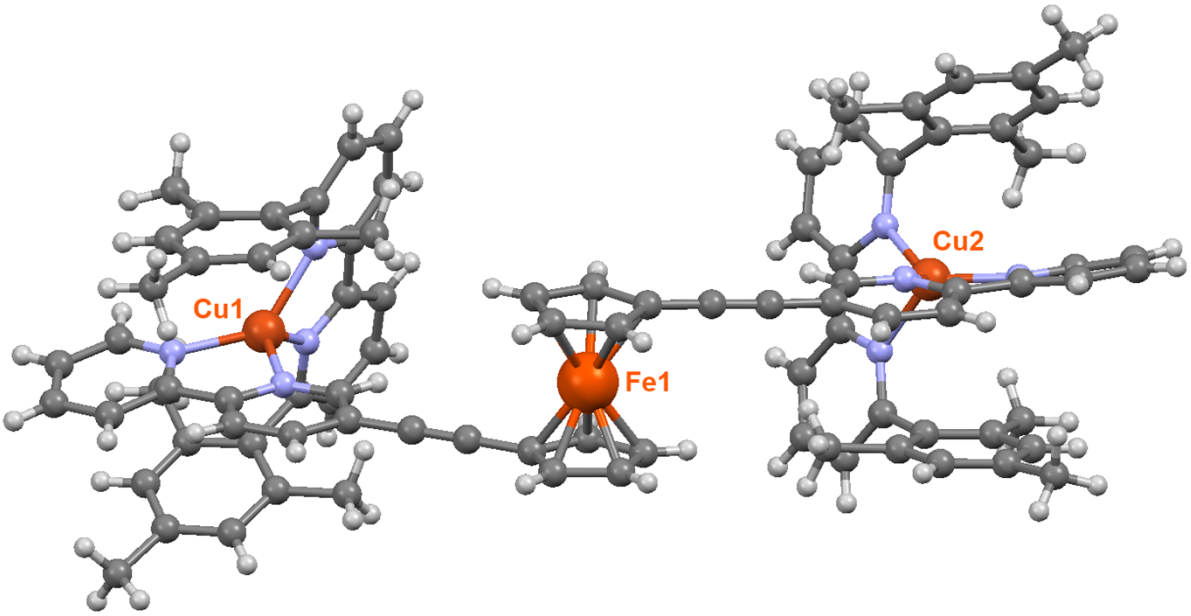

Figure S101 Mercury ball-and-stick plot of $[Cu_2(\mathbf{1a})(\mathbf{3})_2](PF_6)_2$. Selected bond lengths (Å) and angles (°): Cu1-N104: 2.045(5), Cu1-N105: 2.010(4), Cu1-N106: 1.993(4), Cu1-N107: 2.045(4), Cu2-N100: 2.066(5), Cu2-N101: 2.006(6), Cu2-N102: 2.020(5), Cu2-N103: 2.054(7), N104-Cu1-N105: 82.1(2), N106-Cu1-N107: 80.5(2), N104-Cu1-N106: 125.8(2), N105-Cu1-N107: 132.8(2), N100-Cu2-N101: 82.0(2), N102-Cu2-N103: 80.4(2), N100-Cu2-N102: 124.1(2), N101-Cu2-N103: 131.5(2)). Counterions omitted for clarity. $[Cu_2(\mathbf{1a})(\mathbf{3})_2](PF_6)_2$ was subject to Platon Squeeze, details of which follow.

PLATON SQUEEZE details for $[Cu_2(\mathbf{1a})(\mathbf{3})_2](PF_6)_2$

Void number	1	2	3	4	5	6	7	8
Average x	0.000	0.096	0.158	0.500	0.239	0.260	0.739	0.760
Average y	0.000	0.250	0.750	0.500	0.044	0.544	0.456	0.956
Average z	1.000	0.614	0.639	0.500	0.454	0.046	0.954	0.546
Volume	786	1167	1167	786	11	11	11	11
Electron count	239	396	393	240	2	2	2	2

Details

The packing of the crystal shows sizeable solvent channels (Figure S101) containing significant amounts of diffuse electron density, accounted for by disordered solvent which could not be modelled adequately as discrete molecules. This includes a minimum of 5 highly disordered acetonitrile molecules that could be located in the asymmetric unit, but were too disordered to refine. As such, PLATON SQUEEZE was employed to calculate the contribution to the diffraction from the solvent channels and thereby produced a set of solvent-free diffraction intensities.

SQUEEZE estimated 8 voids with a total contribution of approximately 1276 electrons per unit cell. Due to this being a monoclinic space group with 4 asymmetric units per unit cell, this amounts to approximately 1276/4 = 319 electrons per asymmetric unit. This can be accounted for by 10 molecules of acetonitrile (10x22 = 220) and 10 molecules of water (10x10 = 100) per asymmetric unit.

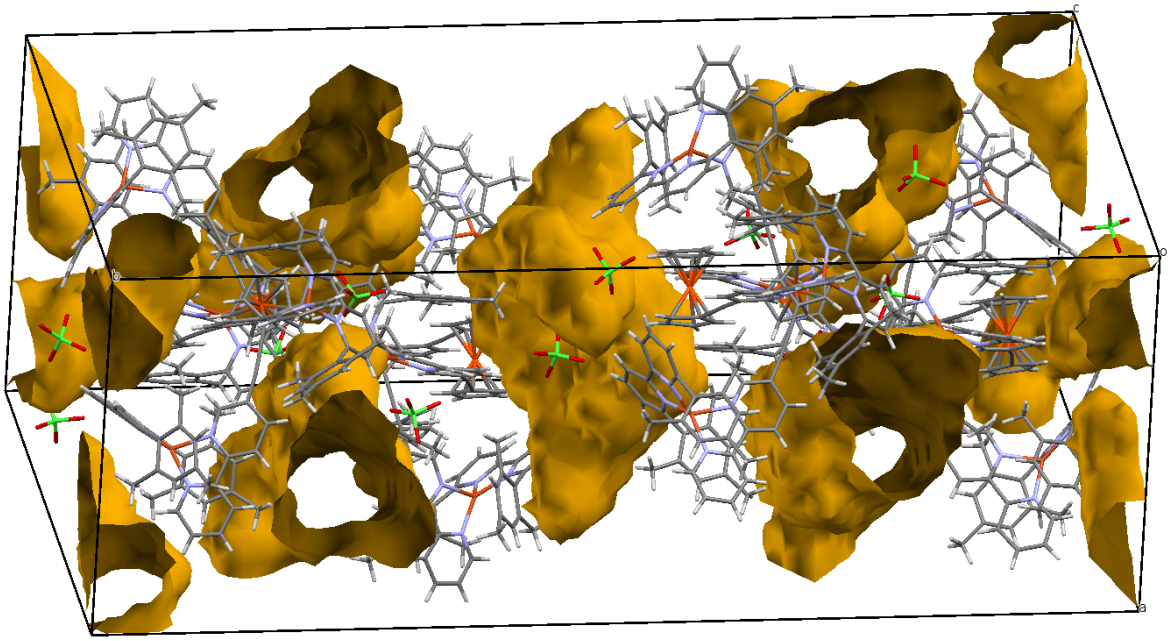

Figure S102 Mercury plot of the calculated solvent voids within the unit cell of $[Cu_2(\mathbf{1a})(\mathbf{3})_2](PF_6)_2$. The total void space is estimated to be approximately 3408.92 Å^3, and takes up 18.3% of the unit cell.

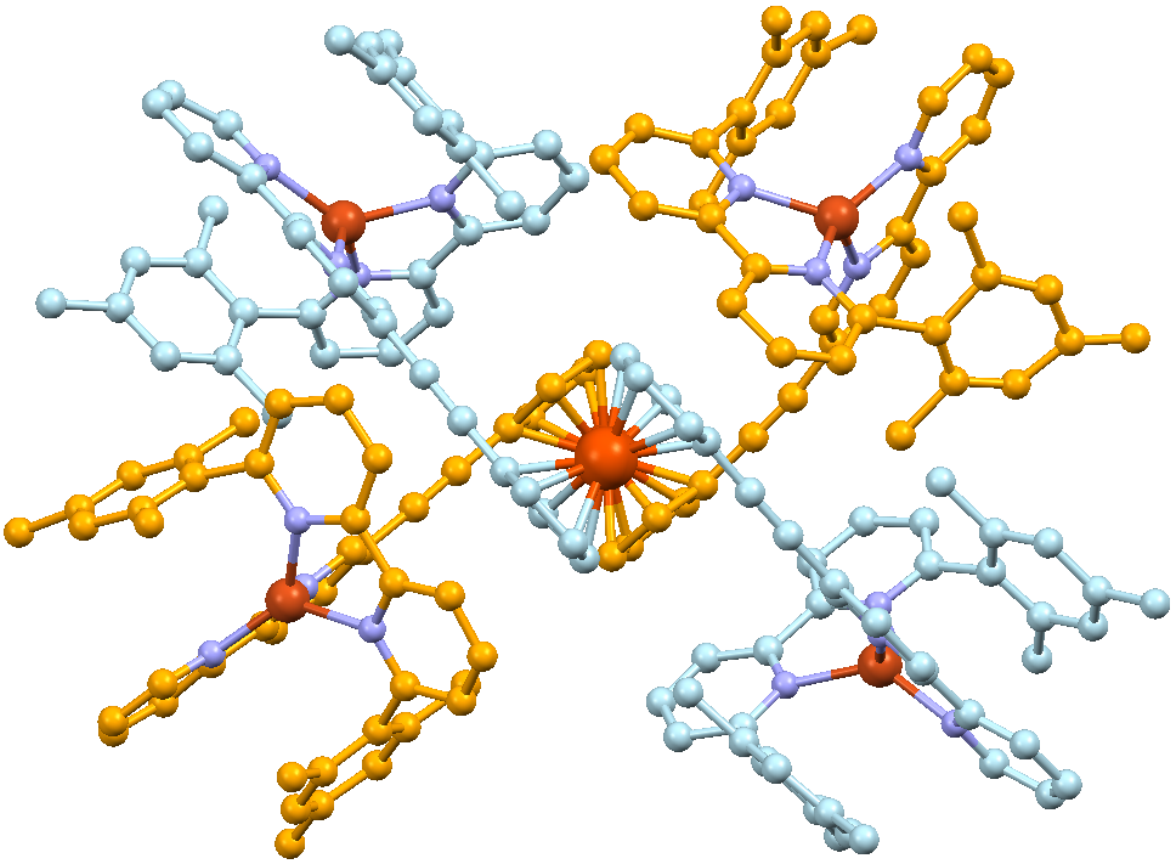

Figure S103 The asymmetric unit of $[Cu_2(\mathbf{1a})(\mathbf{3})_2](PF_6)_2$ consists of two discrete molecules (coloured blue and orange respectively) helically entwined, with the central Fe-Fe distance being 5.189 Å. A variety of H-π interactions stabilise this supramolecular helix. Counterions and hydrogens omitted for clarity.

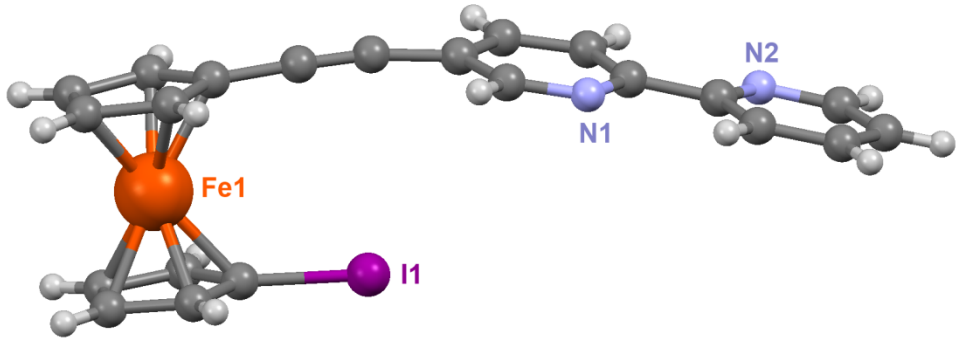

Figure S104 Mercury ball-and-stick plot of **S7**. Significant bowing of the bipyridine substituent is observed due to the intramolecular interaction of the iodine with the π density of the bipyridine.

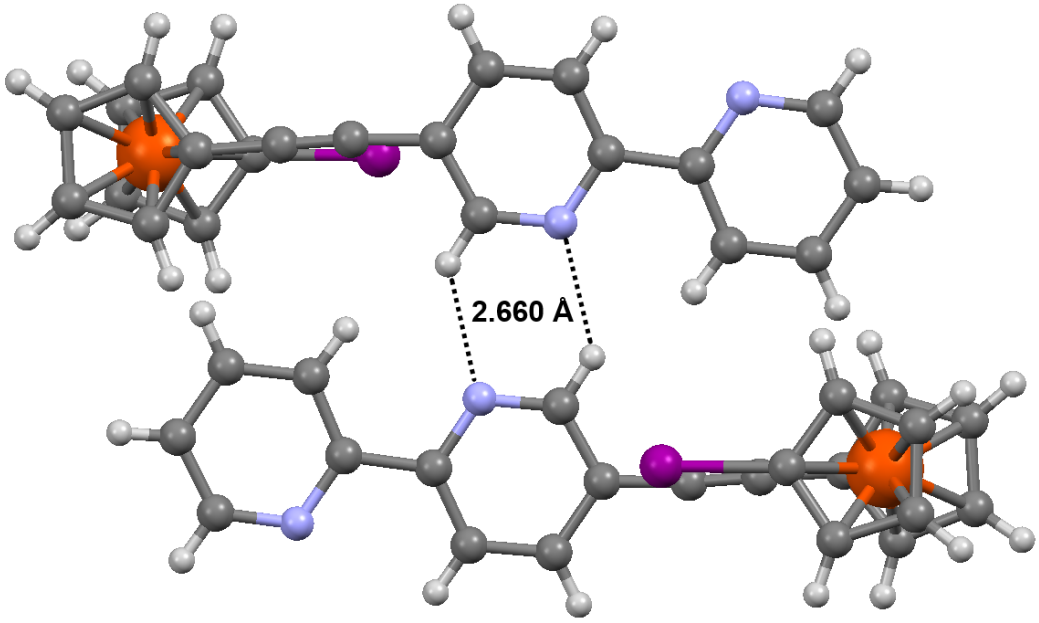

Figure S105 Hydrogen bonding between adjacent molecules within the packing of **S7**, with the N-H bonds labelled.

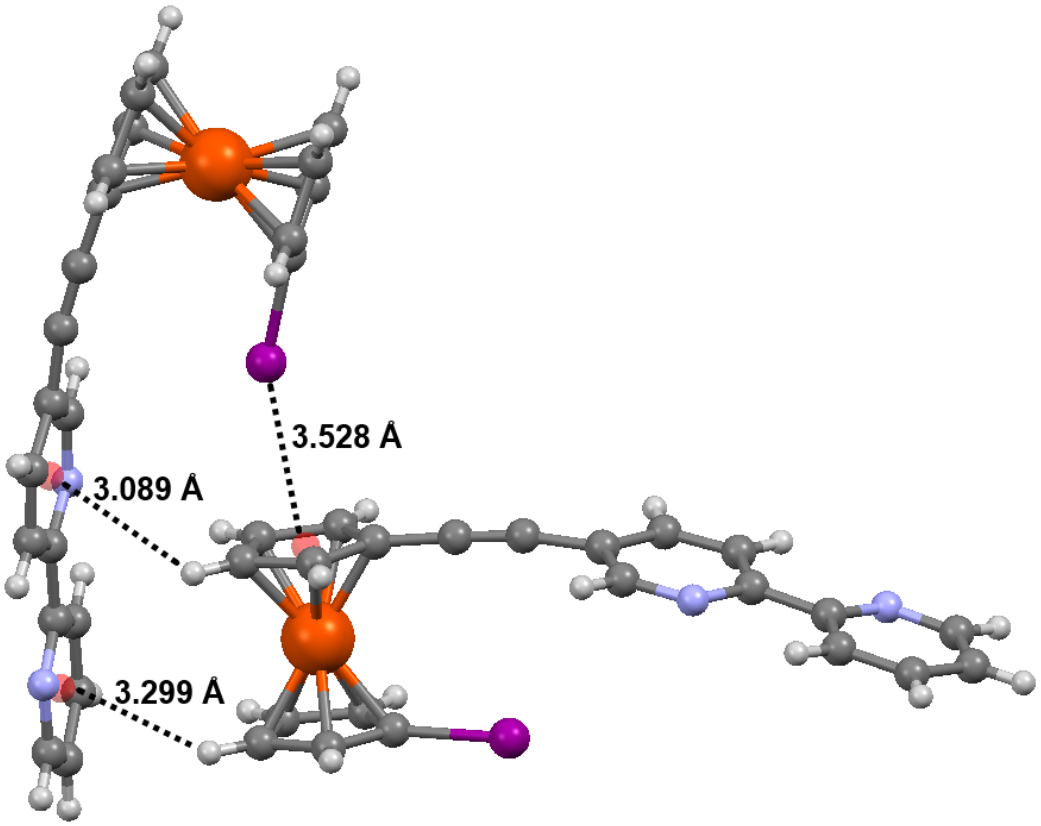

Figure S106 H-π and I-π interactions within the packing of **S7**, with the centroid-H and centroid-I distances labelled.

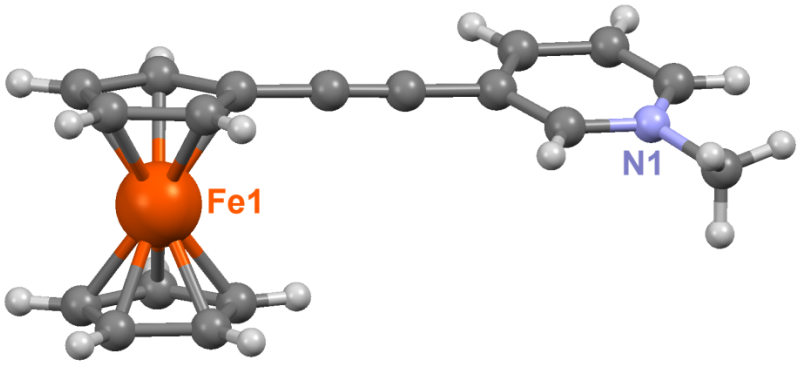

Figure S107 Mercury ball-and-stick plot of **2b**. Counterion omitted for clarity.

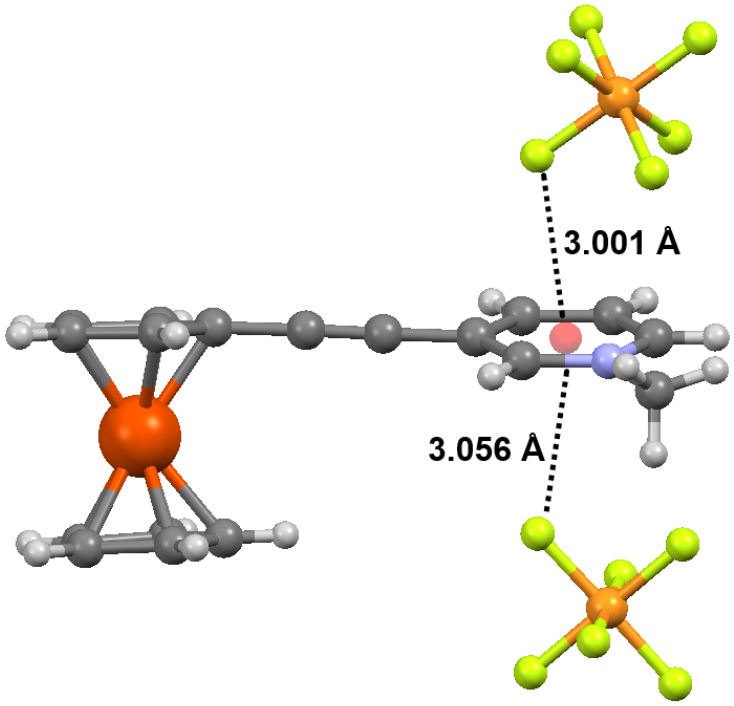

Figure S108 Anion-π interactions observed within the packing of **2b**, with the centroid-F distances labelled.

8 References

1. S.-H. Kim and R. D. Rieke, *Tetrahedron*, 2010, **66**, 3135-3146.
2. V. Grosshenny, F. M. Romero and R. Ziessel, *J. Org. Chem.*, 1997, **62**, 1491-1500.
3. M. S. Inkpen, S. Du, M. Driver, T. Albrecht and N. J. Long, *Dalton Trans.*, 2013, **42**, 2813-2816.
4. M. S. Inkpen, T. Albrecht and N. J. Long, *Organometallics*, 2013, **32**, 6053-6060.
5. E. Lindner, R. Zong and K. Eichele, *Phosphorus, Sulfur Silicon Relat. Elem.*, 2001, **168-169**, 543-546.
6. R. Packheiser, B. Walfort and H. Lang, *Organometallics*, 2006, **25**, 4579-4587.
7. E. Lindner, R. Zong, K. Eichele and M. Strobele, *J. Organomet. Chem.*, 2002, **660**, 78-84.
8. M. Schmittel, A. Ganz, W. A. Schenk and M. Hagel, *Z. Naturforsch., B Chem. Sci.*, 1999, **54**, 559-564.
9. I. Noviandri, K. N. Brown, D. S. Fleming, P. T. Gulyas, P. A. Lay, A. F. Masters and L. Phillips, *J. Phys. Chem. B*, 1999, **103**, 6713-6722.
10. F. Barrière and W. E. Geiger, *J. Am. Chem. Soc.*, 2006, **128**, 3980-3989.
11. M. J. Frisch, G. W. Trucks, H. B. Schlegel, G. E. Scuseria, M. A. Robb, J. R. Cheeseman, G. Scalmani, V. Barone, B. Mennucci, G. A. Petersson, H. Nakatsuji, M. Caricato, X. Li, H. P. Hratchian, A. F. Izmaylov, J. Bloino, G. Zheng, J. L. Sonnenberg, M. Hada, M. Ehara, K. Toyota, R. Fukuda, J. Hasegawa, M. Ishida, T. Nakajima, Y. Honda, O. Kitao, H. Nakai, T. Vreven, J. A. Montgomery Jr., J. E. Peralta, F. Ogliaro, M. J. Bearpark, J. Heyd, E. N. Brothers, K. N. Kudin, V. N. Staroverov, R. Kobayashi, J. Normand, K. Raghavachari, A. P. Rendell, J. C. Burant, S. S. Iyengar, J. Tomasi, M. Cossi, N. Rega, N. J. Millam, M. Klene, J. E. Knox, J. B. Cross, V. Bakken, C. Adamo, J. Jaramillo, R. Gomperts, R. E. Stratmann, O. Yazyev, A. J. Austin, R. Cammi, C. Pomelli, J. W. Ochterski, R. L. Martin, K. Morokuma, V. G. Zakrzewski, G. A. Voth, P. Salvador, J. J. Dannenberg, S. Dapprich, A. D. Daniels, Ö. Farkas, J. B. Foresman, J. V. Ortiz, J. Cioslowski and D. J. Fox, *Gaussian 09*, (2009) Gaussian, Inc., Wallingford, CT, USA.
12. T. Yanai, D. P. Tew and N. C. Handy, *Chem. Phys. Lett.*, 2004, **393**, 51-57.
13. J. Tomasi, B. Mennucci and R. Cammi, *Chem. Rev. (Washington, DC, U. S.)*, 2005, **105**, 2999-3093.
14. N. M. O'Boyle, A. L. Tenderholt and K. M. Langner, *J. Comput. Chem.*, 2008, **29**, 839-845.
15. C. Lee, W. Yang and R. G. Parr, *Phys. Rev. B: Condens. Matter*, 1988, **37**, 785-789.
16. G. Schaftenaar and J. H. Noordik, *J. Comput.-Aided Mol. Des.*, 2000, **14**, 123-134.
17. G. M. Sheldrick, *SADABS: Program for Absorption Correction*, University of Goettingen, Goettingen, Germany, 1996.
18. A. Altomare, M. C. Burla, M. Camalli, G. L. Cascarano, C. Giacovazzo, A. Guagliardi, A. G. G. Moliterni, G. Polidori and R. Spagna, *J. Appl. Crystallogr.*, 1999, **32**, 115-119.
19. L. J. Barbour, *Journal of Supramolecular Chemistry*, 2001, **1**, 189-191.
20. G. M. Sheldrick, *Acta Crystallogr., Sect. A: Found. Crystallogr.*, 2008, **64**, 112-122.